Simulations of Idealized Solid Electrolytes for Solid State Battery Designs*

N. A. W. Holzwarth**

Department of Physics

Wake Forest University, Winston-Salem, NC, USA, 27109

*Supported by NSF Grant DMR-1105485 and WFU's Center for Energy, Environment, and Sustainability.

**With help from: Nicholas Lepley, Ahmad Al-Qawasmeh, Jason Howard, and Larry Rush (physics graduate students), Yaojun Du (previous physics postdoc) and colleagues from WFU chemistry department – Dr. Keerthi Senevirathne (currently at Florida A & M U.), Dr. Cynthia Day, Professor Michael Gross, Professor Abdessadek Lachgar, and Zachary Hood (currently at ORNL)

Outline

- Motivation – Why solid electrolytes?
- Computational tools & reality checks
- Some examples
  - LiPON
  - Li thiophosphates

  } Bulk properties
  } Interface properties
- Summary and remaining challenges

Motivation –
Why solid electrolytes?

Materials components of a Li ion battery

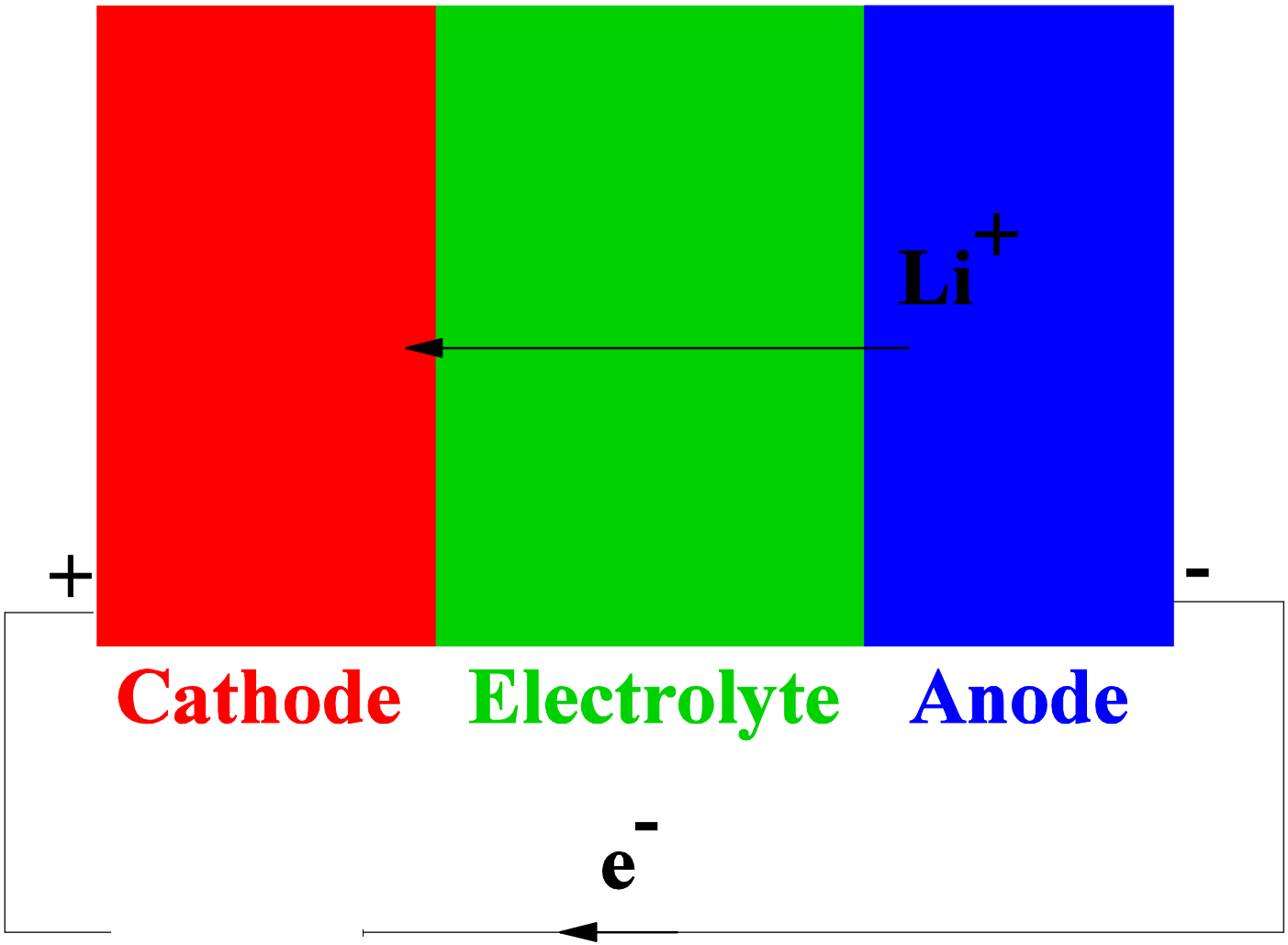

$$V = IR$$

$$\xrightarrow{\quad} I$$

From Oak Ridge National Laboratory:

Materials Views
www.MaterialsViews.com
Adv. Energy Mater. **2015**, *5*, 1401408
DOI: 10.1002/aenm.201401408
ADVANCED ENERGY MATERIALS
www.advenergymat.de

Solid Electrolyte: the Key for High-Voltage Lithium Batteries

Juchuan Li, Cheng Ma, Miaofang Chi, Chengdu Liang, and Nancy J. Dudney**

Advantages

- **Compatible and stable with high voltage cathodes and with Li metal anodes**

Disadvantages

- **Relatively low ionic conductivity (Compensated with the use of less electrolyte?)**
- **Lower total capacity**

Demonstrated for $LiNi_{0.5}Mn_{1.5}O_4$/LiPON/Li

- **10^{-6} m LiPON electrolyte layer achieved adequate conductivity**
- **10,000 cycles* with 90% capacity retention**

***1 cycle per day for 27 years**

From Toyota Motor Company Website:

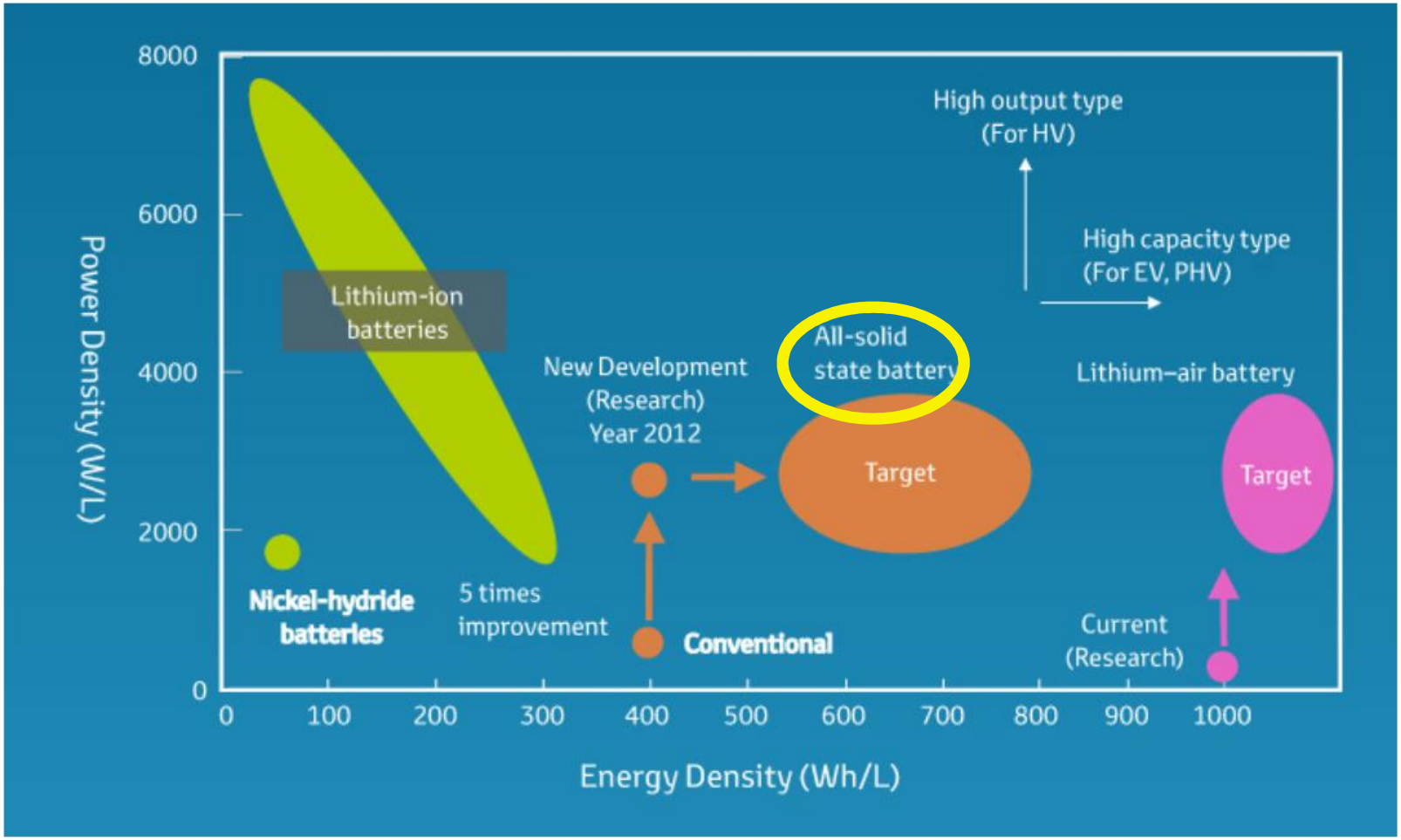

Figure1 R&D of Next-Generation Batteries Promote research and de facto standards for next-generation batteries with collaboration framework between R&D and production engineering

http://www.toyota-global.com/innovation/environmental_technology/next_generation_secondary_batteries.html

Motivation: Paper by N. Kayama, *et. al* in ***Nature Materials* 10**, 682-686 (2011)

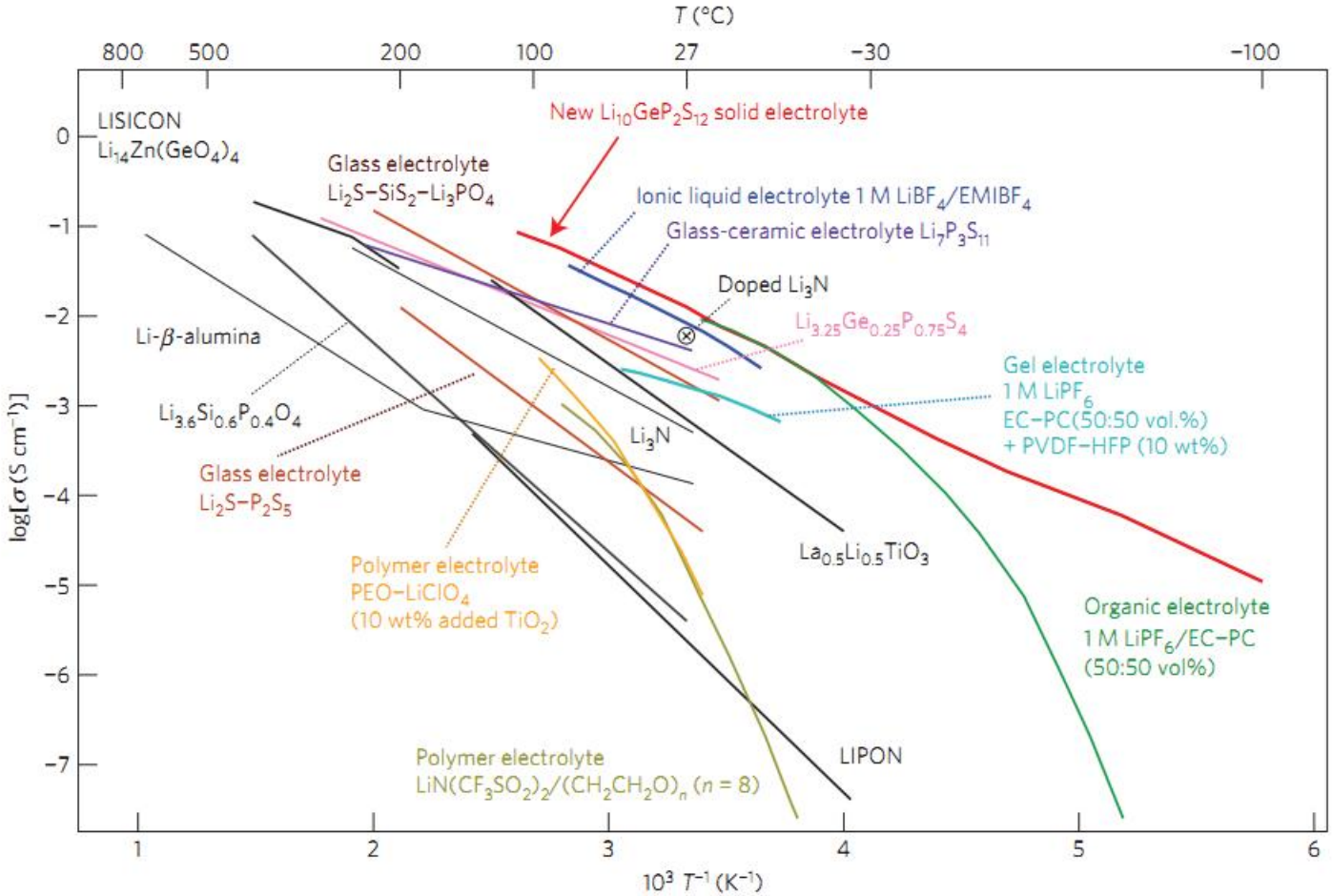

Figure 3 | Thermal evolution of ionic conductivity of the new $Li_{10}GeP_2S_{12}$ phase, together with those of other lithium solid electrolytes, organic liquid electrolytes, polymer electrolytes, ionic liquids and gel electrolytes[3-8,13-16,20,22]. The new $Li_{10}GeP_2S_{12}$ exhibits the highest lithium ionic conductivity (12 m S cm^{-1} at 27 °C) of the solid lithium conducting membranes of inorganic, polymer or composite systems. Because organic electrolytes usually have transport numbers below 0.5, inorganic lithium electrolytes have extremely high conductivities.

Motivation: Paper by N. Kamaya, *et. al* in ***Nature Materials*** **10**, 682-686 (2011)

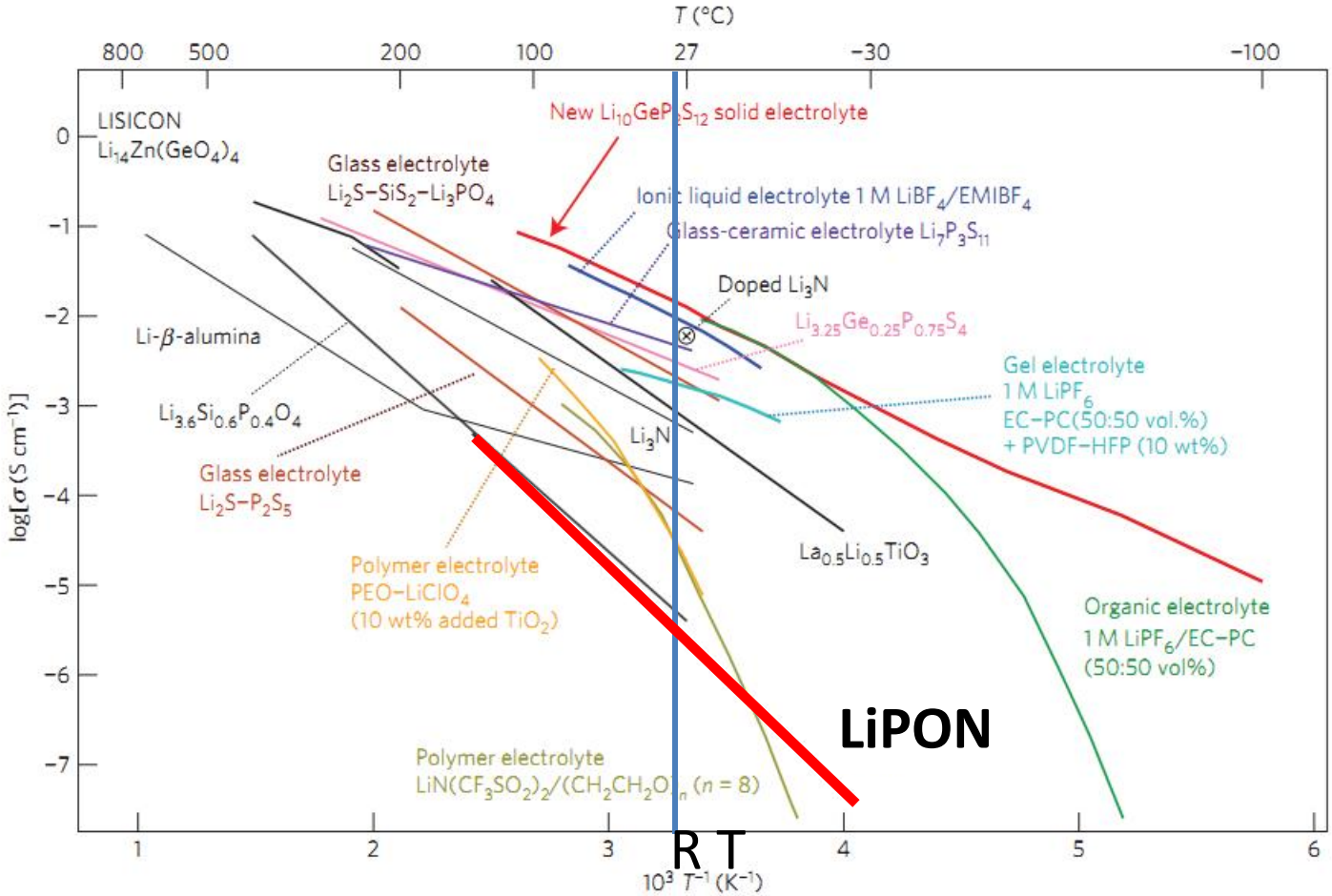

Figure 3 | Thermal evolution of ionic conductivity of the new $Li_{10}GeP_2S_{12}$ phase, together with those of other lithium solid electrolytes, organic liquid electrolytes, polymer electrolytes, ionic liquids and gel electrolytes[3-8,13-16,20,22]**.** The new $Li_{10}GeP_2S_{12}$ exhibits the highest lithium ionic conductivity (12 m S cm^{-1} at 27 °C) of the solid lithium conducting membranes of inorganic, polymer or composite systems. Because organic electrolytes usually have transport numbers below 0.5, inorganic lithium electrolytes have extremely high conductivities.

Motivation: Paper by N. Kamaya, *et. al* in ***Nature Materials*** **10**, 682-686 (2011)

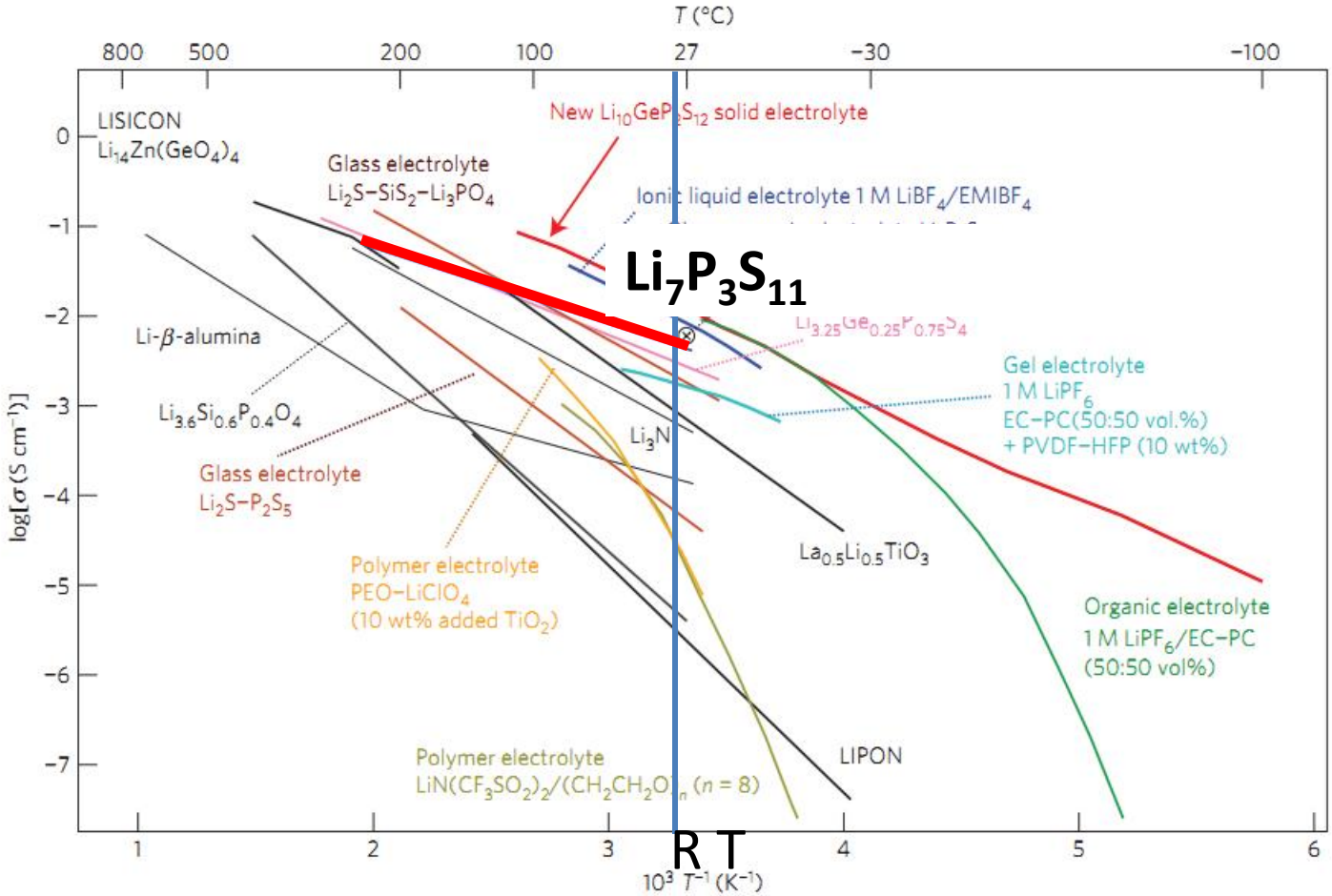

Figure 3 | Thermal evolution of ionic conductivity of the new $Li_{10}GeP_2S_{12}$ phase, together with those of other lithium solid electrolytes, organic liquid electrolytes, polymer electrolytes, ionic liquids and gel electrolytes[3-8,13-16,20,22]**.** The new $Li_{10}GeP_2S_{12}$ exhibits the highest lithium ionic conductivity (12 m S cm^{-1} at 27 °C) of the solid lithium conducting membranes of inorganic, polymer or composite systems. Because organic electrolytes usually have transport numbers below 0.5, inorganic lithium electrolytes have extremely high conductivities.

Motivation: Paper by N. Kamaya, *et. al* in ***Nature Materials*** **10**, 682-686 (2011)

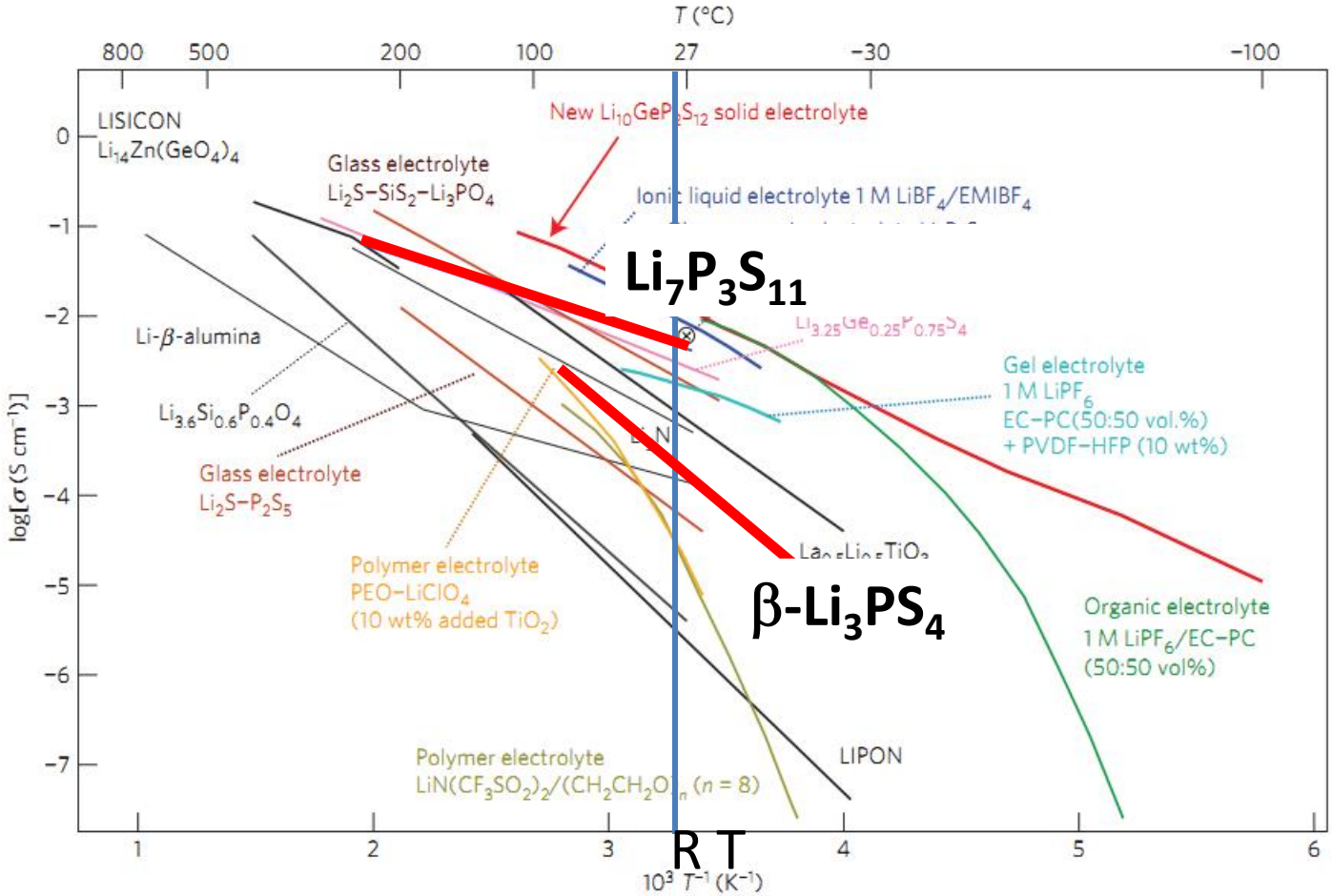

Figure 3 | Thermal evolution of ionic conductivity of the new $Li_{10}GeP_2S_{12}$ phase, together with those of other lithium solid electrolytes, organic liquid electrolytes, polymer electrolytes, ionic liquids and gel electrolytes[3-8,13-16,20,22]**.** The new $Li_{10}GeP_2S_{12}$ exhibits the highest lithium ionic conductivity (12 m S cm^{-1} at 27 °C) of the solid lithium conducting membranes of inorganic, polymer or composite systems. Because organic electrolytes usually have transport numbers below 0.5, inorganic lithium electrolytes have extremely high conductivities.

Motivation: Paper by N. Kamaya, *et. al* in ***Nature Materials*** **10**, 682-686 (2011)

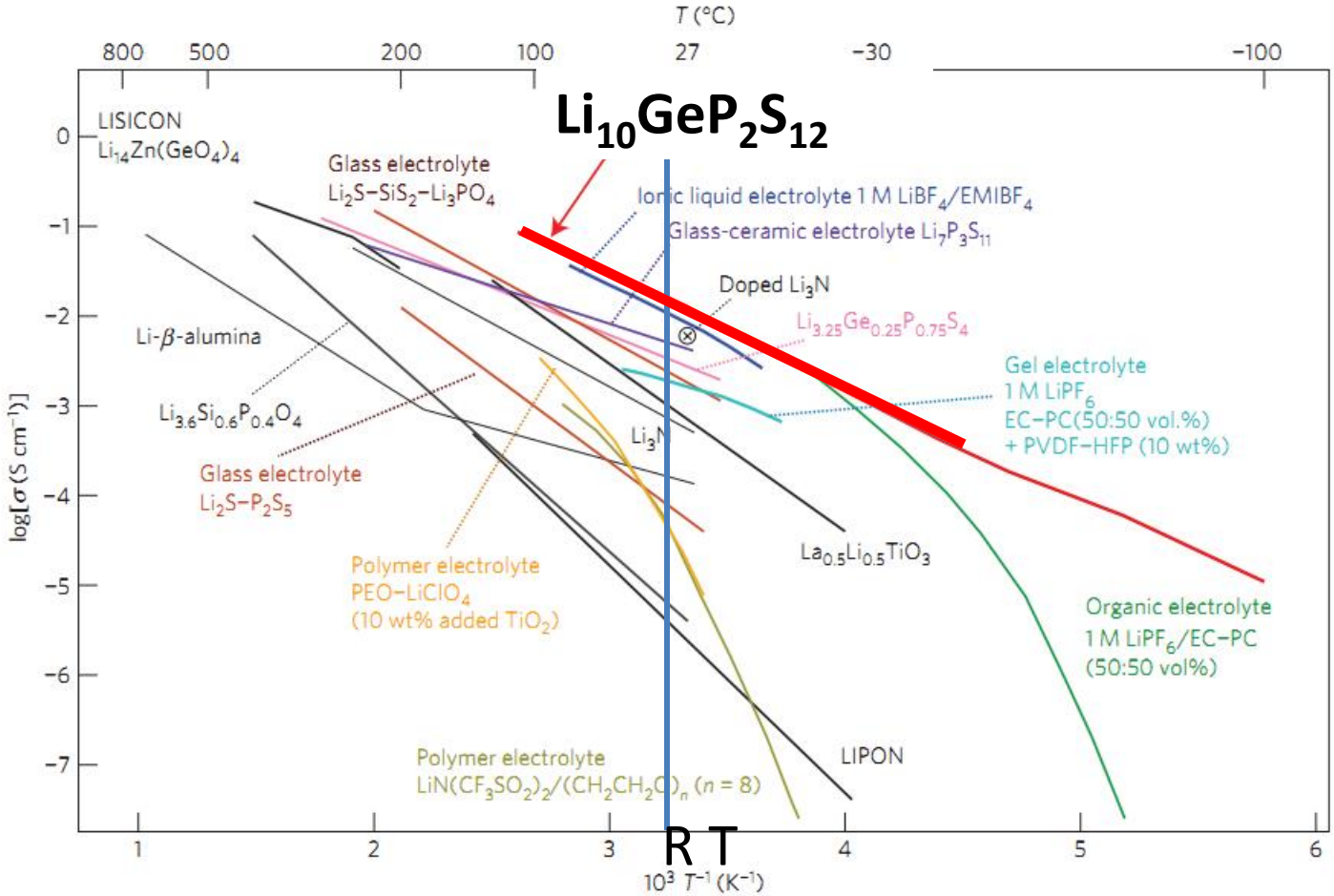

Figure 3 | Thermal evolution of ionic conductivity of the new $Li_{10}GeP_2S_{12}$ phase, together with those of other lithium solid electrolytes, organic liquid electrolytes, polymer electrolytes, ionic liquids and gel electrolytes[3-8,13-16,20,22]**.** The new $Li_{10}GeP_2S_{12}$ exhibits the highest lithium ionic conductivity (12 m S cm^{-1} at 27 °C) of the solid lithium conducting membranes of inorganic, polymer or composite systems. Because organic electrolytes usually have transport numbers below 0.5, inorganic lithium electrolytes have extremely high conductivities.

Solid Electrolyte Families Investigated in this Study:

$Li_xPO_yN_z$

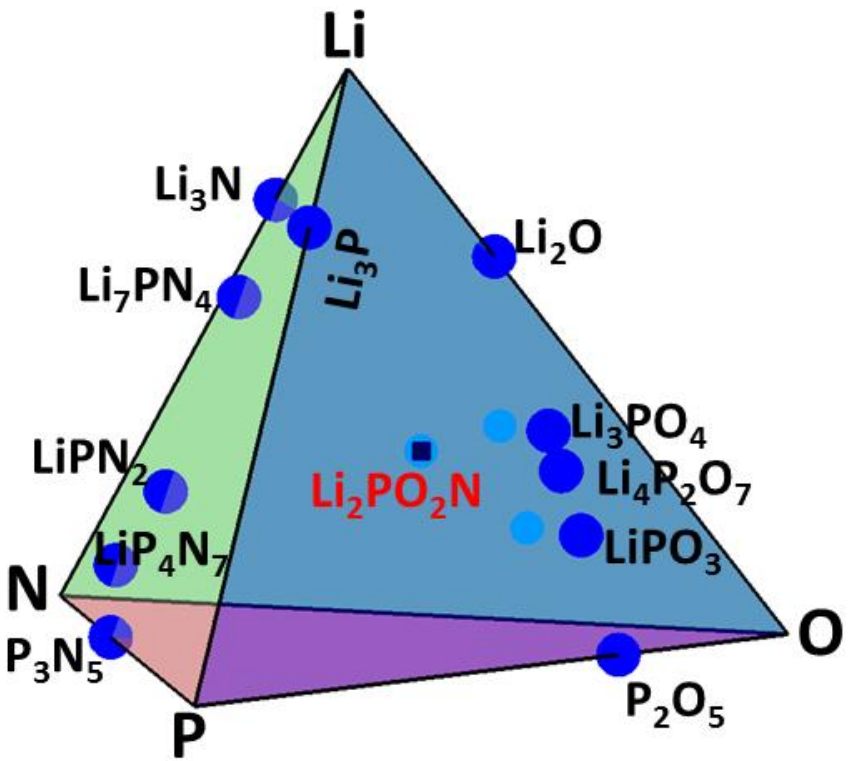

Li_xPS_y

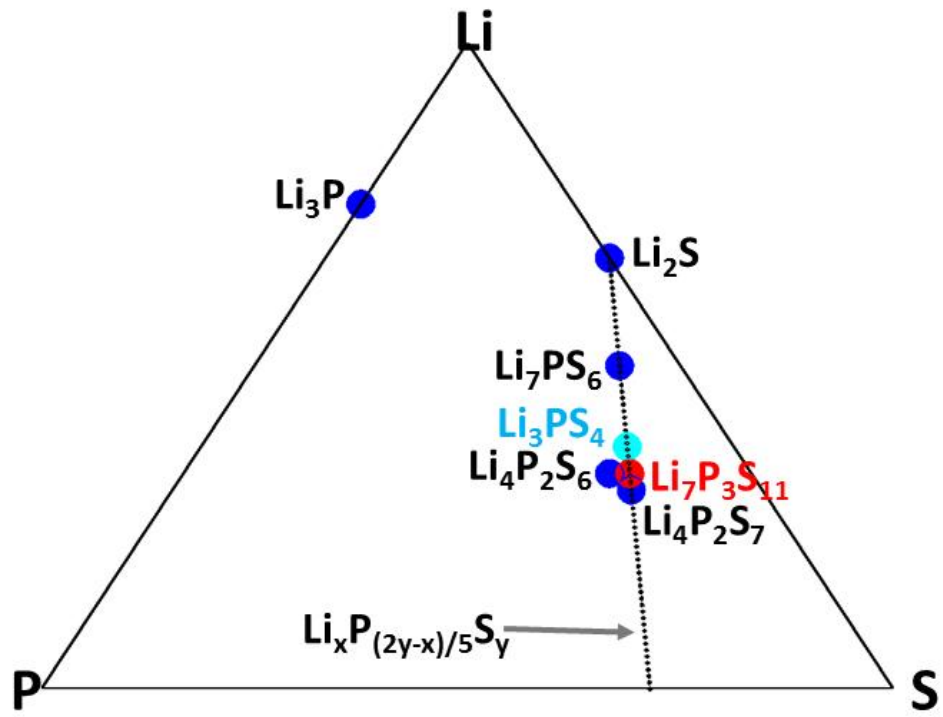

Computational tools

Summary of "first-principles" calculation methods

Electronic coordinates

Atomic coordinates

Exact Schrödinger equation:

$$\mathcal{H}(\{\mathbf{r}_i\},\{\mathbf{R}^a\})\Psi_\alpha(\{\mathbf{r}_i\},\{\mathbf{R}^a\}) = E_\alpha \Psi_\alpha(\{\mathbf{r}_i\},\{\mathbf{R}^a\})$$

where

$$\mathcal{H}(\{\mathbf{r}_i\},\{\mathbf{R}^a\}) = \mathcal{H}^{\text{Nuclei}}(\{\mathbf{R}^a\}) + \mathcal{H}^{\text{Electrons}}(\{\mathbf{r}_i\},\{\mathbf{R}^a\})$$

Born-Oppenheimer approximation

Born & Huang, **Dynamical Theory of Crystal Lattices**, Oxford (1954)

Approximate factorization:

$$\Psi_\alpha(\{\mathbf{r}_i\},\{\mathbf{R}^a\}) = X_\alpha^{\text{Nuclei}}(\{\mathbf{R}^a\})\Upsilon_\alpha^{\text{Electrons}}(\{\mathbf{r}_i\},\{\mathbf{R}^a\})$$

Treated with classical mechanics

Treated with density functional theory

Electronic Schrödinger equation:

$$\mathcal{H}^{\text{Electrons}}(\{\mathbf{r}_i\},\{\mathbf{R}^a\})\Upsilon_\alpha^{\text{Electrons}}(\{\mathbf{r}_i\},\{\mathbf{R}^a\}) = U_\alpha(\{\mathbf{R}^a\})\Upsilon_\alpha^{\text{Electrons}}(\{\mathbf{r}_i\},\{\mathbf{R}^a\})$$

$$\mathcal{H}^{\text{Electrons}}(\{\mathbf{r}_i\},\{\mathbf{R}^a\}) = -\frac{\hbar^2}{2m}\sum_i \nabla_i^2 - \sum_{a,i}\frac{Z^a e^2}{|\mathbf{r}_i - \mathbf{R}^a|} + \sum_{i<j}\frac{e^2}{|\mathbf{r}_i - \mathbf{r}_j|}$$

For electronic ground state: $\alpha \Rightarrow 0$

Density functional theory

Hohenberg and Kohn, *Phys. Rev*. **136** B864 (1964)
Kohn and Sham, *Phys. Rev*. **140** A1133 (1965)

Mean field approximation: $U_0(\{\mathbf{R}^a\}) \Rightarrow U_0(\{\rho(\mathbf{r})\},\{\mathbf{R}^a\})$

Electron density

Kohn-Sham construction: $\rho(\mathbf{r}) \approx \rho_K(\mathbf{r}) = \sum_n |\psi_n(\mathbf{r})|^2$

$$\mathcal{H}_{\text{KS}}^{\text{Electrons}}(\mathbf{r},\rho(\mathbf{r}),\{\mathbf{R}^a\})\psi_n(\mathbf{r}) = \varepsilon_n\psi_n(\mathbf{r})$$

Independent electron wavefunction

More computational details:

$$\mathcal{H}_{\mathrm{KS}}^{\mathrm{Electrons}}(\mathbf{r},\rho(\mathbf{r}),\{\mathbf{R}^a\}) = -\frac{\hbar^2\nabla^2}{2m} + \underbrace{\sum_a \frac{-Z^a e^2}{|\mathbf{r}-\mathbf{R}^a|}}_{\text{electron-nucleus}} + \underbrace{e^2\int d^3r'\frac{\rho(\mathbf{r}')}{|\mathbf{r}-\mathbf{r}'|}}_{\text{electron-electron}} + \underbrace{V_{xc}\left(\rho(\mathbf{r})\right)}_{\text{exchange-correlation}}$$

Exchange-correlation functionals:

LDA: J. Perdew and Y. Wang, Phys. Rev. B **45**, 13244 (1992)

GGA: J. Perdew, K. Burke, and M. Ernzerhof, PRL **77**, 3865 (1996)

HSE06: J. Heyd, G. E. Scuseria, and M. Ernzerhof, JCP **118**, 8207 (2003)

Numerical methods:

"Muffin-tin" construction: Augmented Plane Wave developed by Slater → "linearized" version by Andersen:

J. C. Slater, Phys. Rev. **51** 846 (1937)

O. K. Andersen, Phys. Rev. B **12** 3060 (1975) (LAPW)

Pseudopotential methods:

J. C. Phillips and L. Kleinman, Phys. Rev. **116** 287 (1959) -- original idea

P. Blöchl, Phys. Rev. B. 50 17953 (1994) – Projector Augmented Wave (PAW) method

Outputs of calculations:

Ground state energy:

$$U_0(\{\rho(\mathbf{r})\},\{\mathbf{R}^a\}) \quad \Rightarrow \quad \text{Determine formation energies}$$

$$\min\Big|_{\{\mathbf{R}^a\}}\left(U_0(\{\rho(\mathbf{r})\},\{\mathbf{R}^a\})\right) \quad \Rightarrow \quad \text{Determine structural parameters}$$

$$\Rightarrow \quad \text{Stable and meta-stable structures}$$

$$\rho(\mathbf{r}) = \sum_n |\psi_n(\mathbf{r})|^2 \quad \Rightarrow \quad \text{Self-consistent electron density}$$

$$\{\varepsilon_n\} \quad \Rightarrow \quad \text{One-electron energies; densities of states}$$

Nuclear Hamiltonian (usually treated classically)

$$\mathcal{H}^{\text{Nuclei}}\left(\{\mathbf{R}^a\}\right) = \sum_a \frac{\mathbf{P}^{a2}}{2M^a} + U_0(\{\rho(\mathbf{r})\},\{\mathbf{R}^a\})$$

➔ Normal modes of vibration

Codes used for calculations

Function	Code	Website
Generate atomic datasets	ATOMPAW	http://pwpaw.wfu.edu
DFT; optimize structure	PWscf abinit	http://www.quantum-espresso.org http://www.abinit.org
Structural visualization	XCrySDen VESTA	http://ww.xcrysden.org http://jp-minerals.org/vesta/en/

ATOMPAW Code for generating atomic datasets for PAW calculations

Holzwarth, Tackett, and Matthews, CPC 135 329 (2001) http://pwpaw.wfu.edu

- ATOMPAW
- INFO
- DATASETS
- CONTRIBUTERS
- CONTACT INFO
- NAWH Web
- PHYSICS Web
- WFU Web

ATOMPAW

Download source code and example files:

- atompaw-4.0.0.12.tar.gz (5.4mb) 12/23/2014: Slight update of new version of atompaw code. In additon to previous updates, added PBESOL output for Quantum Espresso interface and added interface for SOCORRO.
- atompaw-3.1.0.3.tar.gz (3.8mb) Updated version of *atompaw* code (01/03/2014 and 09/18/2013 -- Marc Torrent and Francois Jollet introduced improvements to the XML and abinit dataset generation routines; 07/09/2013 -- Marc Torrent introduced small corrections; 06/22/2013 -- Marc Torrent and Francois Jollet added a new option for outputting a file in XML format according to the specifications set up by the GPAW group . The output file format is controled by a menu at

Atomic PAW datasets

1 H																	2 He
3 Li	4 Be											5 B	6 C	7 N	8 O	9 F	10 Ne
11 Na	12 Mg											13 Al	14 Si	15 P	16 S	17 Cl	18 Ar
19 K	20 Ca	21 Sc	22 Ti	23 V	24 Cr	25 Mn	26 Fe	27 Co	28 Ni	29 Cu	30 Zn	31 Ga	32 Ge	33 As	34 Se	35 Br	36 Kr
37 Rb	38 Sr	39 Y	40 Zr	41 Nb	42 Mo	43 Tc	44 Ru	45 Rh	46 Pd	47 Ag	48 Cd	49 In	50 Sn	51 Sb	52 Te	53 I	54 Xe
55 Cs	56 Ba		72 Hf	73 Ta	74 W	75 Re	76 Os	77 Ir	78 Pt	79 Au	80 Hg	81 Tl	82 Pb	83 Bi	84 Po	85 At	86 Rn

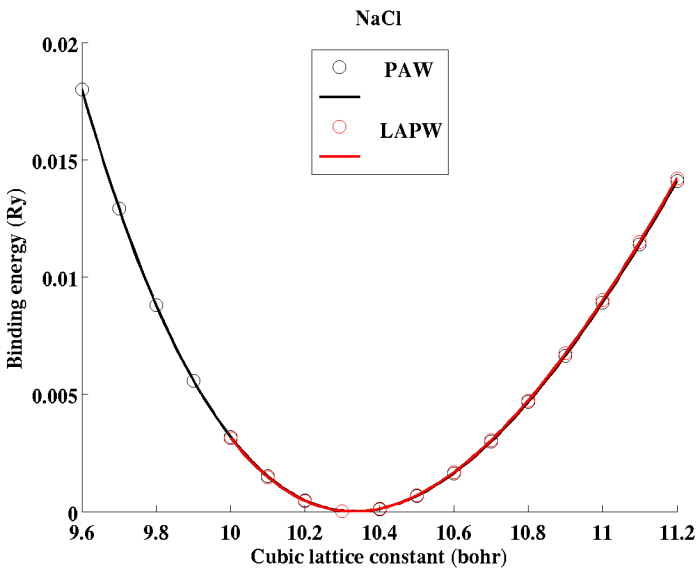

1 H																	2 He
3 Li	4 Be											5 B	6 C	7 N	8 O	9 F	10 Ne
11 Na	12 Mg											13 Al	14 Si	15 P	16 S	17 Cl	18 Ar
19 K	20 Ca	21 Sc	22 Ti	23 V	24 Cr	25 Mn	26 Fe	27 Co	28 Ni	29 Cu	30 Zn	31 Ga	32 Ge	33 As	34 Se	35 Br	36 Kr
37 Rb	38 Sr	39 Y	40 Zr	41 Nb	42 Mo	43 Tc	44 Ru	45 Rh	46 Pd	47 Ag	48 Cd	49 In	50 Sn	51 Sb	52 Te	53 I	54 Xe
55 Cs	56 Ba		72 Hf	73 Ta	74 W	75 Re	76 Os	77 Ir	78 Pt	79 Au	80 Hg	81 Tl	82 Pb	83 Bi	84 Po	85 At	86 Rn

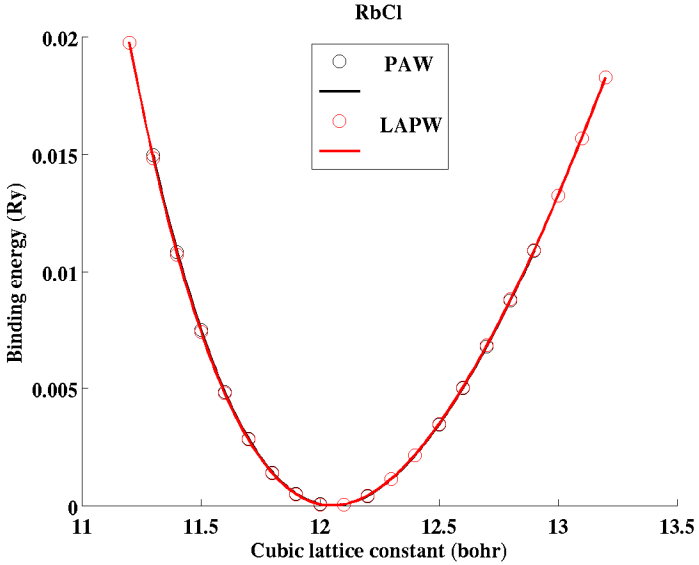

Validation

Li_3PO_4 crystals

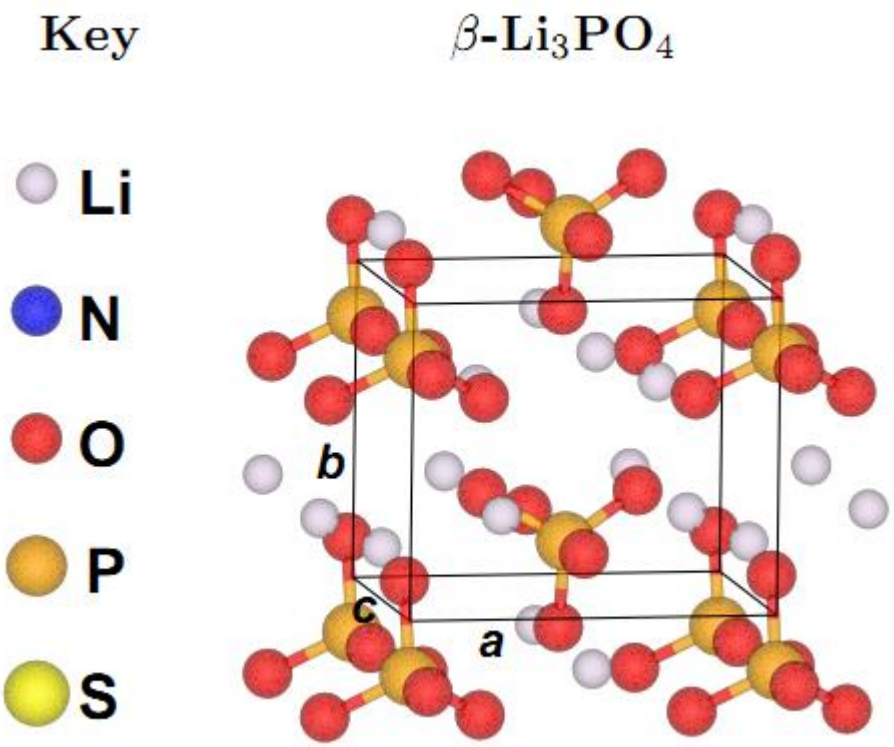

(Pmn2$_1$)

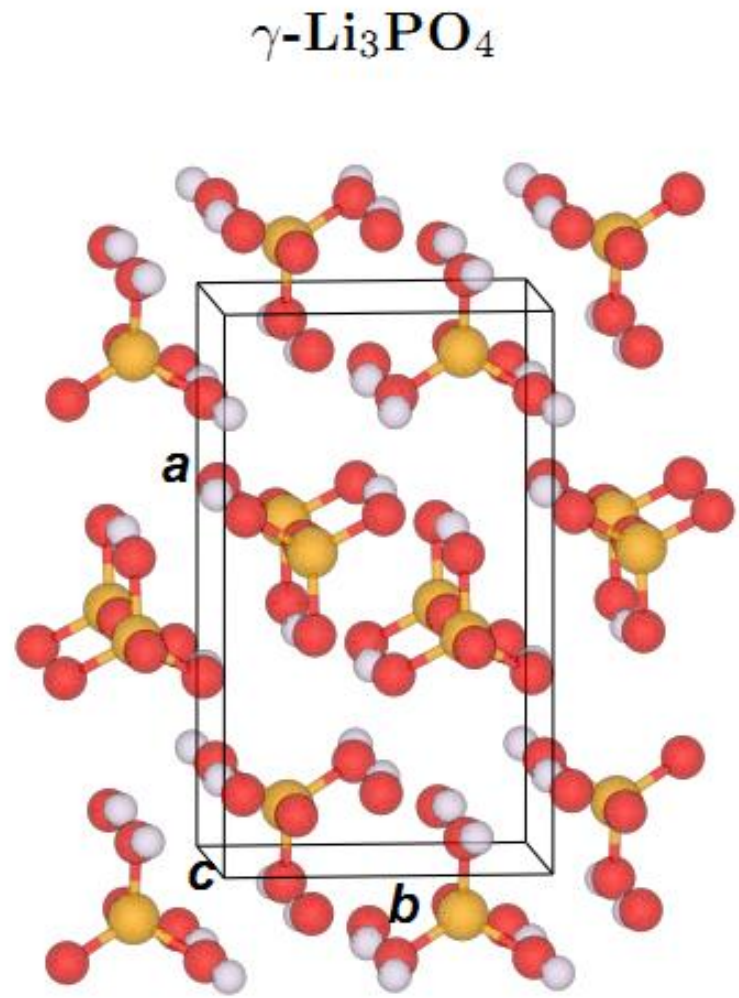

(Pnma)

Validation of calculations

Raman spectra – Experiment & Calculation

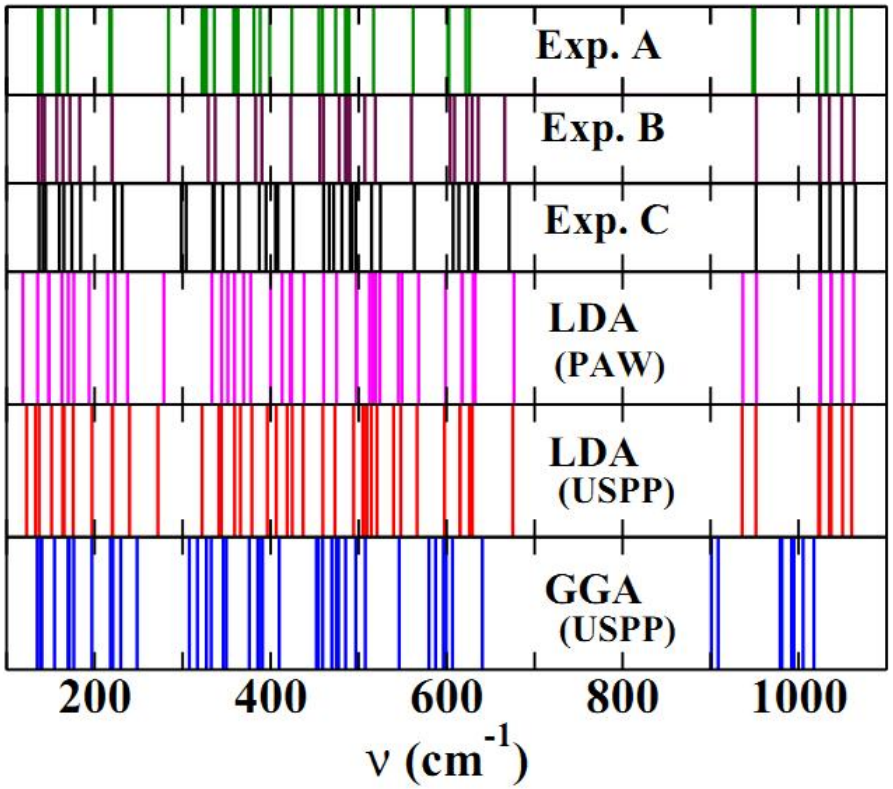

γ-Li_3PO_4

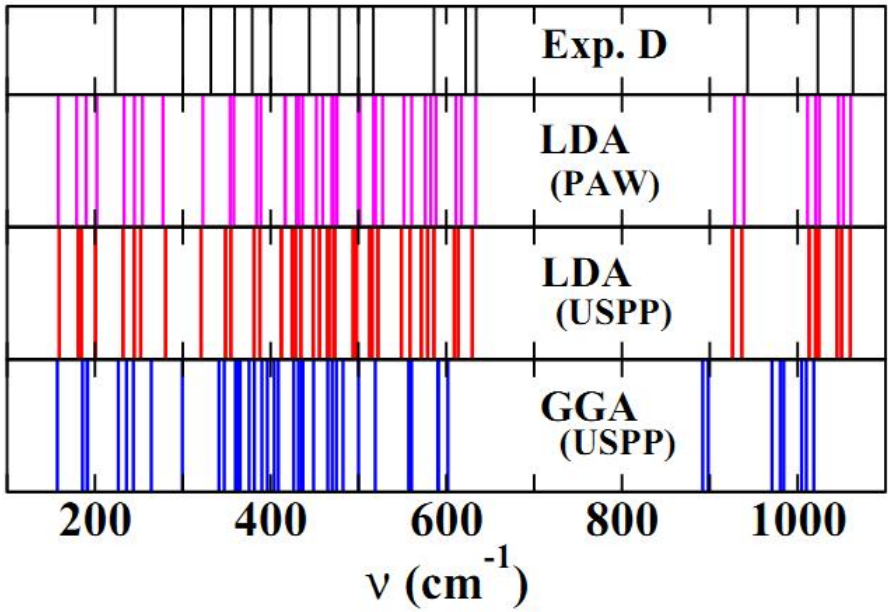

β-Li_3PO_4

A: B. N. Mavrin et al, J. Exp. Theor. Phys. **96**,53 (2003); B: F. Harbach and F. Fischer, Phys. Status Solidi B **66**, 237 (1974) – room temp. C: Ref. B at liquid nitrogen temp.; D: L. Popović et al, J. Raman Spectrosc. **34**,77 (2003).

Heats of formation – Experiment & Calculation

Table 1. Calculated heats of formation for Li phosphates, phospho-nitrides, and thiophosphates and related materials. The structural designation uses the the notation defined in the International Table of Crystallography[85] based on structural information reported in the International Crystal Structure Database.[86] The heats of formation ΔH (eV/FU) are given in units of eV per formula unit. When available from Ref. [31] and [32] experiment values are indicated in parentheses. Those indicated with "*" were used fitting the O and N reference energies as explained in the text.

Material	Structure	ΔH (eV/FU)
β-Li_3PO_4	$Pmn2_1$ (#31)	-21.23
γ-Li_3PO_4	$Pnma$ (#62)	-21.20 (-21.72*)
γ-Li_3PS_4	$Pmn2_1$ (#31)	- 8.37
β-Li_3PS_4	$Pnma$ (#62)	- 8.28
$Li_4P_2O_6$	$P\bar{3}1m$ (#162)	-29.72
$Li_4P_2O_7$	$P\bar{1}$ (#2)	-33.97
$Li_5P_2O_6N$	$P\bar{1}$ (#2)	-33.18
$Li_4P_2S_6$	$P\bar{3}1m$ (#162)	-12.42
$Li_4P_2S_7$	$P\bar{1}$ (#2)	-11.59
$Li_7P_3O_{11}$	$P\bar{1}$ (#2)	-54.84
$Li_7P_3S_{11}$	$P\bar{1}$ (#2)	-20.01
$LiPO_3$	$P2/c$ (#13)	-12.75
$LiPN_2$	$I\bar{4}2d$ (#122)	- 3.65
$s1$-Li_2PO_2N	$Pbcm$ (#57)	-12.35
SD-Li_2PO_2N	$Cmc2_1$ (#36)	-12.47
SD-Li_2PS_2N	$Cmc2_1$ (#36)	- 5.80

Material	Structure	ΔH (eV/FU)
N_2O_5	$P6_3/mmc$ (#194)	- 0.94 (- 0.45*)
P_3N_5	$C2/c$ (#15)	- 3.02 (- 3.32*)
h-P_2O_5	$R3c$ (#161)	-15.45 (-15.53*)
o-P_2O_5	$Fdd2$ (#43)	-15.78
P_2S_5	$P\bar{1}$ (#2)	- 1.93
P_4S_3	$Pnma$ (#62)	- 2.45 (- 2.33)
SO_3	$Pna2_1$ (#33)	- 4.84 (- 4.71*)
Li_3N	$P6/mmm$ (#191)	- 1.60 (- 1.71*)
Li_2O	$Fm\bar{3}m$ (#225)	- 6.10 (- 6.20*)
Li_2O_2	$P6_3/mmc$ (#194)	- 6.35 (- 6.57*)
Li_3P	$P6_3/mmc$ (#194)	- 3.47
Li_2S	$Fm\bar{3}m$ (#225)	- 4.30 (- 4.57)
Li_2S_2	$P6_3/mmc$ (#194)	- 4.09
$LiNO_3$	$R\bar{3}c$ (#167)	- 5.37 (- 5.01*)
Li_2SO_4	$P2_1/c$ (#14)	-14.63 (-14.89*)

Estimate of ionic conductivity assuming activated hopping

Schematic diagram of minimal energy path

Approximated using NEB algorithm[a]
– "Nudged Elastic Band"

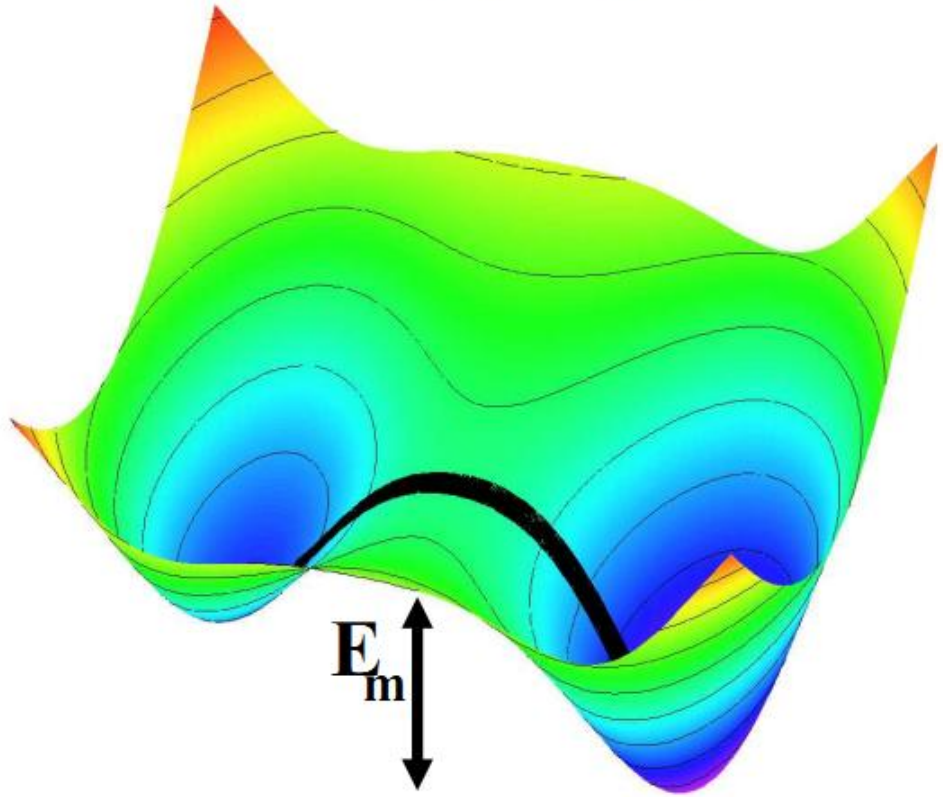

[a] Henkelman and Jónsson, *JCP* **113**, 9978 (2000)

Arrhenius relation

$$\sigma \cdot T = K e^{-E_A/kT}$$

From: Ivanov-Shitz and co-workers, *Cryst. Reports* **46**, 864 (2001):

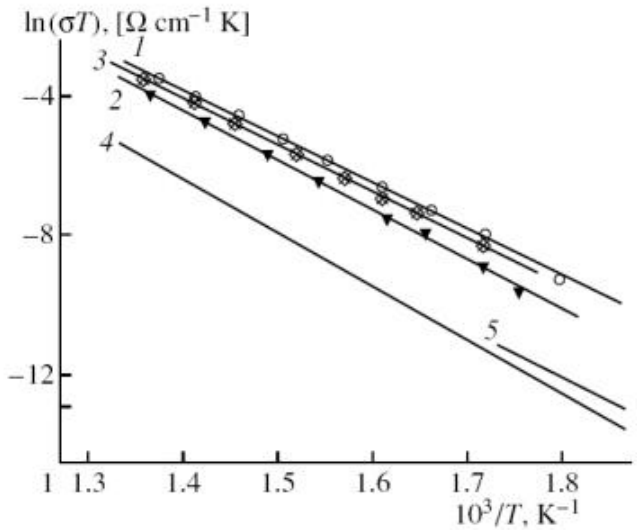

Fig. 2. Temperature dependences of conductivity in γ-Li_3PO_4: (*1–3*) for single crystals measured along the (*1*) *a*-axis, (*2*) *b*-axis, (*3*) *c*-axis and (*4, 5*) for a polycrystal (*4*) according to [4, 5] and (*5*) according to [7].

E_A = 1.14, 1.23, 1.14, 1.31, 1.24 eV for 1,2,3,4,5, respectively.

Arrhenius activation energies – Experiment and Calculation

Table 3. Calculated migration energies (E_m^{cal}) for Li ion vacancies (vac) and interstitials (int), vacancy-interstitial formation energies (E_f^{cal}), and corresponding the activation energies (E_A^{cal}) for crystalline materials computed using the NEB method in idealized supercells. When available, experimental activation energies E_A^{exp} are also listed together with additional information including the literature reference indicated in [ ] brackets. For γ-Li_3PO_4, results for different crystallographic directions are quoted to compare with single crystal experiment; in other cases, only the minimum energies are given. All energies are given in eV.

Material	vac E_m^{cal}	int E_m^{cal}	E_f^{cal}	E_A^{cal}	E_A^{exp}	Reference
β-Li_3PO_4	0.7	0.4	2.1	1.4		
γ-Li_3PO_4	0.7, 0.7	0.4, 0.3	1.7	1.3, 1.1	1.23, 1.14	(sngl. cryst.) [100]
$Li_{2.88}PO_{3.73}N_{0.14}$					0.97	(poly cryst.) [58]
$Li_{3.3}PO_{3.9}N_{0.17}$					0.56	(amorphous) [58]
$Li_{1.35}PO_{2.99}N_{0.13}$					0.60	(amorphous) [101]
$LiPO_3$	0.6	0.7	1.2	1.2	1.4	(poly cryst.) [97]
					0.76-1.2	(amorphous) [97]
$LiPN_2$	0.4		2.5	1.7	0.6	(poly cryst.) [99]
SD-Li_2PO_2N	0.4	0.8	2.0	1.4	0.6	(poly cryst.) [52]
γ-Li_3PS_4	0.3		0.8	0.7	0.5	(poly cryst.) [102]
β-Li_3PS_4	0.2		0.0	0.2	0.4	(nano cryst.) [103]
$Li_7P_3S_{11}$	0.2	0.5	0.0	0.2	0.1	(poly cryst.) [76]

➢What is meant by "first principles"?

A series of well-controlled approximations

- ❑ Born-Oppenheimer Approximation
- ❑ Density Functional Approximation
- ❑ Local density Approximation (LDA)
- ❑ Numerical method: Projector Augmented Wave

Validation

- ❑ Lattice vibration modes
- ❑ Heats of formation
- ❑ Activation energies for lattice migration

How can computer simulations contribute to the development of materials?

- Computationally examine known materials and predict new materials and their properties
  - Structural forms
  - Relative stabilities
  - Direct comparisons of simulations and experiment
  - Investigate properties that are difficult to realize experimentally including

Of particular interest in battery materials --

- Model ion migration mechanisms
  - Vacancy migration
  - Interstitial migration
  - Vacancy-interstitial formation energies
- Model ideal electrolyte interfaces with anodes

Systematic study of LiPON materials – $Li_xPO_yN_z$ – (Yaojun A. Du and N. A. W. Holzwarth, Phys. Rev. B 81, 184106 (2010))

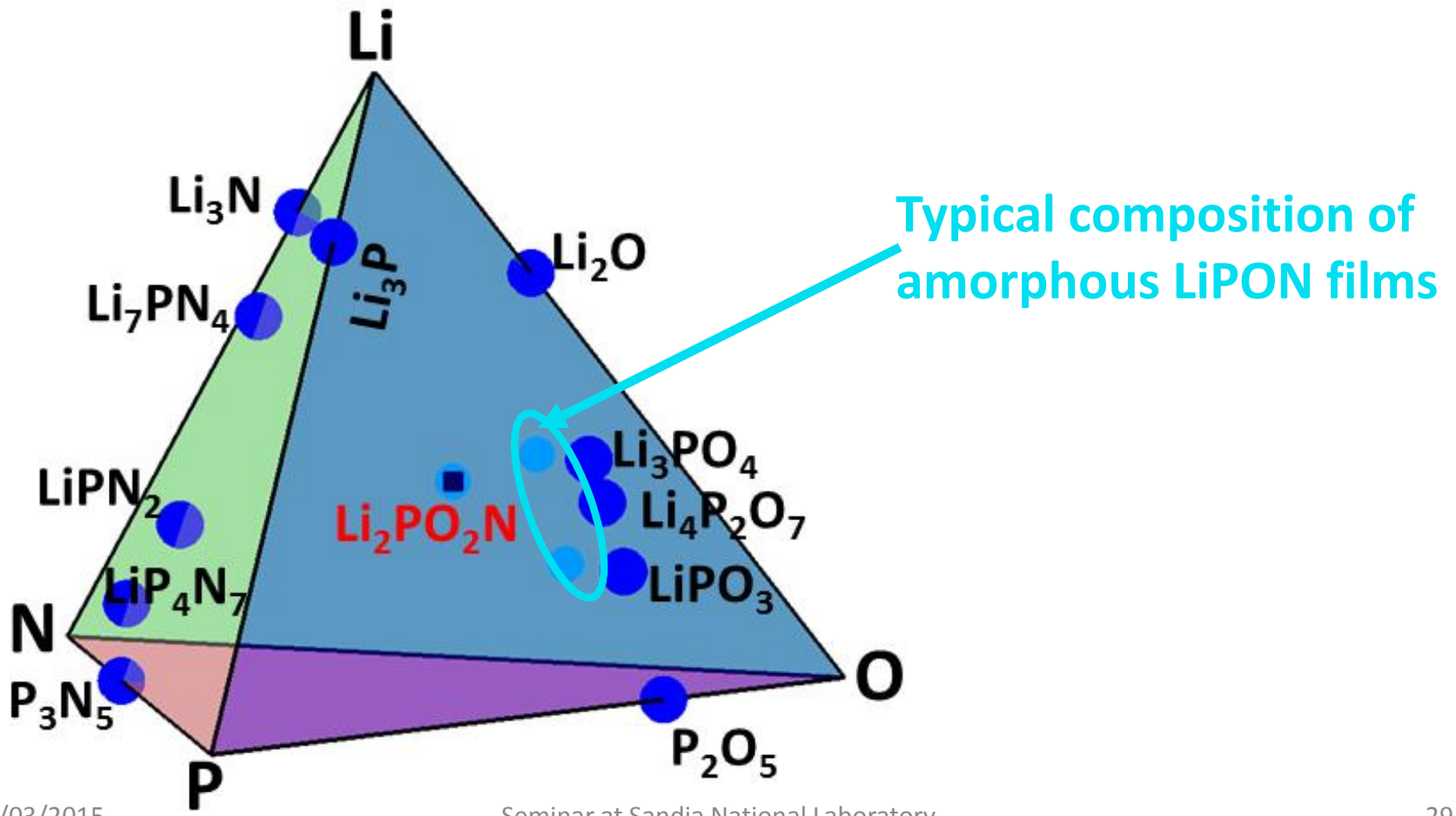

Experimentally known structure

$LiPO_3$

Computationally predicted structure

s_1-Li_2PO_2N

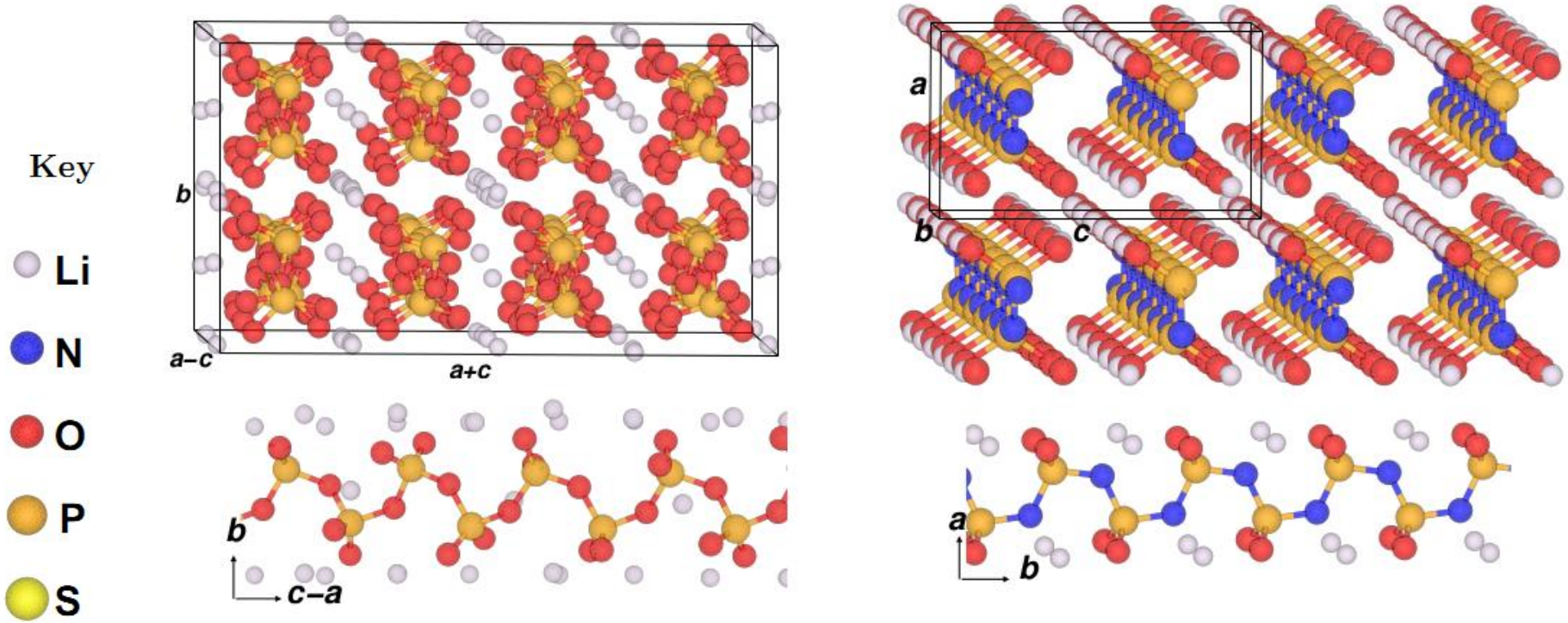

Fig. 7. Ball and stick diagrams for $LiPO_3$ in the $P2/c$ structure (20 formula units per unit cell) and $s1$-Li_2PO_2N in the $Pbcm$ structure (4 formula units per unit cell) from the calculated results. For each crystal diagram, a view of a horizontal chain axis is also provided for a single phosphate or phospho-nitride chain.

Computationally predicted structure

Experimentally realized structure

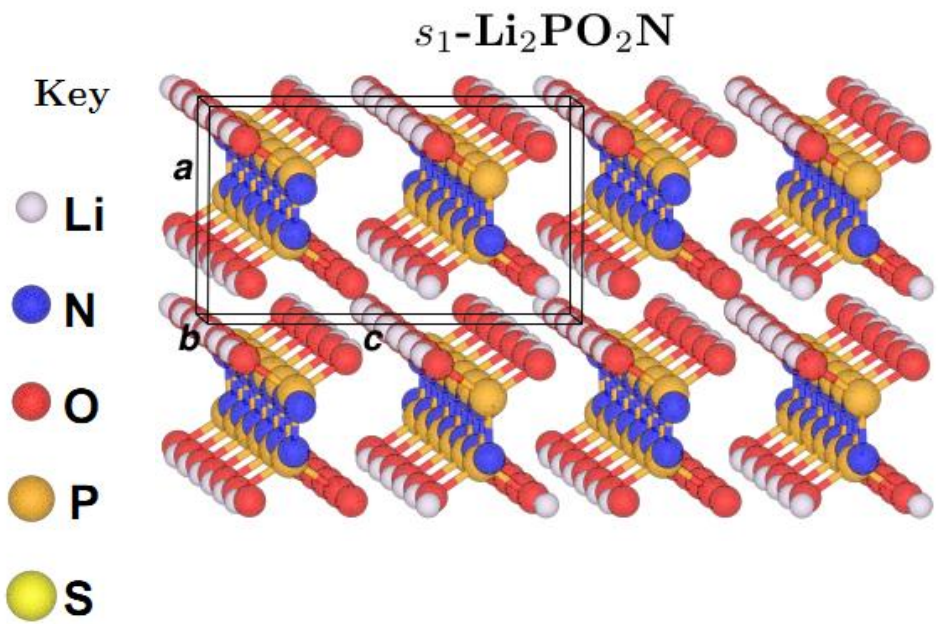

***SD*-Li_2PO_2N**

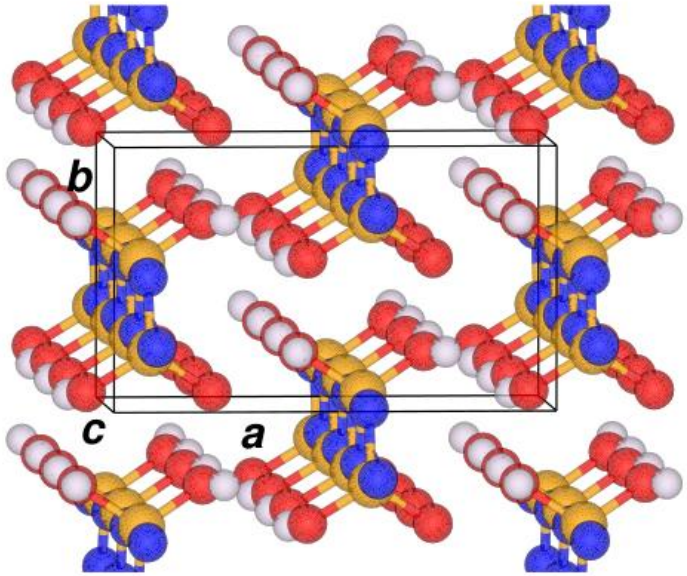

Pbcm

Cmc2$_1$

Synthesis of Li_2PO_2N by Keerthi Senevirathne, Cynthia Day, Michael Gross, and Abdessadek Lachgar

Method: High temperature solid state synthesis based on reaction

$$Li_2O + \tfrac{1}{5}P_2O_5 + \tfrac{1}{5}P_3N_5 \rightarrow Li_2PO_2N$$

Structure from X-ray refinement: $Cmc2_1$

Li P O N

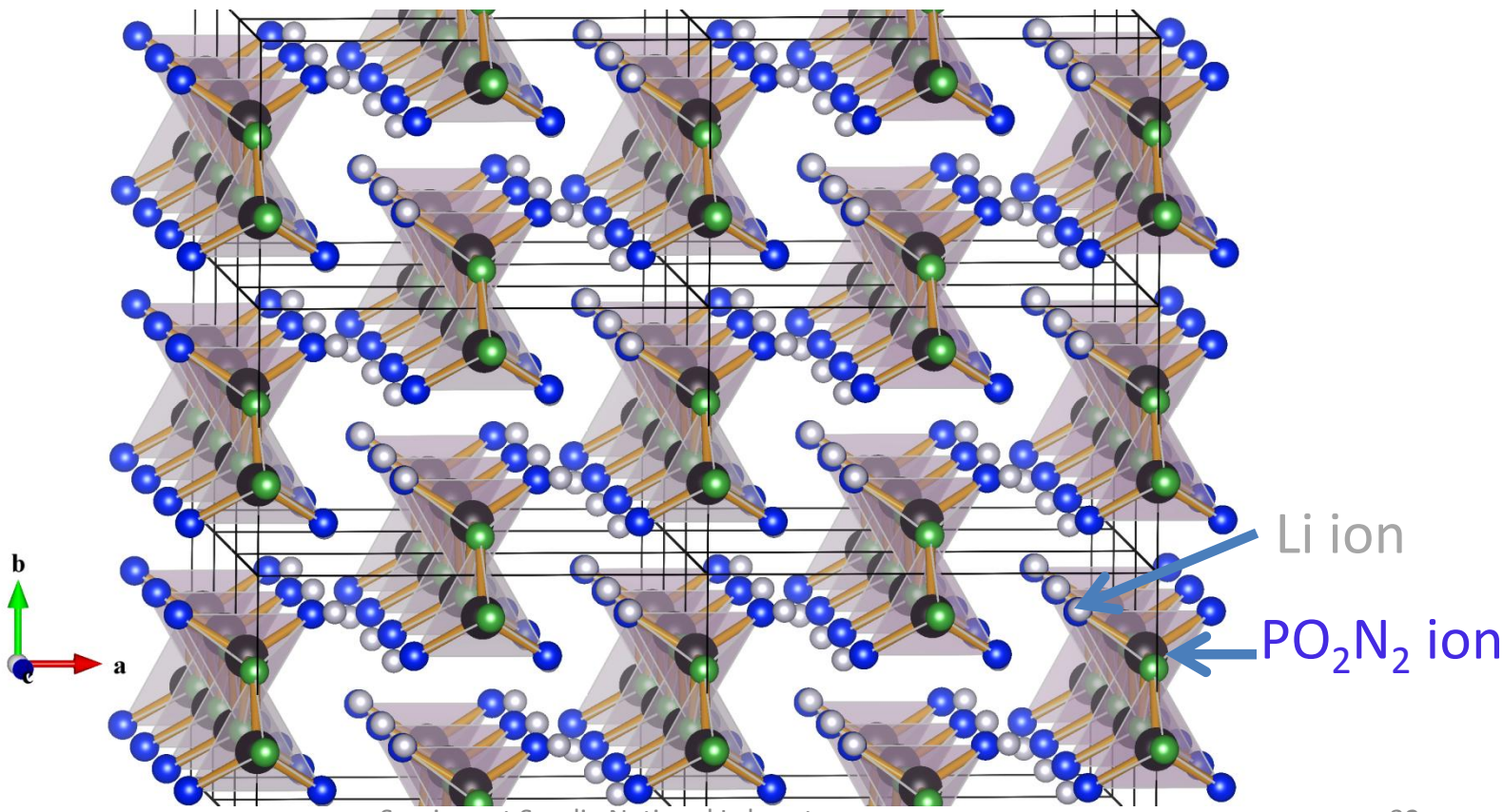

Comparison of synthesized and predicted structures of Li_2PO_2N:

Synthesized

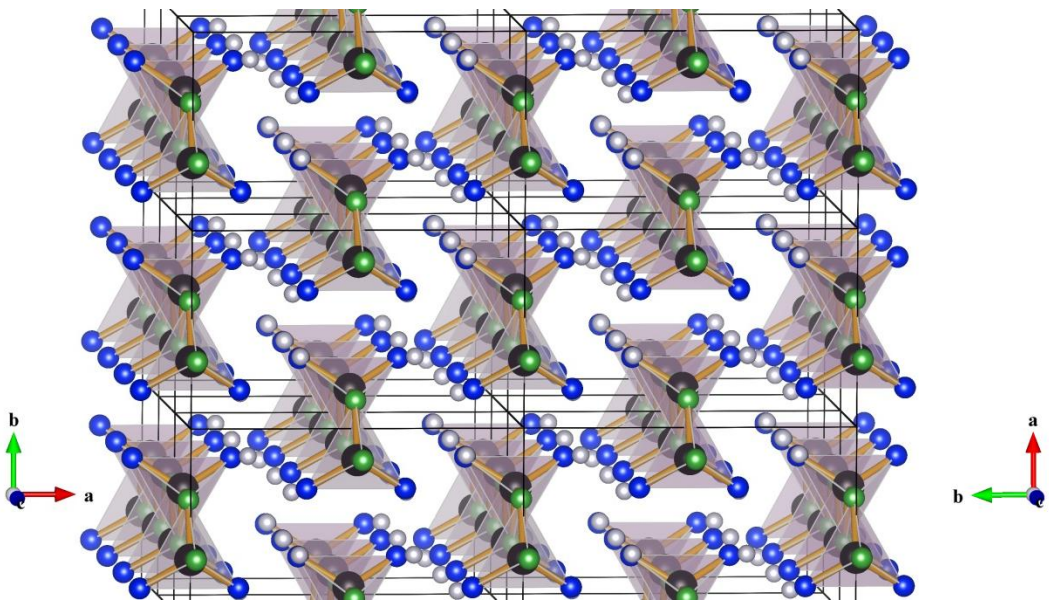

***SD*-Li_2PO_2N (*Cmc2$_1$*)**

Predicted

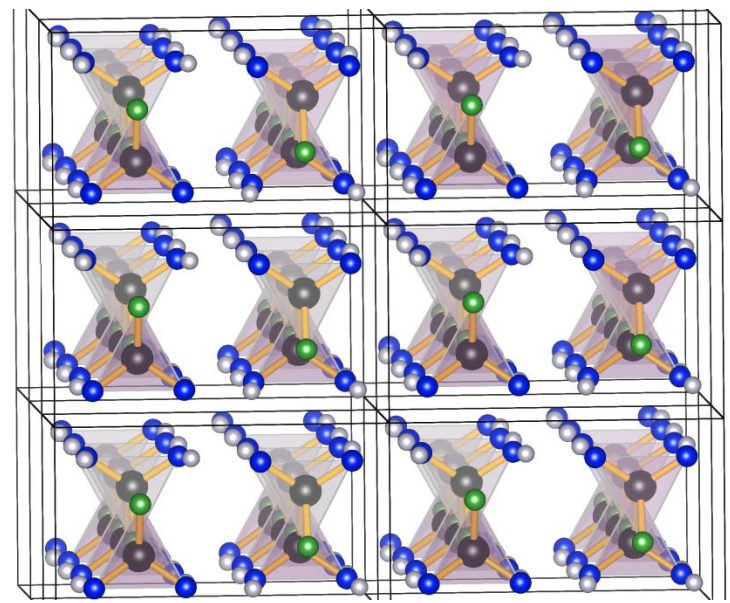

***s$_2$*-Li_2PO_2N (*Aem2*)**

Li P O N

Calculations have now verified that the SD structure is more stable than the s_2 structure by 0.1 eV/FU.

Comparison of synthesized Li_2PO_2N with Li_2SiO_3

***SD*-Li_2PO_2N (*Cmc2$_1$*)**

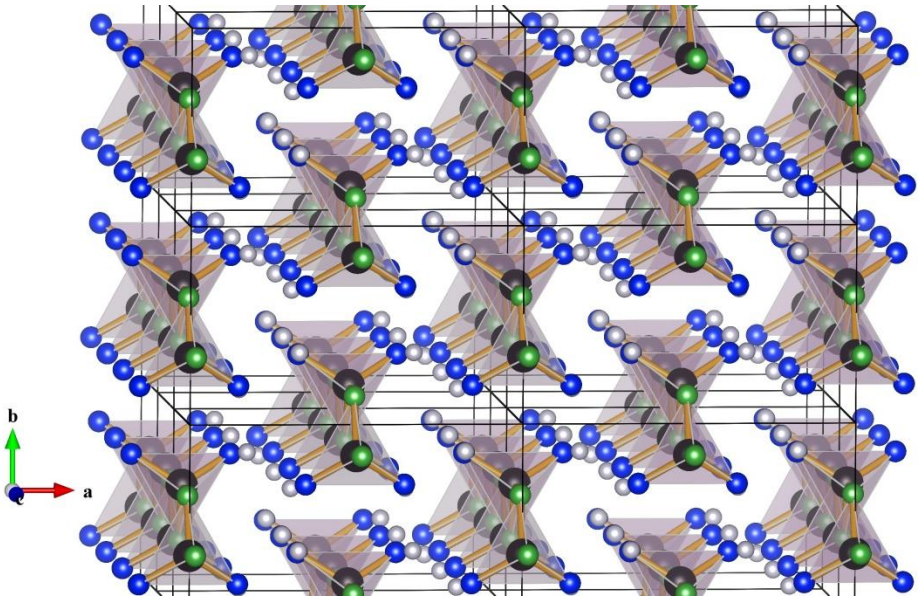

a=9.07 Å, b=5.40 Å, c=4.60 Å

Li_2SiO_3 (*Cmc2$_1$*)

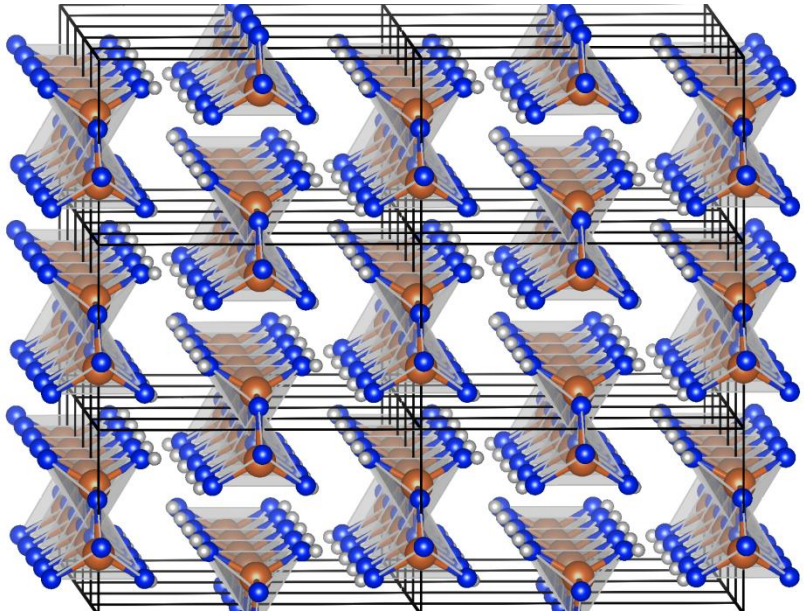

a=9.39 Å, b=5.40 Å, c=4.66 Å

K.-F. Hesse, Acta Cryst. B33, 901 (1977)

Li P O N Si

Electronic band structure of *SD*-Li_2PO_2N

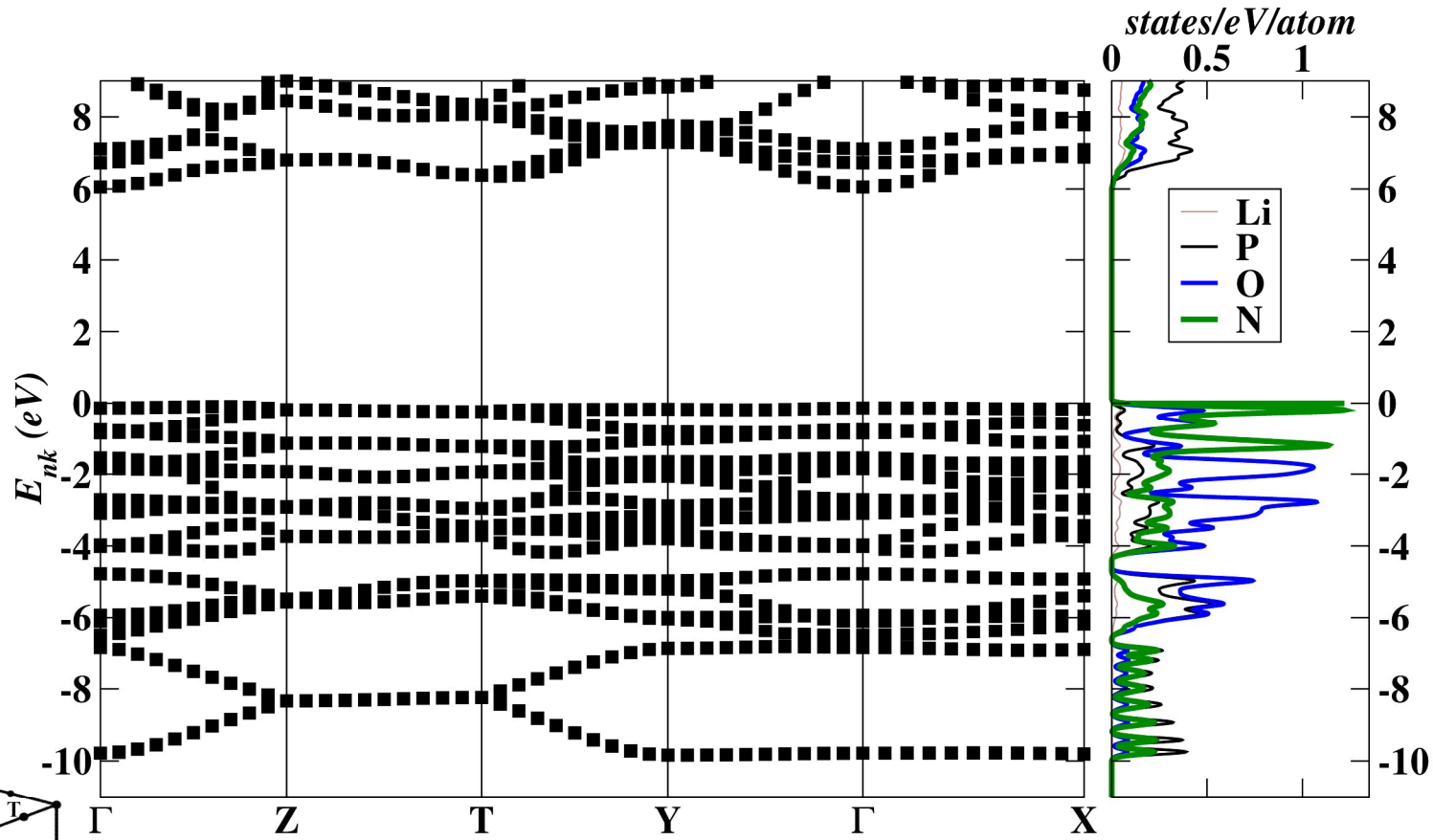

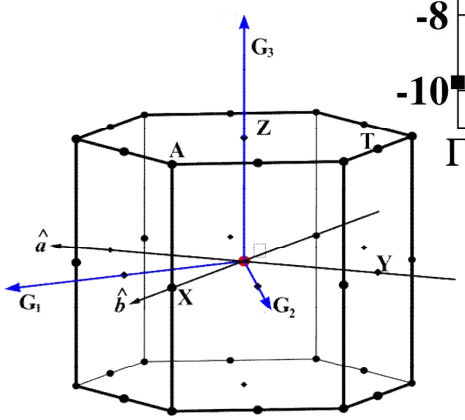

More details of *SD*-Li_2PO_2N structure

Ball and stick model

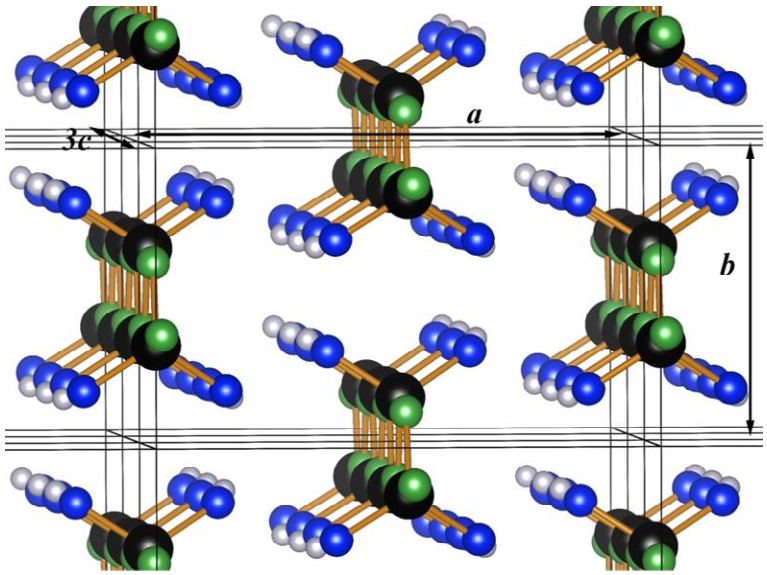

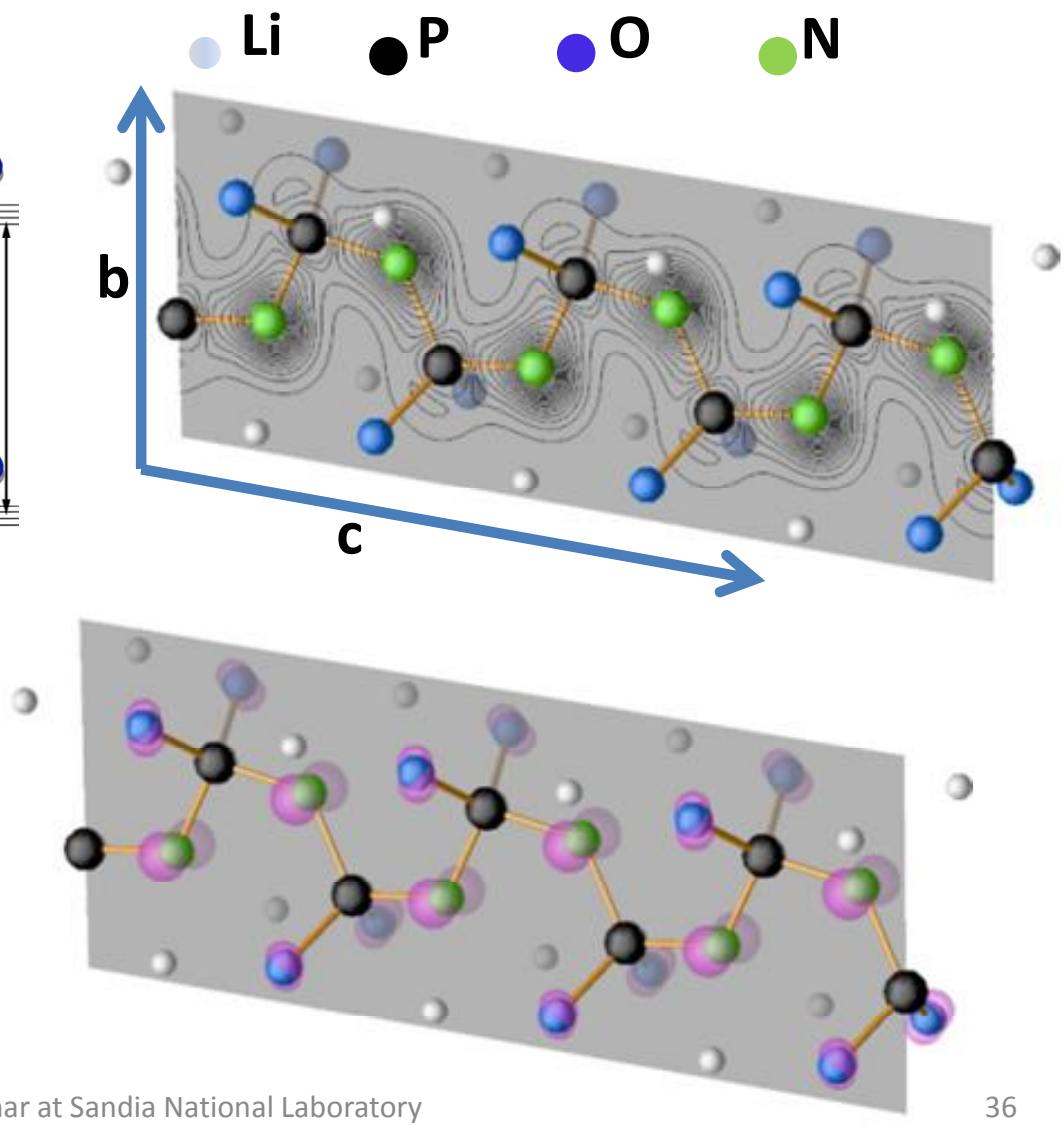

Isosurfaces (maroon) of charge density of states at top of valence band, primarily π states on N.

Vibrational spectrum of *SD*-Li_2PO_2N

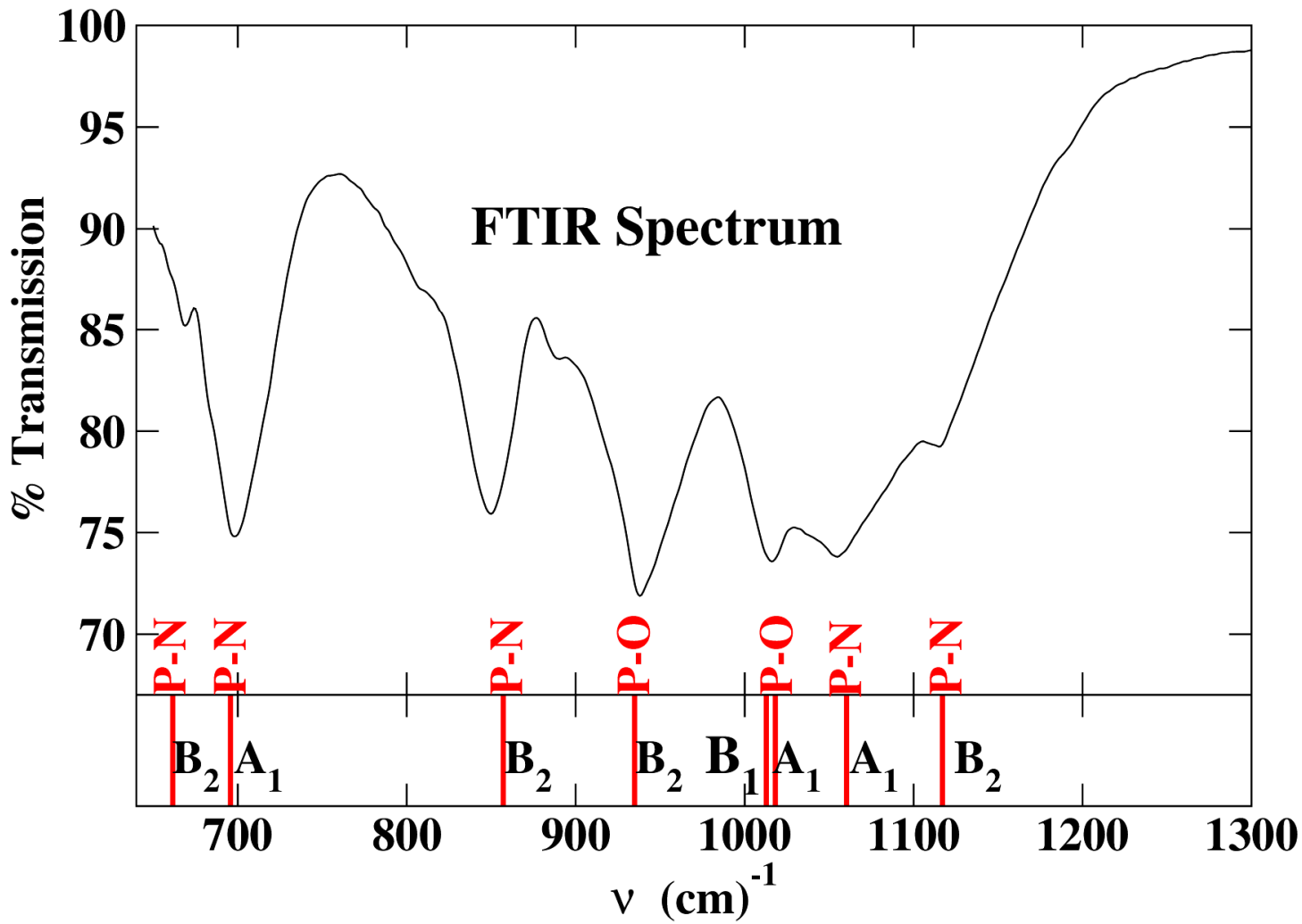

Stability of *SD*-Li_2PO_2N in air

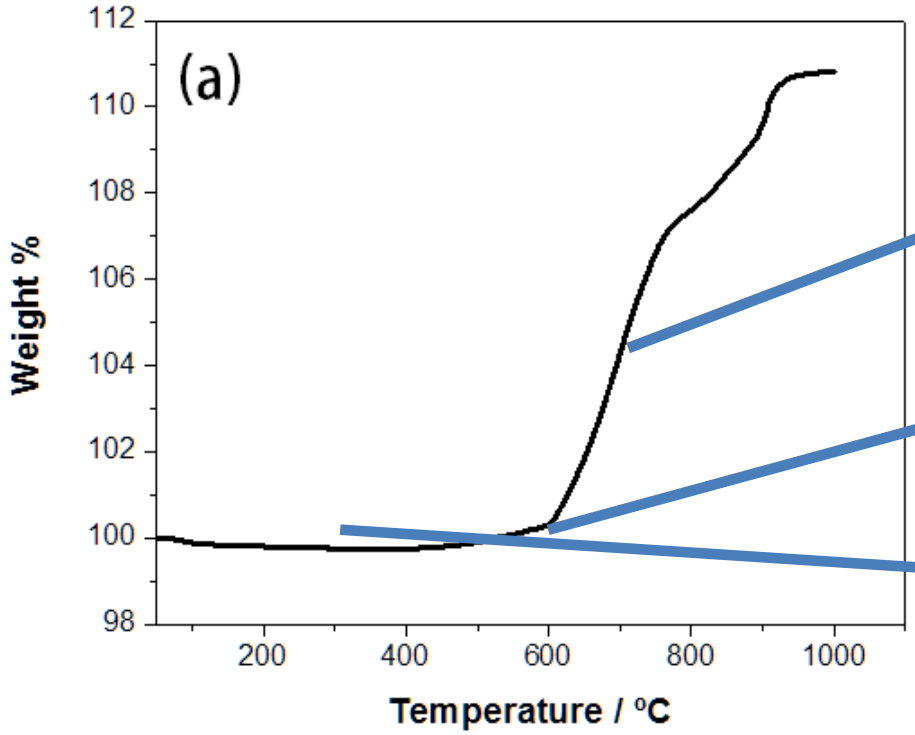

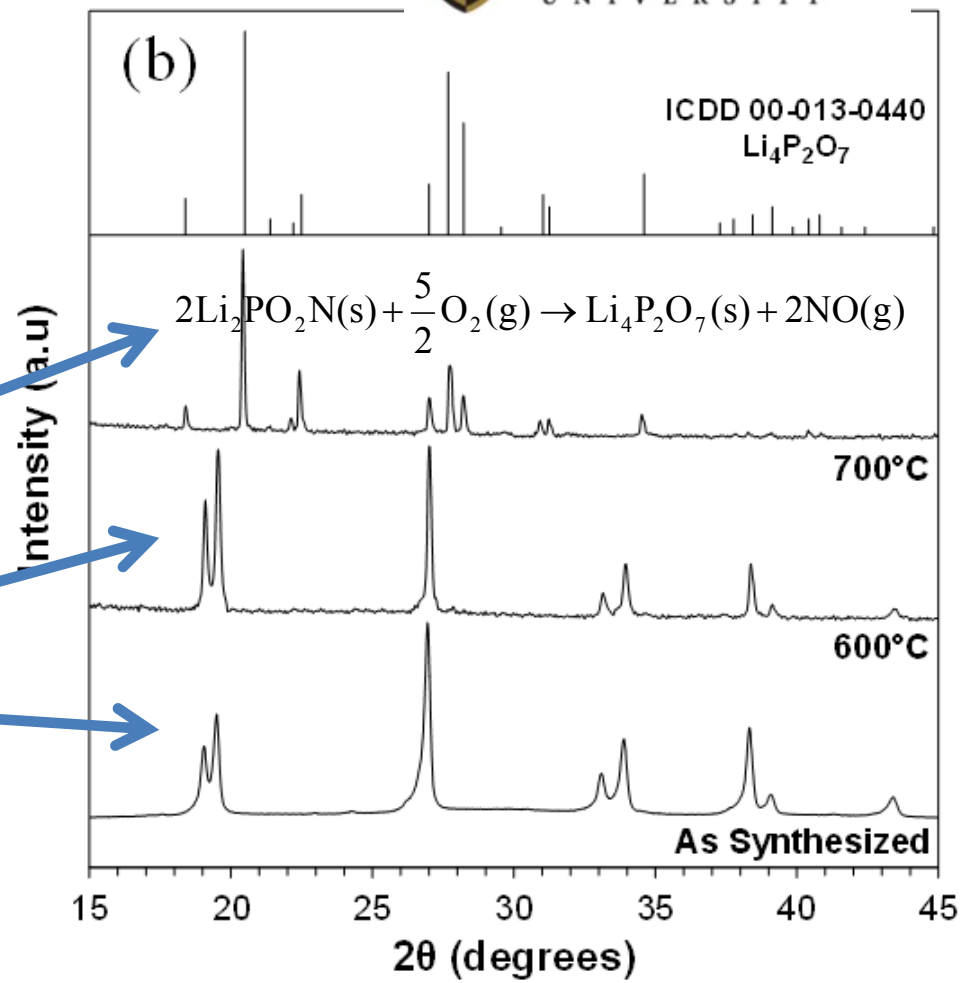

Thermogravimetric analysis curve in air

Note: no structural changes were observed while heating in vacuum up to 1050° C.

Ionic conductivity of *SD*-Li_2PO_2N

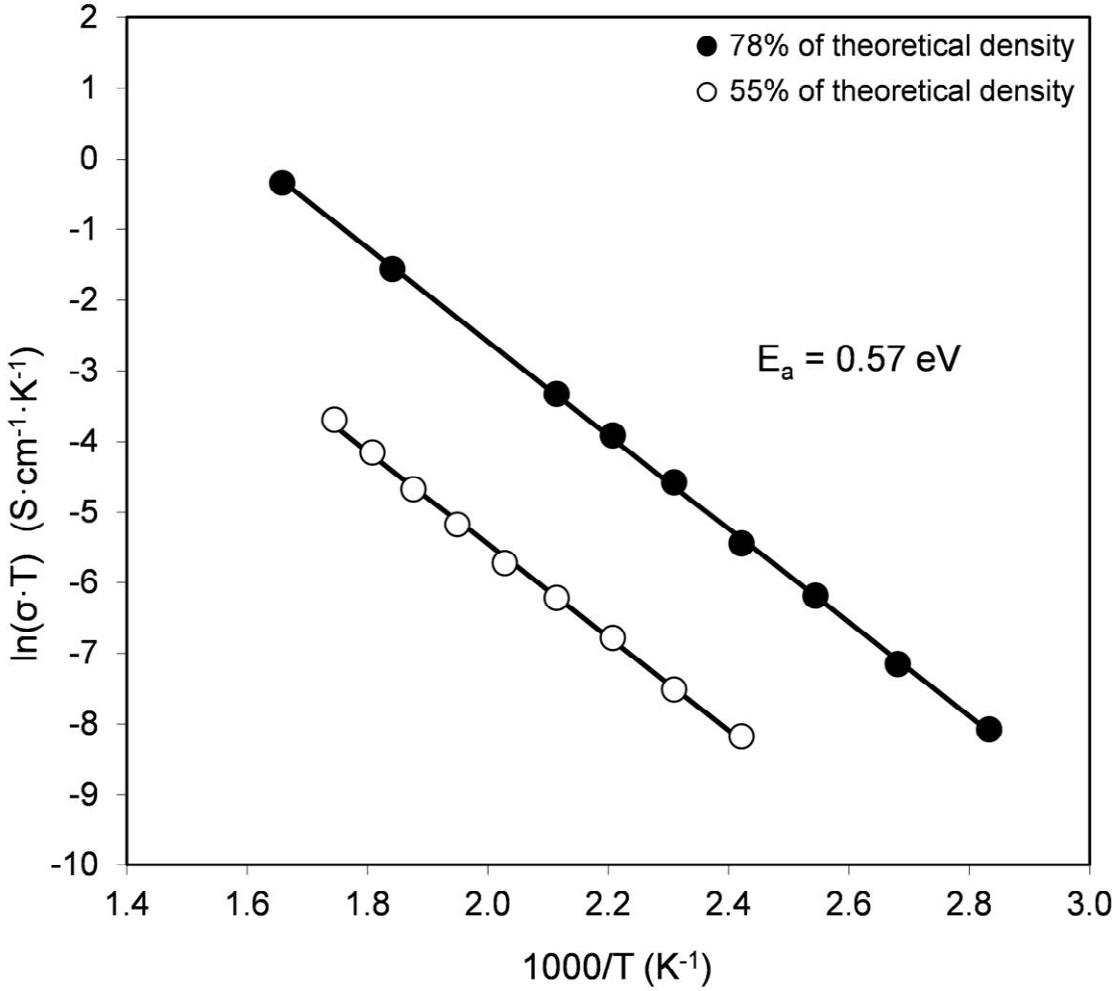

$$\sigma \approx 10^{-6}\ \text{S/cm} \quad \text{at } 80^{o}\ \text{C}$$

NEB analysis of E_m (vacancy mechanism)

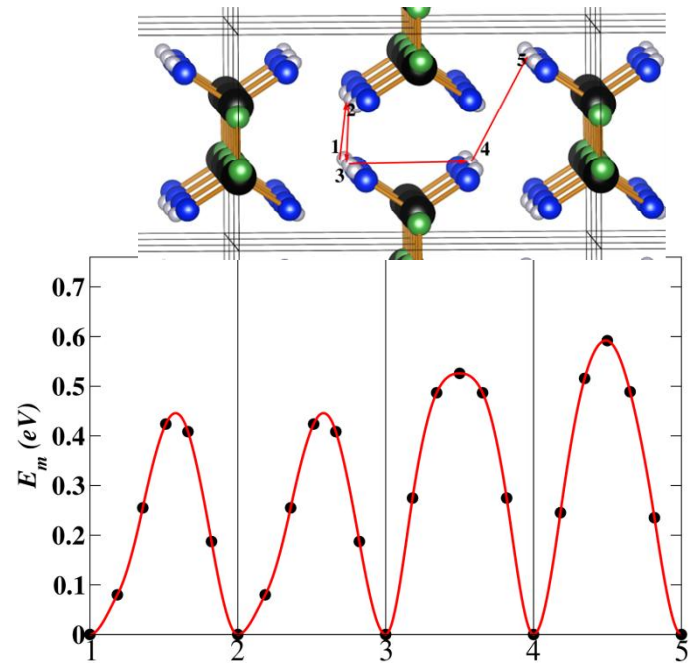

$$E_m \approx 0.4\ \text{eV}; E_f \approx 2\ \text{eV}$$

$$\Rightarrow E_A = E_m + \tfrac{1}{2}E_f \approx 1.4\ \text{eV}$$

➔Sample has appreciable population of vacancies

Summary of the Li_2PO_2N story

- Predicted on the basis of first principles theory
- Subsequently, experimentally realized by Keerthi Senevirathne and colleagues; generally good agreement between experiment and theory
- Ion conductivity properties not (yet) competitive

Systematic study of Li_xPS_y materials – (N. D. Lepley and N. A. W. Holzwarth, J. Electrochem. Soc. 159, A538 (2012), Phys. Rev. B 88, 104103 (2013))

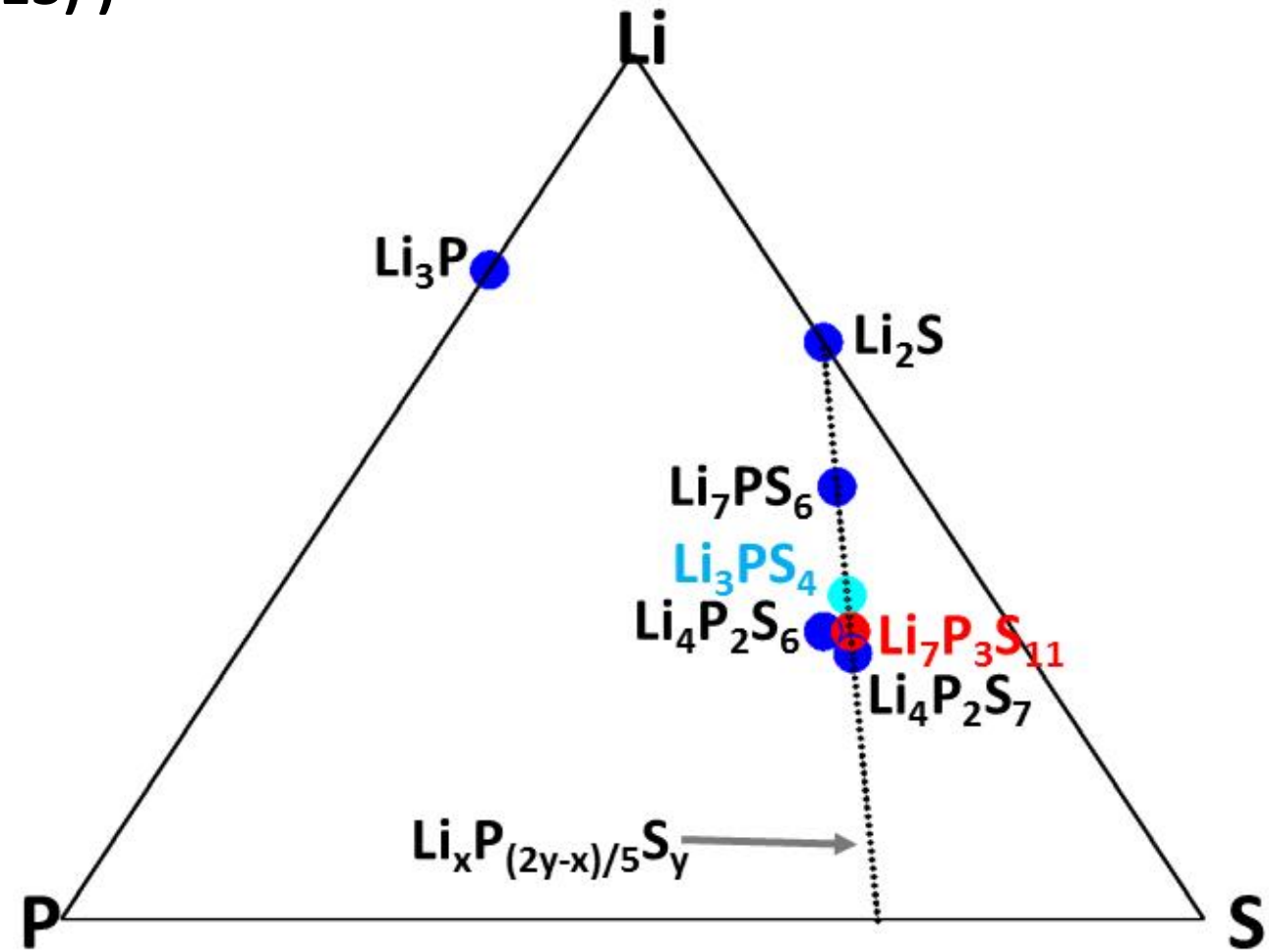

Comparison of some lithium phosphates and thiophosphates

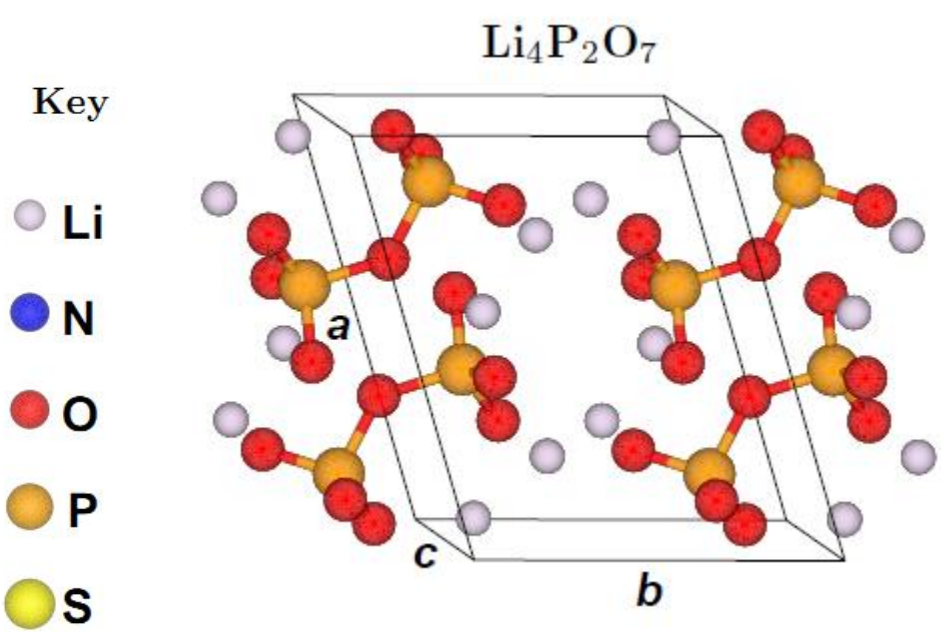

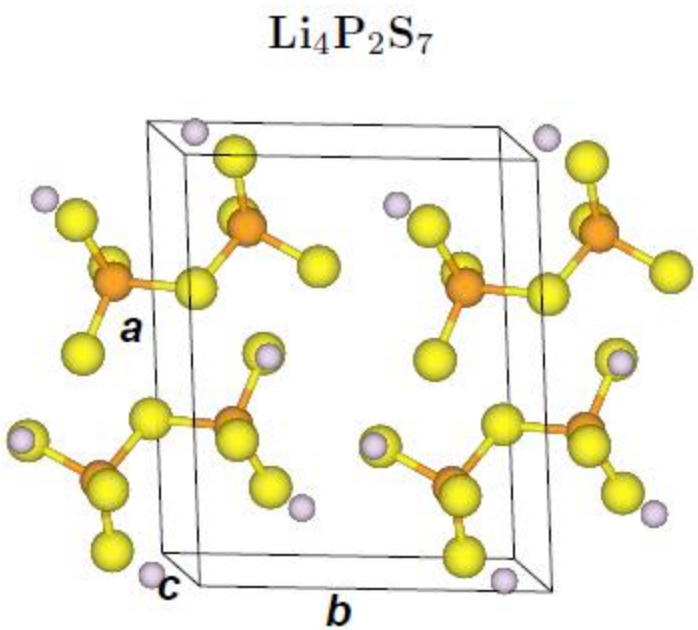

Crystallizes (experimentally and computationally) into $P\bar{1}$ structure

Experimentally amorphous; computationally metastable in $P\bar{1}$ structure

Some lithium thiophosphate crystal structures

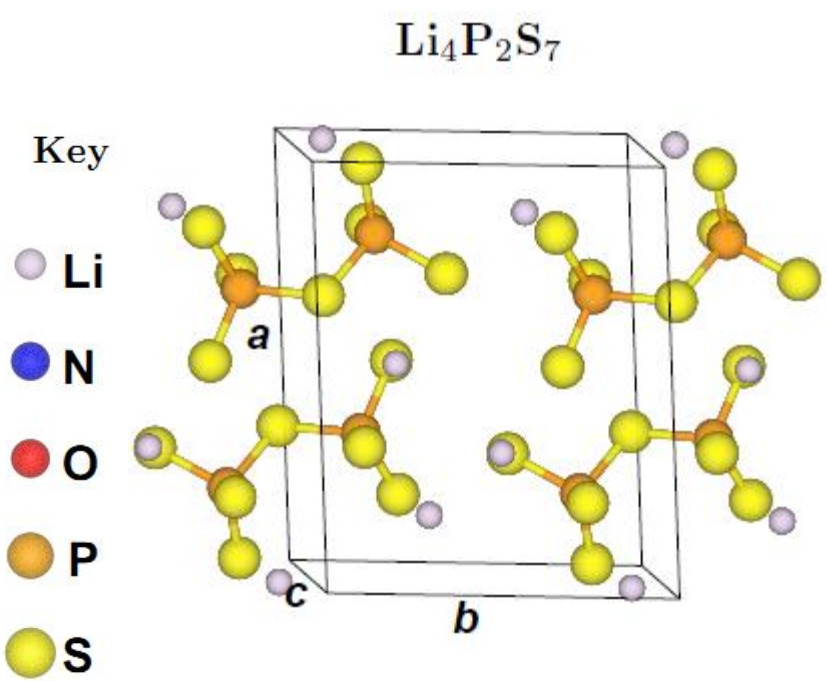

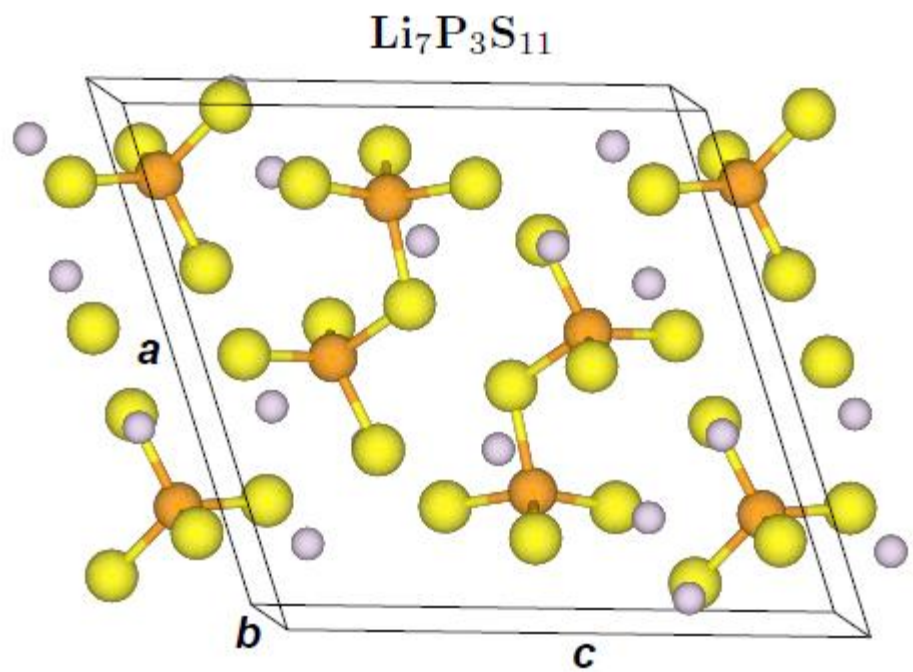

Experimentally amorphous; computationally metastable in $P\bar{1}$ structure

Experimentally and computationally metastable in $P\bar{1}$ structure

Vacancy migration analysis from NEB results for $Li_7P_3S_{11}$:

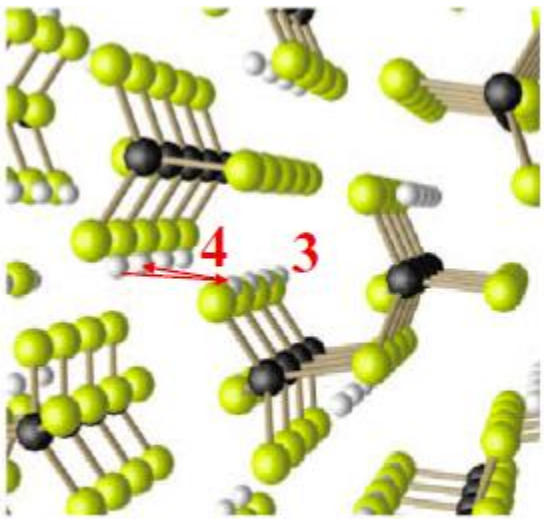

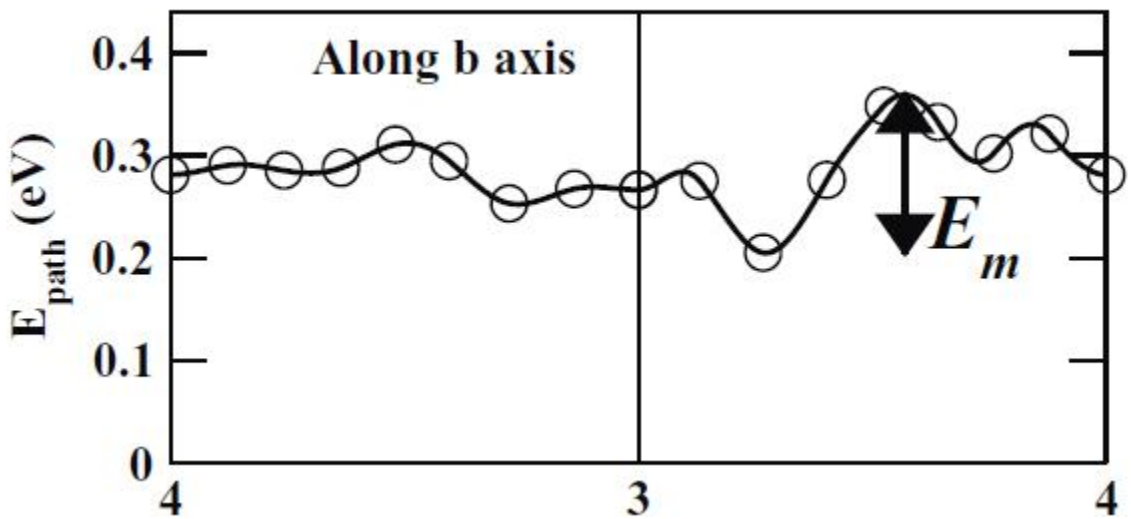

● Li ● P ● S

$$E_m \approx 0.15 \text{ eV}; E_f \approx 0 \text{ eV}$$

$$\Rightarrow E_A = E_m + \tfrac{1}{2} E_f \approx 0.15 \text{ eV}$$

Experiment -- A Hayashi *et al.,* J. Solid State Electrochem. **14**, 1761 (2010):

$$\sigma \approx 2 - 3 \times 10^{-3} \text{ S/cm} \qquad E_A \approx 0.12 - 0.18 \text{ eV}$$

Systematic study of Li_xPS_y materials – (N. D. Lepley and N. A. W. Holzwarth, J. Electrochem. Soc. 159, A538 (2012), Phys. Rev. B 88, 104103 (2013))

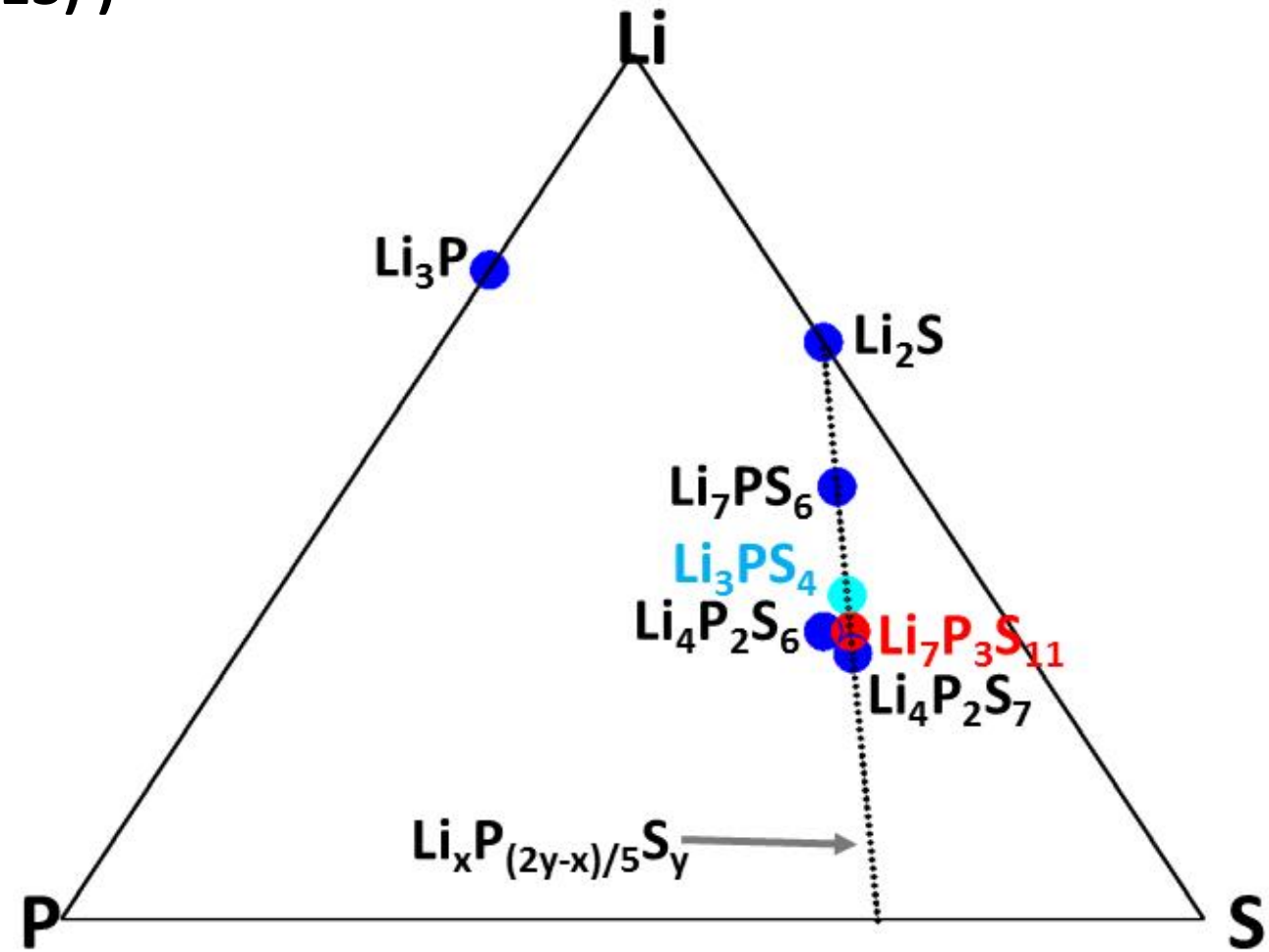

$Pnm2_1$ structured materials

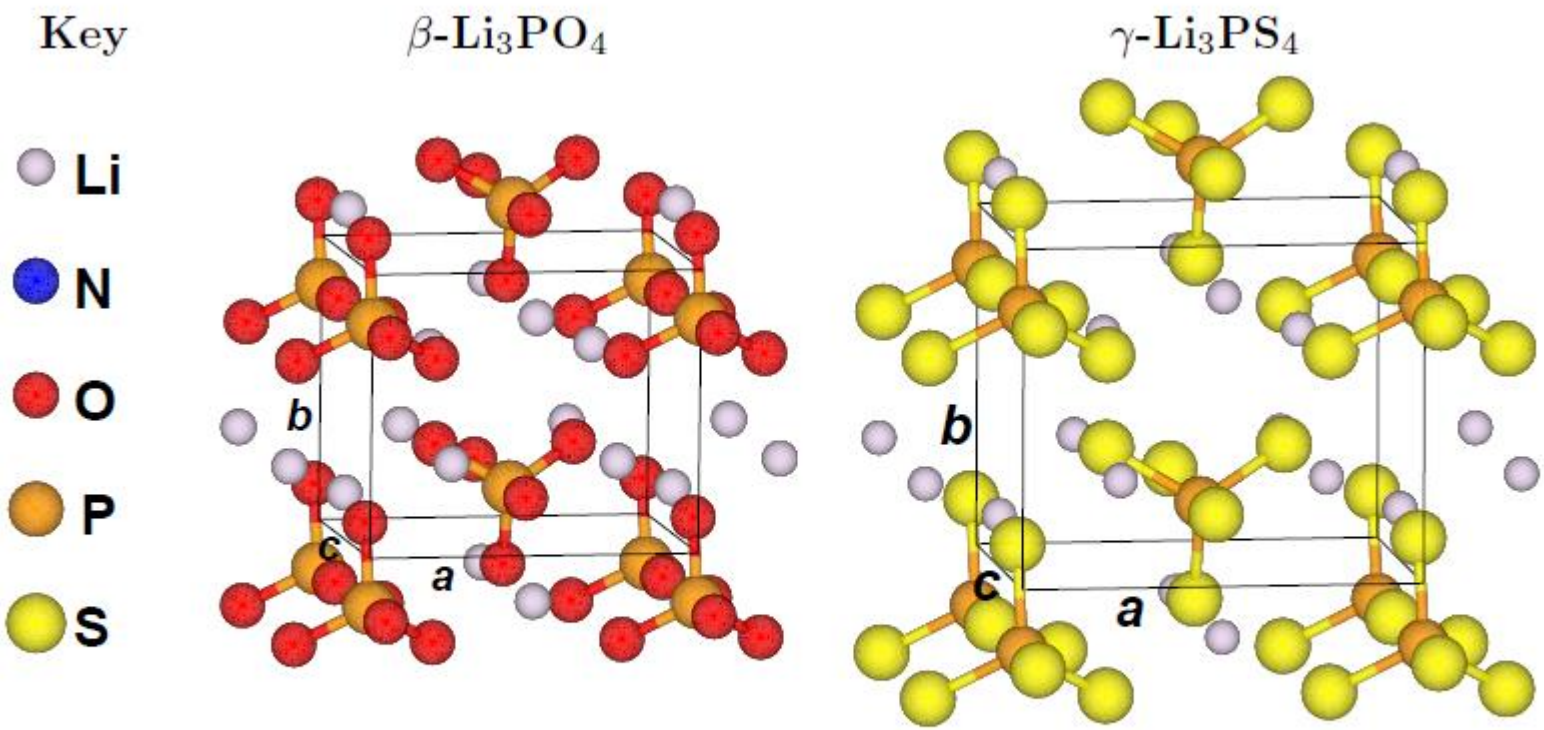

Fig. 2. Ball and stick diagram for the $Pmn2_1$ structures of β-Li_3PO_4 and γ-Li_3PS_4 (2 formula units per unit cell) from computational results. The key shown at the left indicates the ball convention used throughout Sec. 2.

Pnma structured materials

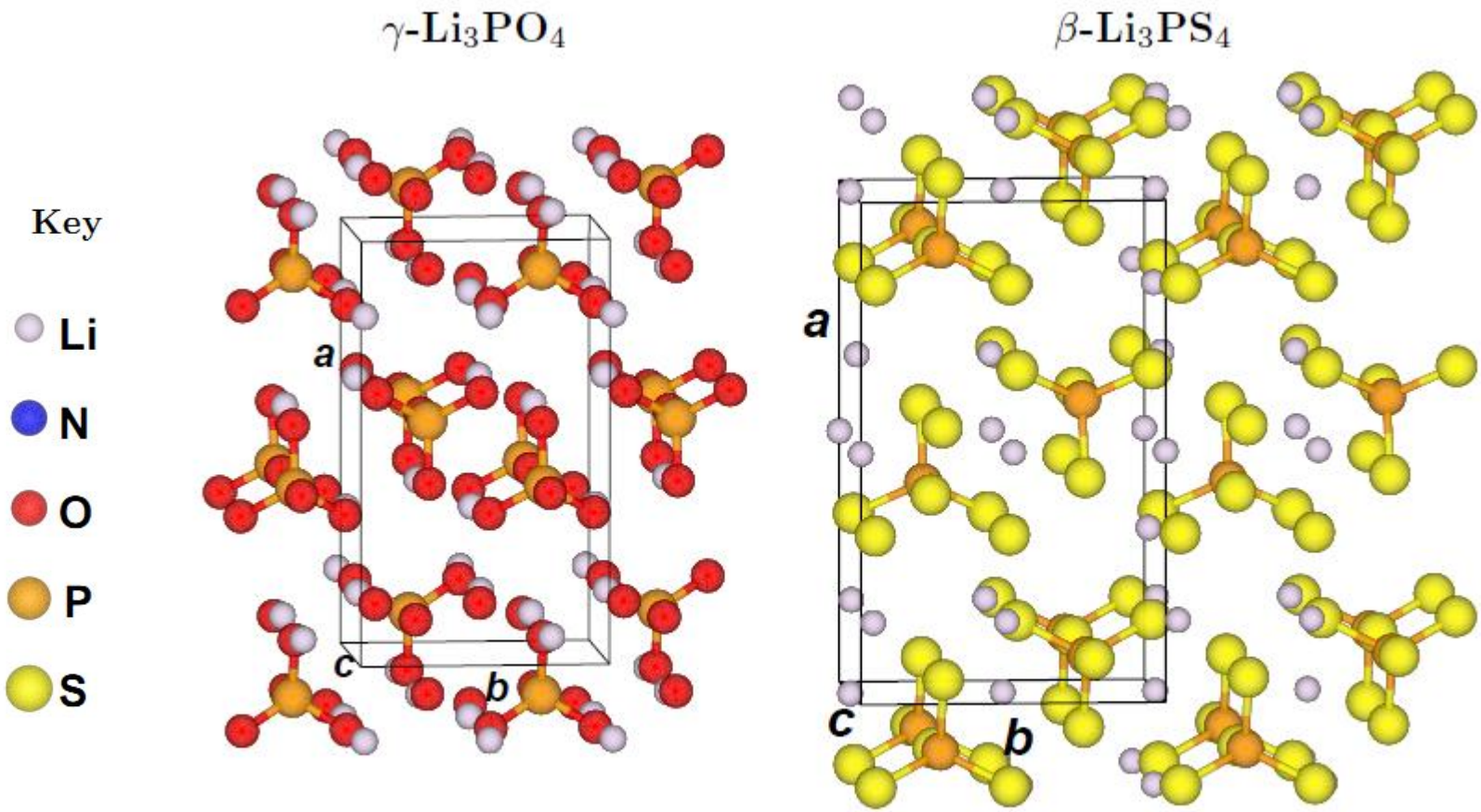

Fig. 3. Ball and stick diagram for the *Pnma* structures of γ-Li_3PO_4 and β-Li_3PS_4 (4 formula units per unit cell) from idealized computational results.

Pnma structured materials

More detailed look at β-Li_3PS_4 structure

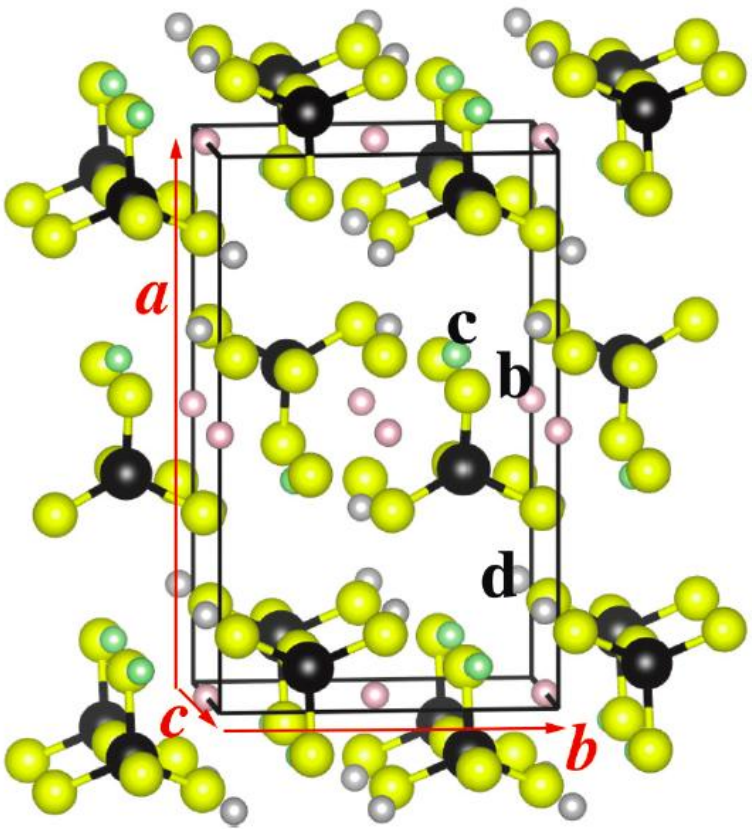

P ● S ●

Li sites:

- d sites (100% occ.)
- b sites (70% occ.)
- c sites (30% occ.)

Possible vacancy migration paths in β-Li_3PS_4

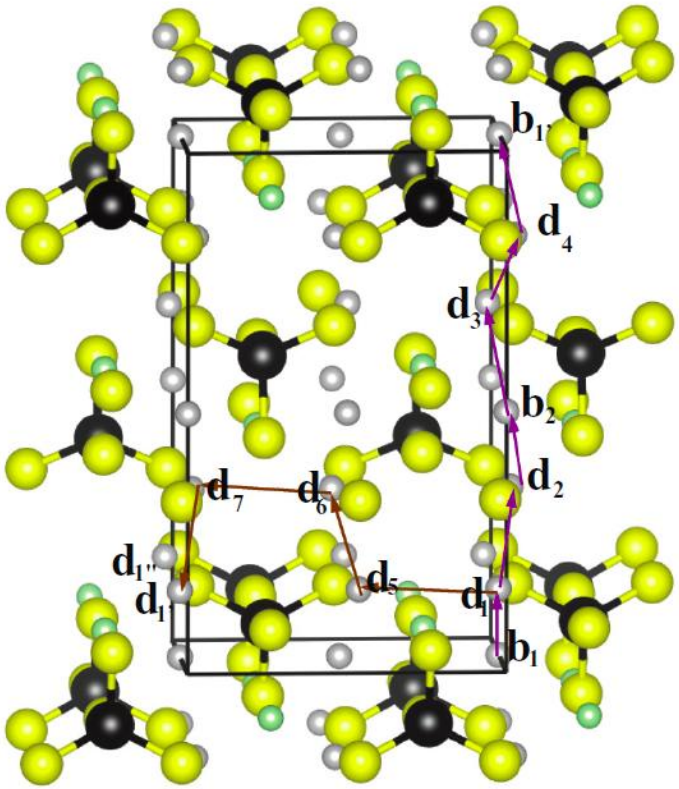

NEB diagram:

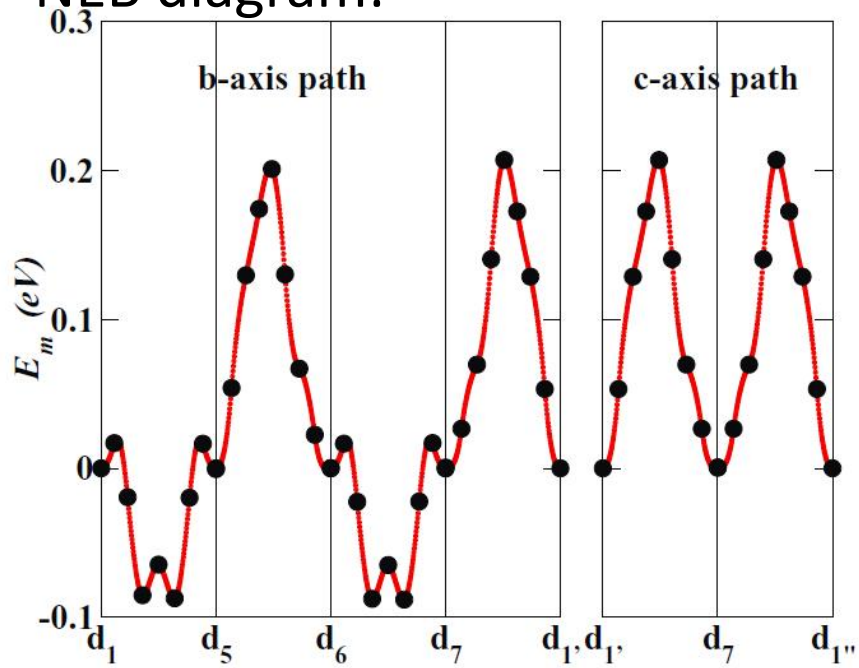

FIG. 8. (Color online) Energy diagram of NEB path for Li vacancy migration along the **b** and **c** axes for β-Li_3PS_4-*b*.

Li sites: **P** ● **S** ●

- d sites (100% occ.)
- b sites (70% occ.)
- c sites (30% occ.)

$$E_m \approx 0.3 \text{ eV}; E_f \approx 0 \text{ eV}$$

$$\Rightarrow E_A = E_m + \tfrac{1}{2} E_f \approx 0.3 \text{ eV}$$

Experimental values:

$$E_A = 0.4 - 0.5 \text{ eV}$$

From ORNL: Experiment on electrolyte Li_3PS_4

WAKE FOREST UNIVERSITY

JACS
JOURNAL OF THE AMERICAN CHEMICAL SOCIETY
Communication
pubs.acs.org/JACS

Anomalous High Ionic Conductivity of Nanoporous β-Li_3PS_4

Zengcai Liu,[†] Wujun Fu,[†] E. Andrew Payzant,[†,‡] Xiang Yu,[†] Zili Wu,[†,§] Nancy J. Dudney,[‡] Jim Kiggans,[‡] Kunlun Hong,[†] Adam J. Rondinone,[†] and Chengdu Liang*,[†]

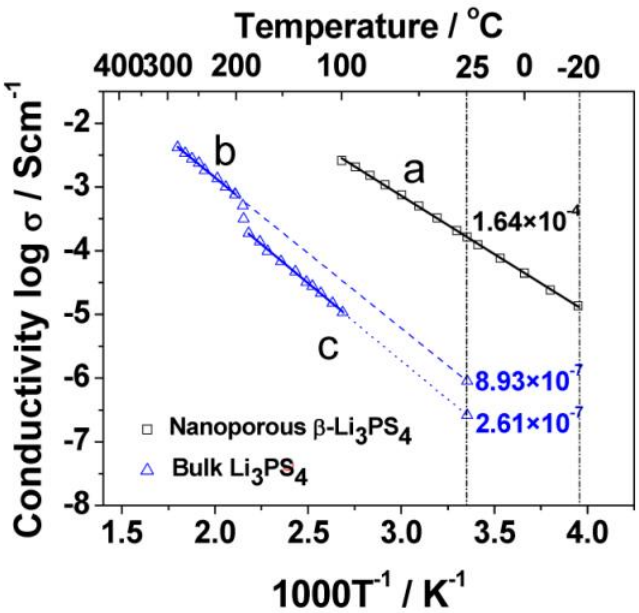

Figure 1. Arrhenius plots for nanoporous β-Li_3PS_4 (line a), bulk β-Li_3PS_4 (line b), and bulk γ-Li_3PS_4 (line c). The conductivity data for bulk Li_3PS_4 are reproduced from the work of Tachez.[10].

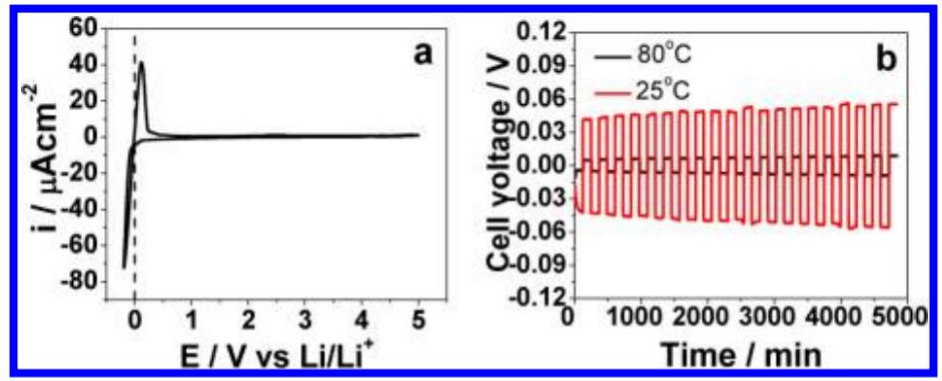

Figure 5. Electrochemical stability of β-Li_3PS_4 and cycling stability with metallic lithium electrodes. (a) CV of a Li/β-Li_3PS_4/Pt cell, where Li and Pt serve as the reference/counter and working electrodes, respectively. (b) Lithium cyclability in a symmetric Li/β-Li_3PS_4/Li cell. The cell was cycled at a current density of 0.1 mA cm^{-2} at room temperature and 80 °C.

Systematic study of Li_xPS_y materials – (N. D. Lepley and N. A. W. Holzwarth, J. Electrochem. Soc. 159, A538 (2012), Phys. Rev. B 88, 104103 (2013))

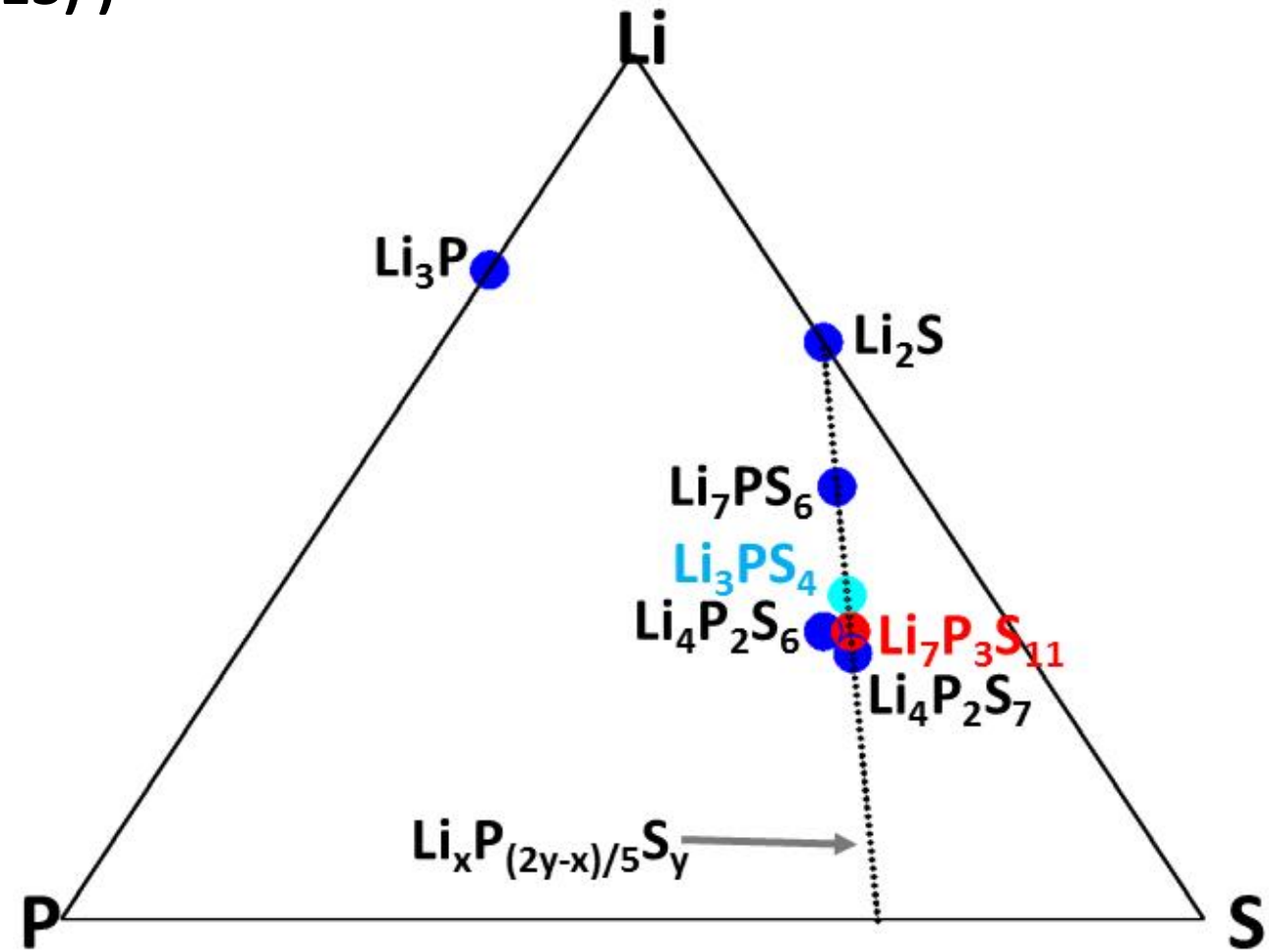

Investigation of $Li_4P_2S_6$

Collaboration with Zachary D. Hood at ORNL

Synthesis:

$$2Li_2S + P_2S_5 \xrightarrow[900^o\,C]{} Li_4P_2S_6 + S$$

Sulfur removed by treatment with solvent; sample prepared for electrochemical applications using ball milling.

Scanning Electron Micrograph of prepared sample:

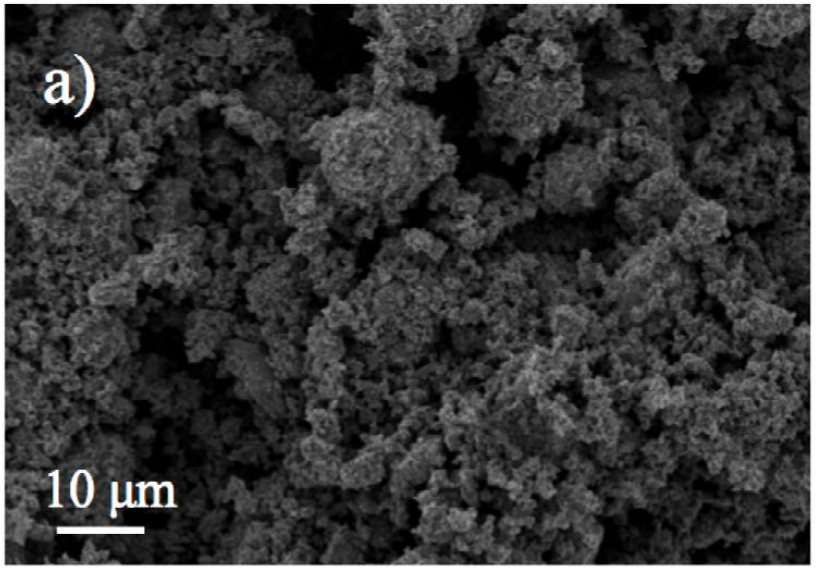

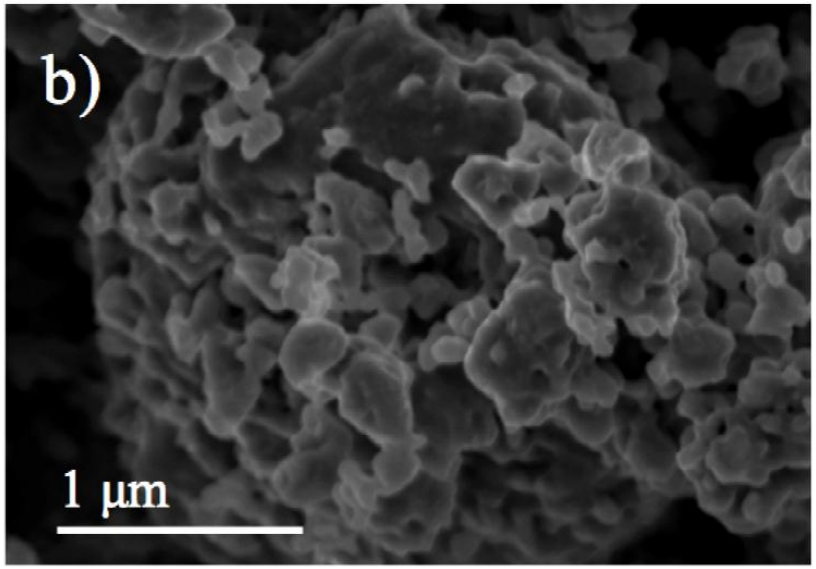

Crystal structure: Space Group $P6_3/mcm$ (#193)

Projection on to hexagonal plane:

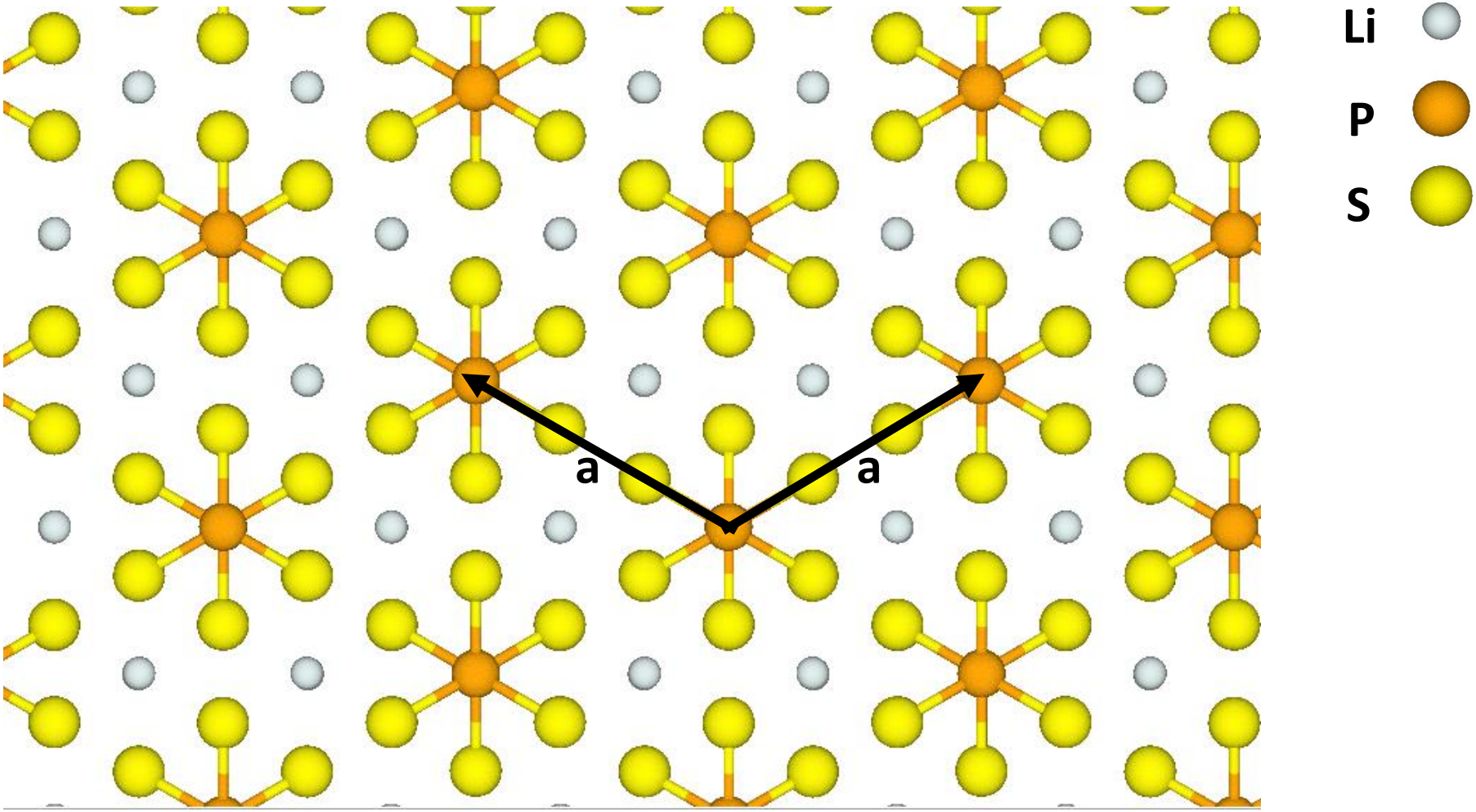

Crystal structure: Space Group *P6$_3$/mcm* (#193)

$Li_4P_2S_6$ units:

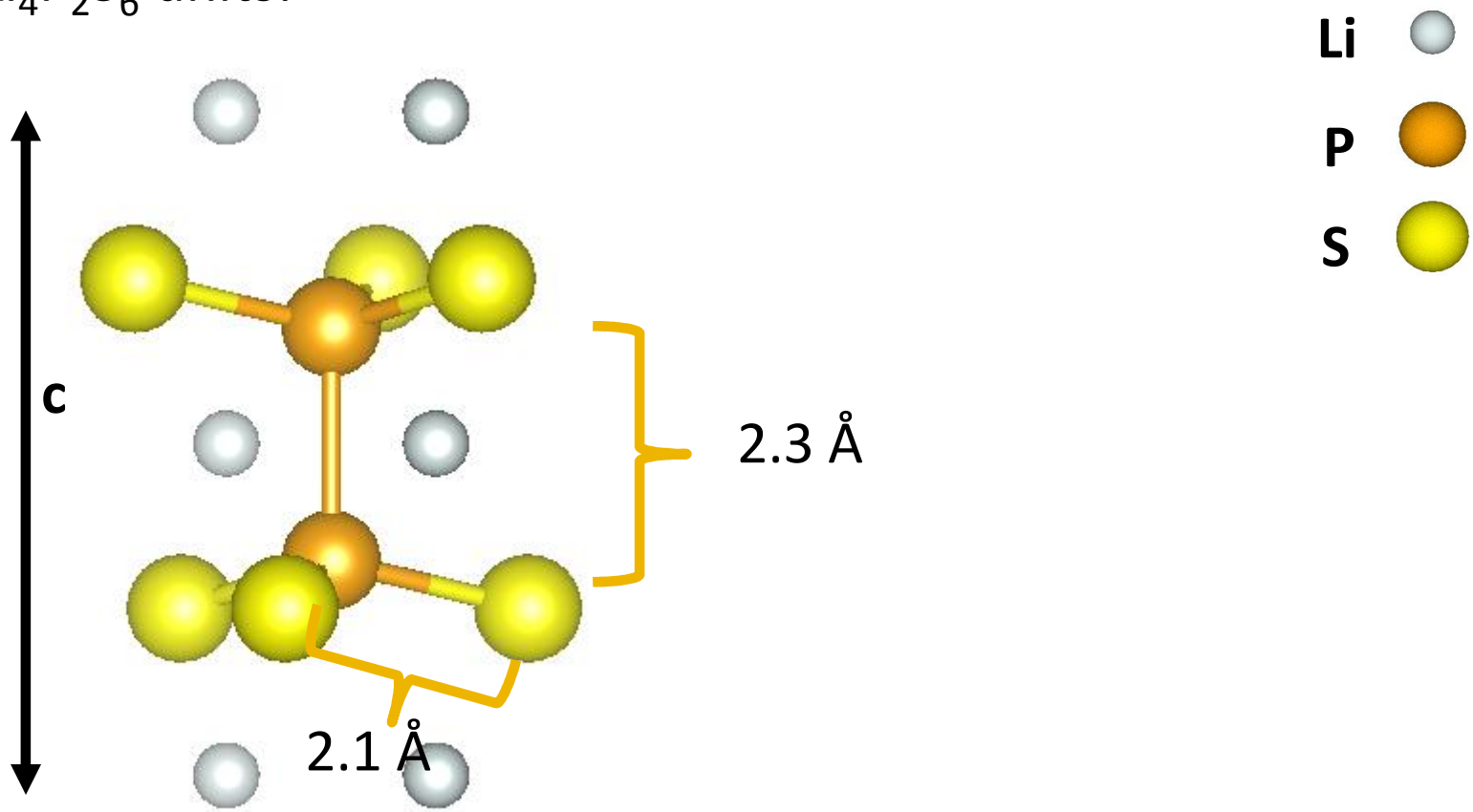

Crystal structure: Space Group *P6$_3$/mcm* (#193)

Disorder in P-P placements:

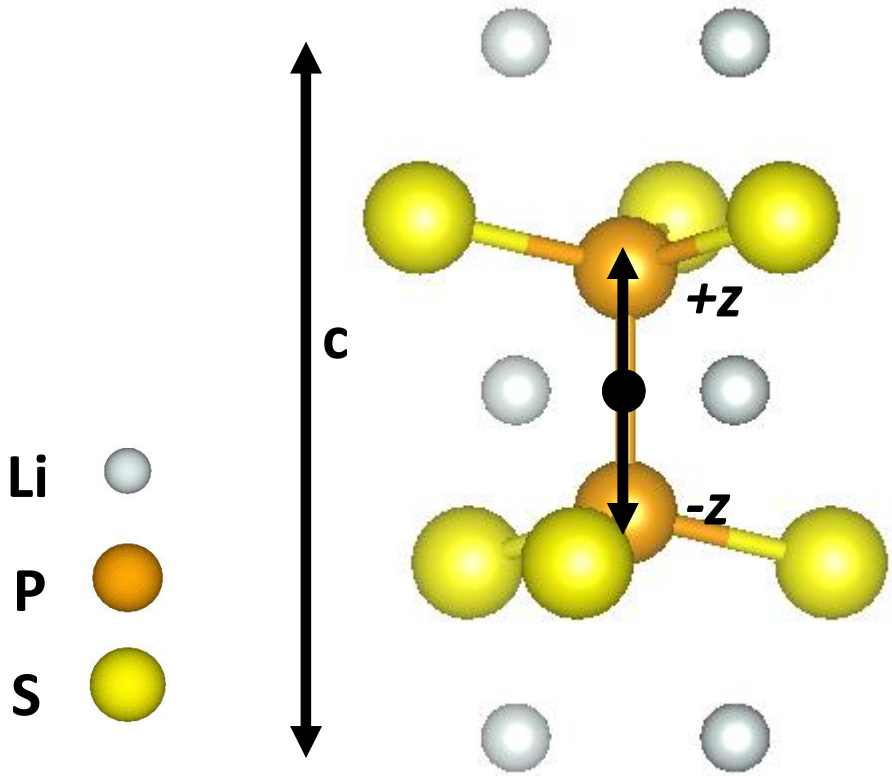

Site label z ↑

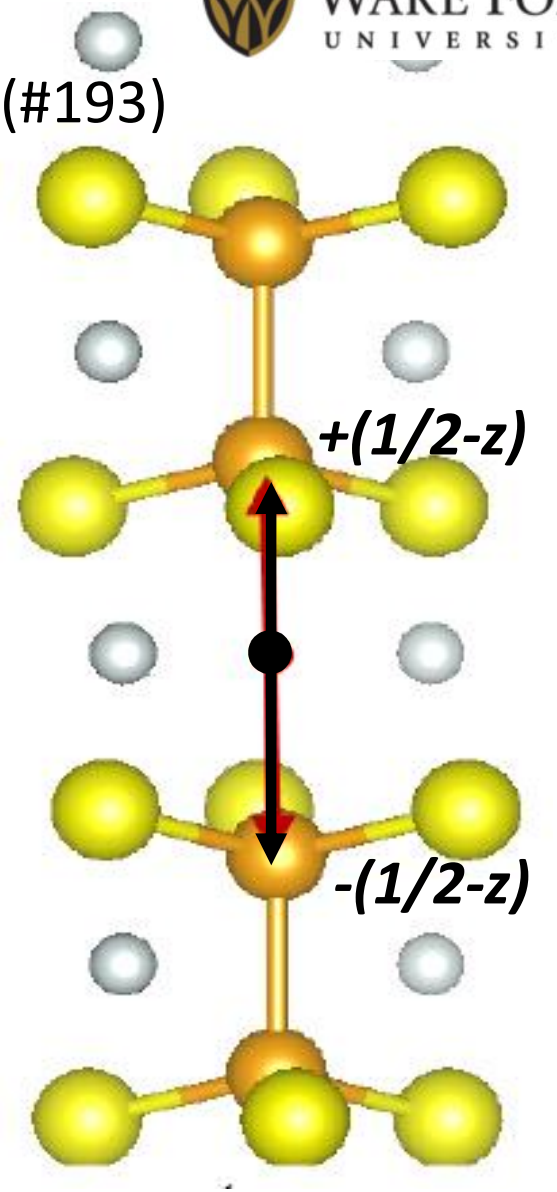

Site label z ↓

Examples:

Structure “b”

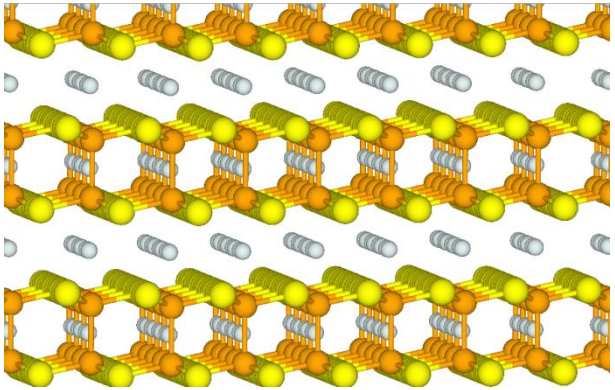

$\Delta E = 0.03\ eV$

100% z↑

Structure “c”

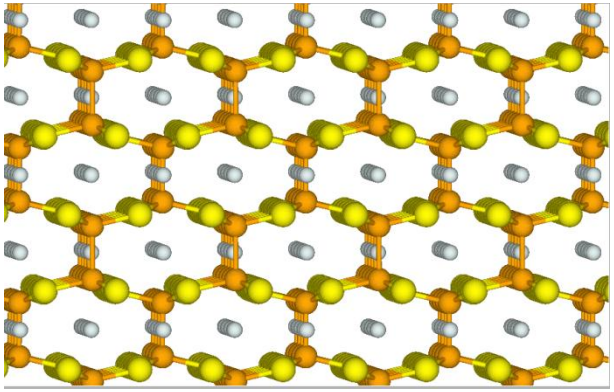

$\Delta E = 0$

50% z↑

50% z↓

Structure “d”

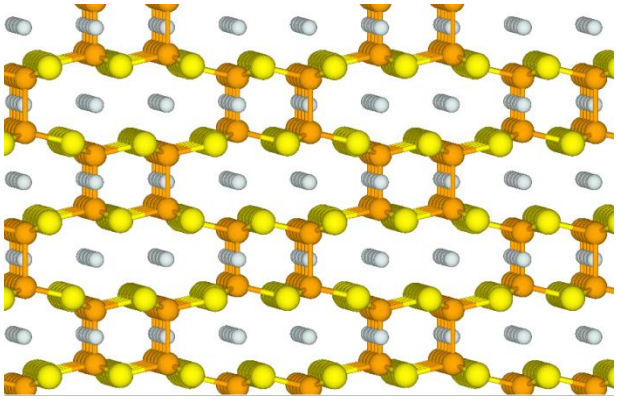

$\Delta E = 0$

50% z↑

50% z↓

Li

P

S

Structural variation can be mapped on to a two-dimensional hexagonal lattice with each P configuration taking z↑ or z↓ settings; Li and S configurations fixed

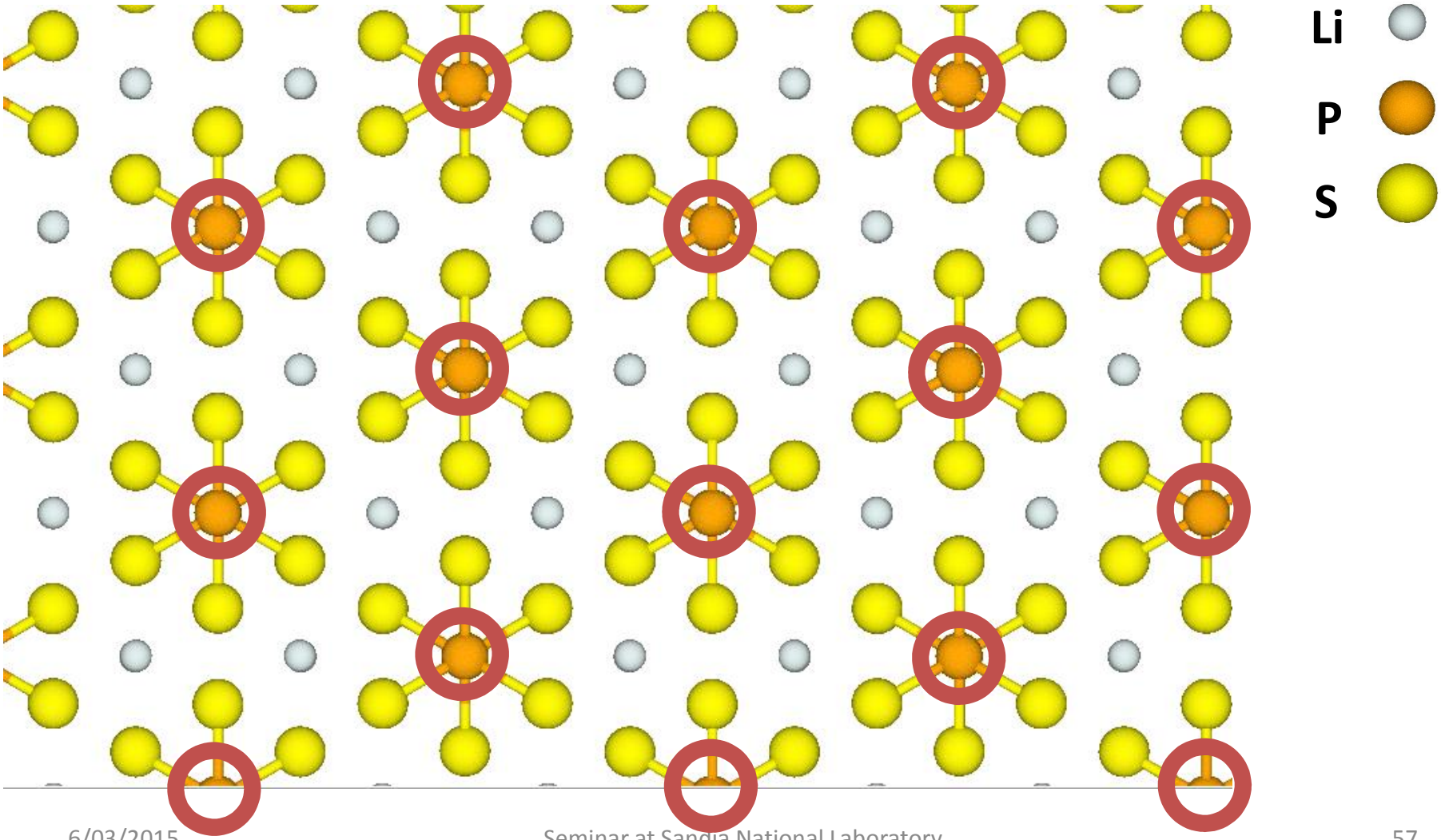

Temperature in dependence of X-ray powder diffraction

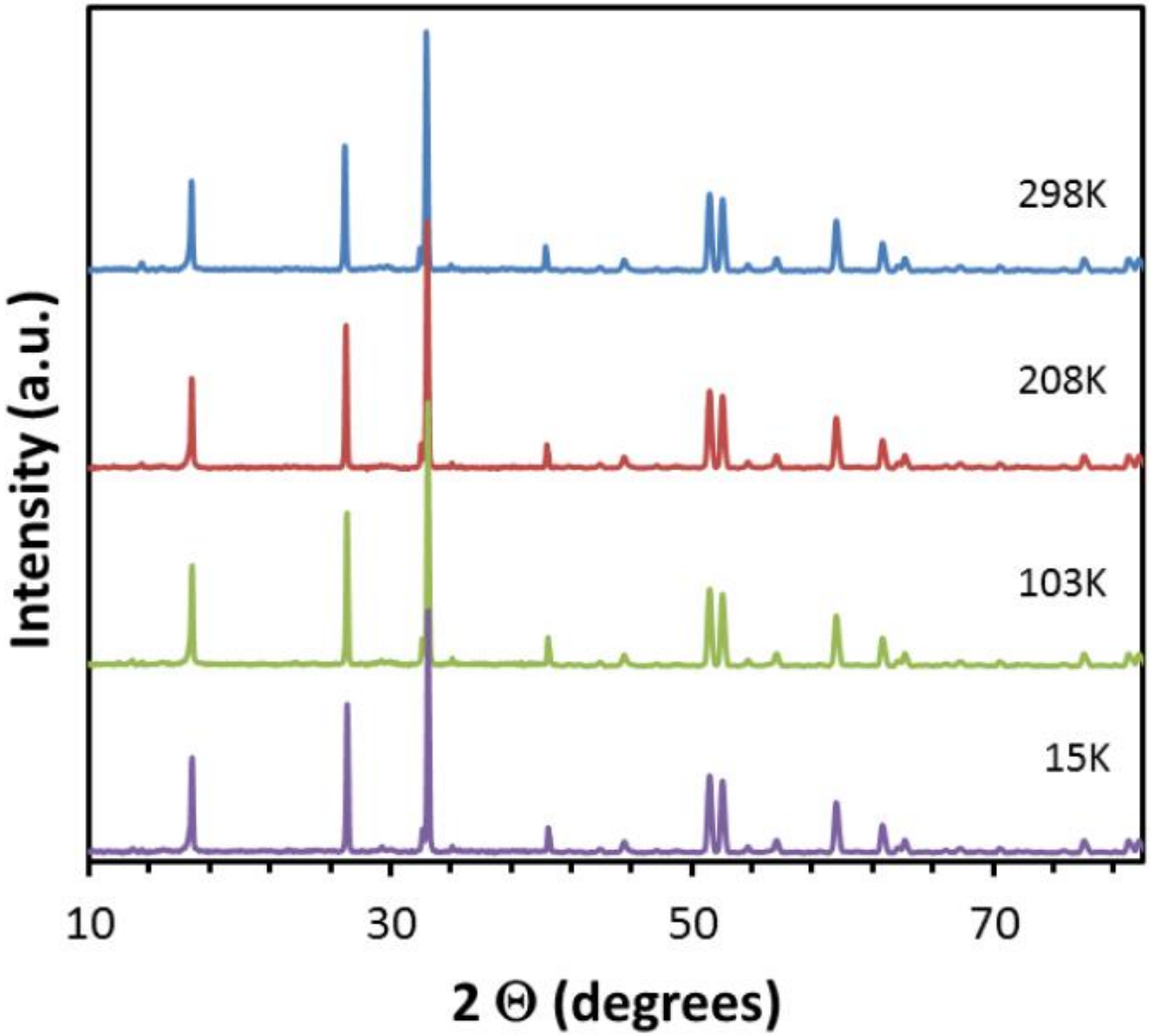

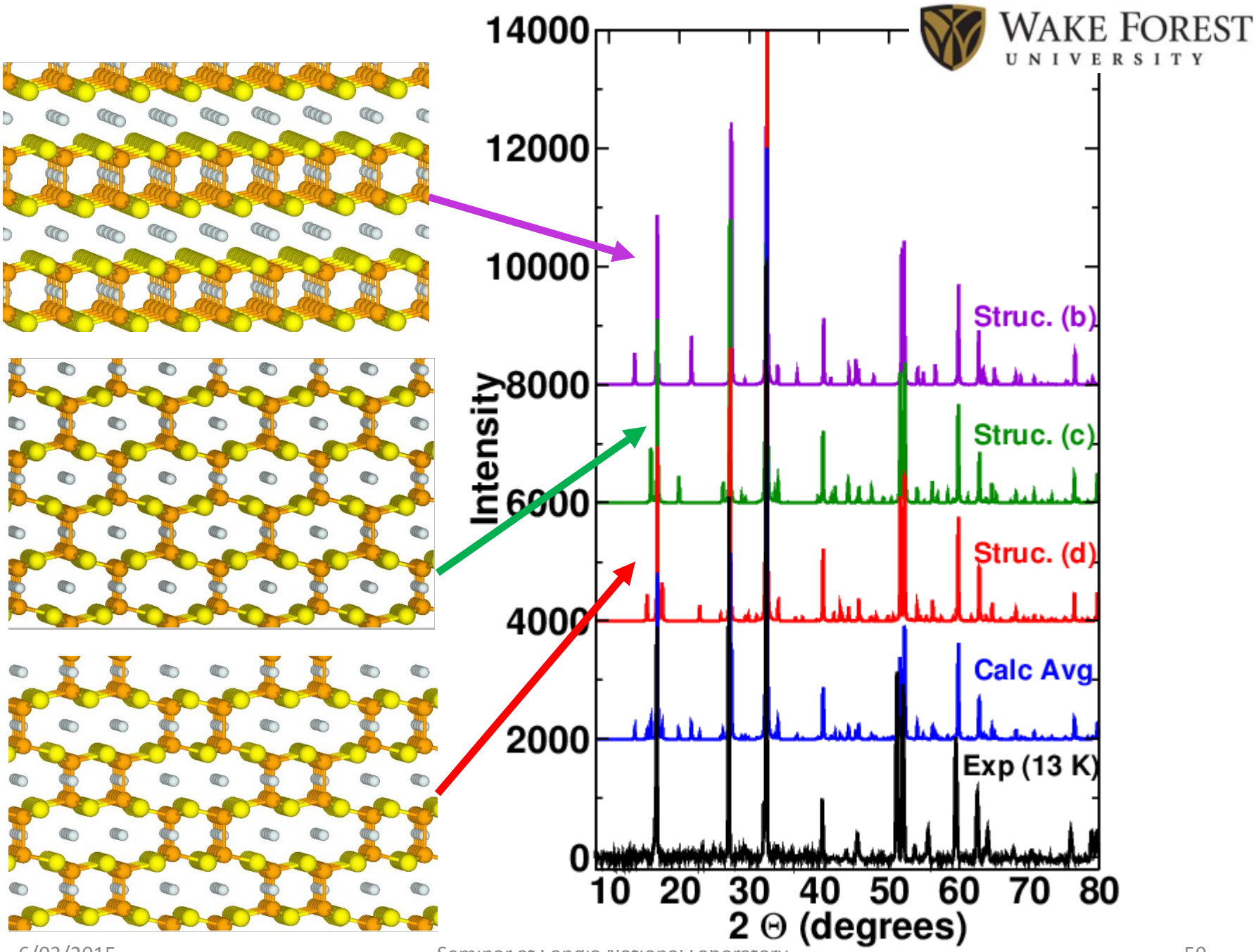
WAKE FOREST
UNIVERSITY
14000
12000
10000
8000
6000
4000
2000
0
Intensity
10
20
30
40
50
60
70
80
2 Θ (degrees)
Struc. (b)
Struc. (c)
Struc. (d)
Calc Avg
Exp (13 K)

Comparison of 13 K X-ray data with simulation

Note: simulations scaled by 102% to compensate for systematic LDA error.

Simulations consistent with incoherent average over all P z↑ and z↓ configurations

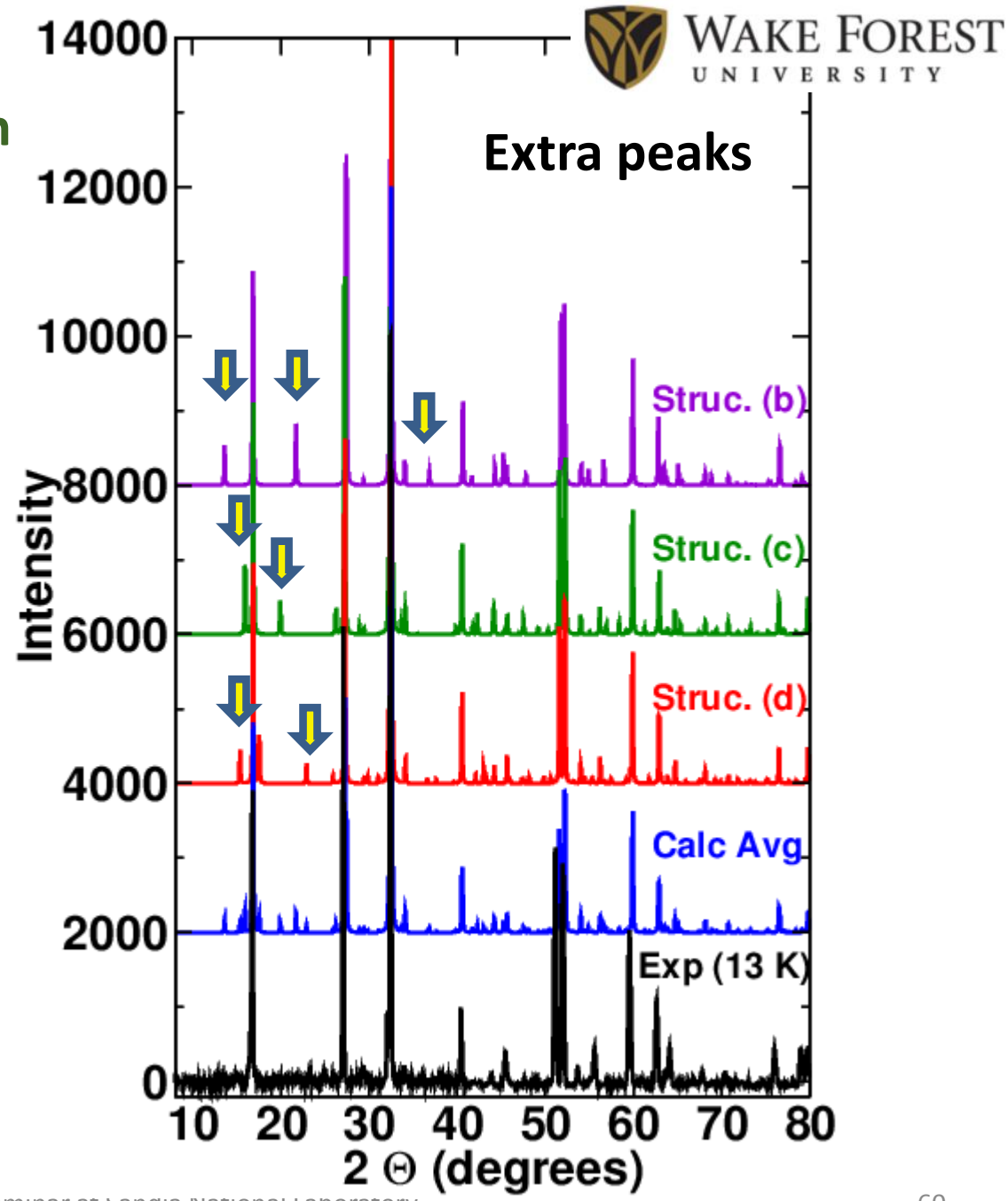

In terms of diffracting plane spacing:

$$d = \lambda / (2\sin\Theta)$$

X-ray spectrum **Neutron spectrum**

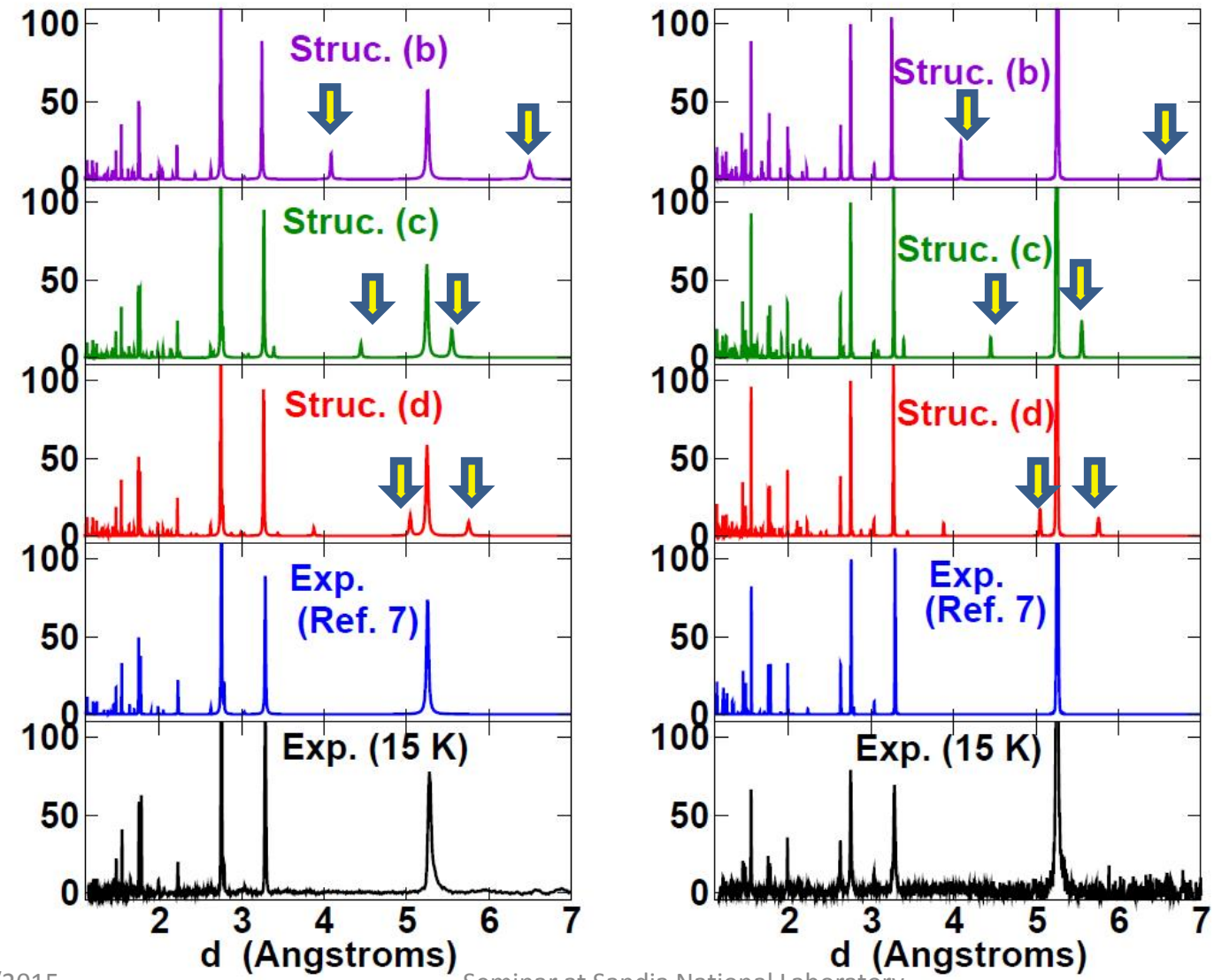

Structural parameters

	a (Å)	c (Å)	z_P	z_S
Exp. 293K (X-ray)*	6.070	6.557	0.1715	0.3237
Exp. 300K (X-ray)	6.075	6.597	0.172	0.324
Exp. 300K (neutron)	6.075	6.595	0.173	0.326
Exp. 15K (X-ray)	6.051	6.548	0.172	0.324
Exp. 15K (neutron)	6.055	6.553	0.172	0.326
Calc. structure "b"	6.07	6.50	0.18	0.33
Calc. structure "c"	6.06	6.54	0.17	0.33
Calc. structure "d"	6.06	6.54	0.17	0.33

Hood *et al.*

with 102% LDA corr.

*Mercier *et al.*, J. Solid State Chem. 43, 151 (1982)

Stability: $Li_4P_2S_6$ is much less reactive than other lithium thio-phosphates, but it decomposes in air, especially at higher temperature

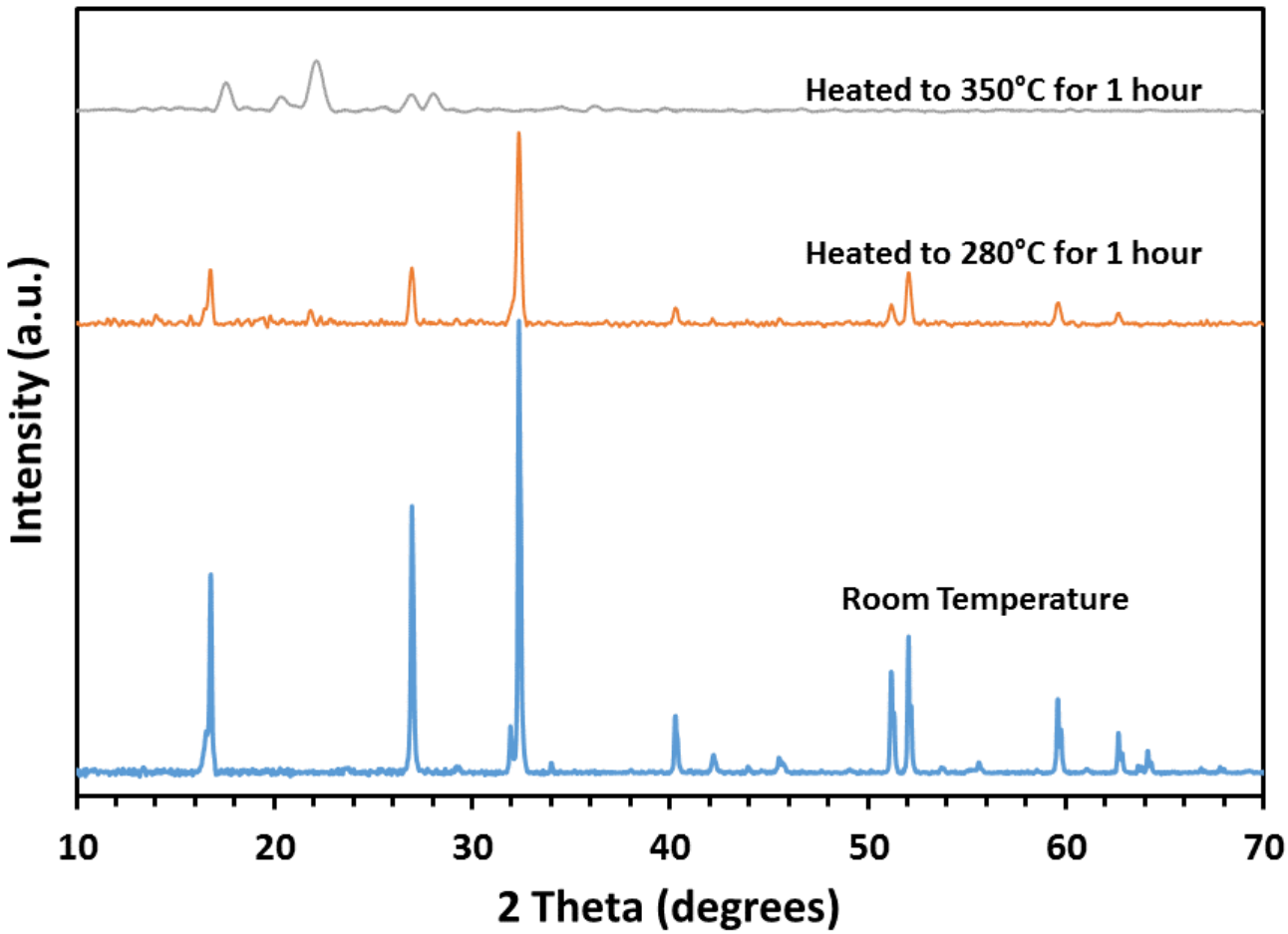

Decomposition products:
P_2O_5
$Li_4P_2O_7$
Li_2SO_4

Ionic conductivity and Activation Energy

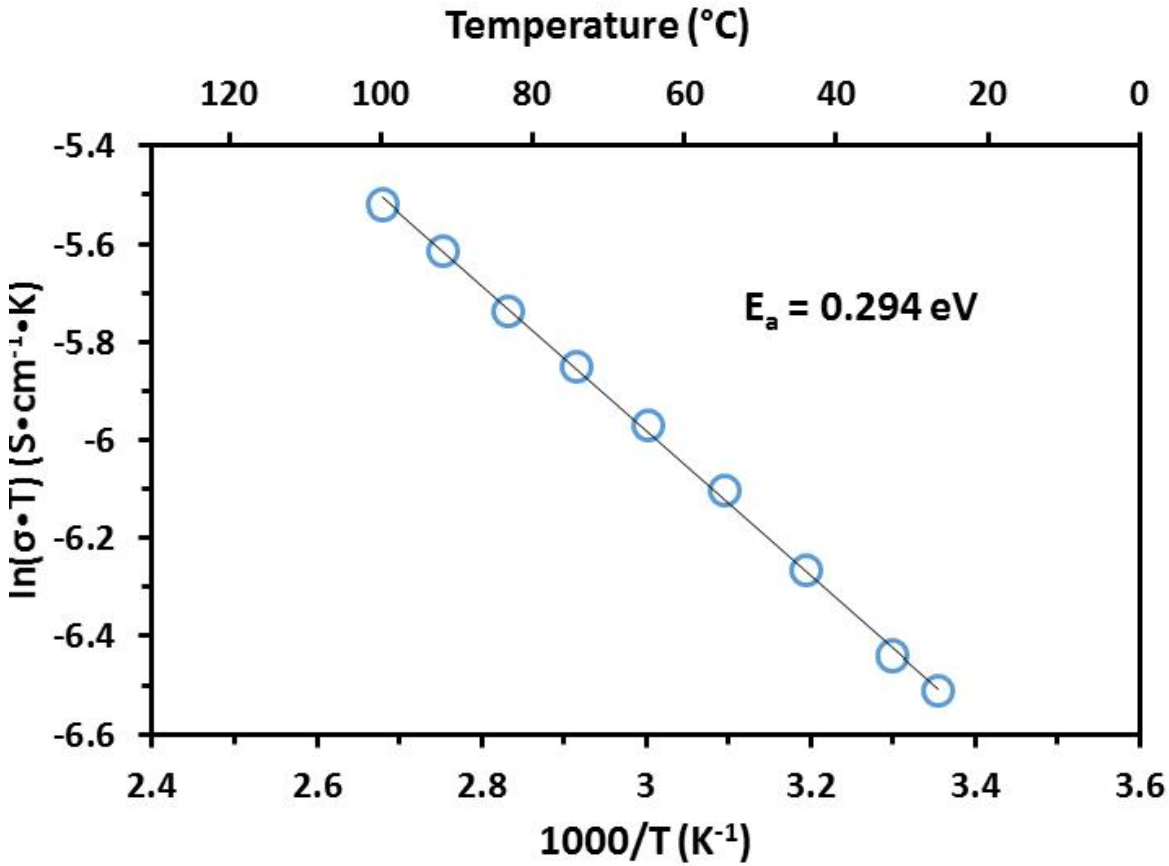

2.38×10^{-7} S/cm at 25˚C and 2.33×10^{-6} S/cm at 100˚C

$Li_4P_2S_6$ pressed pellets with blocking (Al) electrodes

Li/ $Li_4P_2S_6$ /Li cells could not be cycled

Simulations of ion mobility using Nudged Elastic Band Model

Vacancy mechanism:
ΔE>0.6 eV

Li
P
S

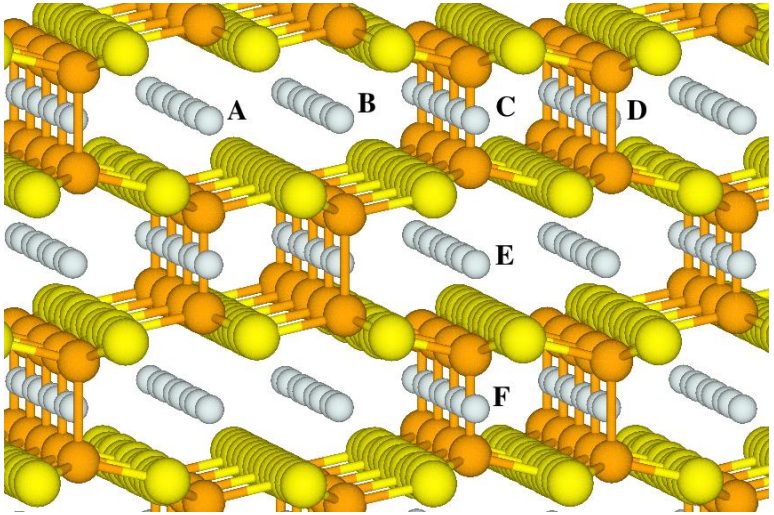

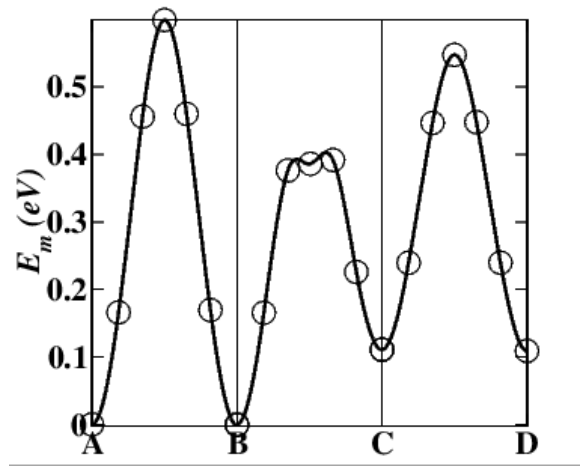

Interstitial mechanism:
ΔE>0.1 eV

Possible interstitial sites

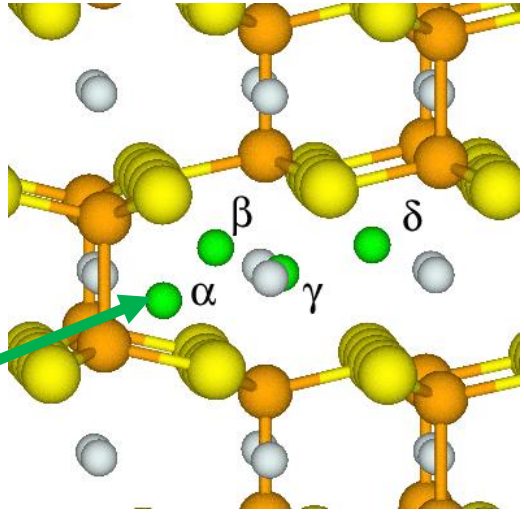

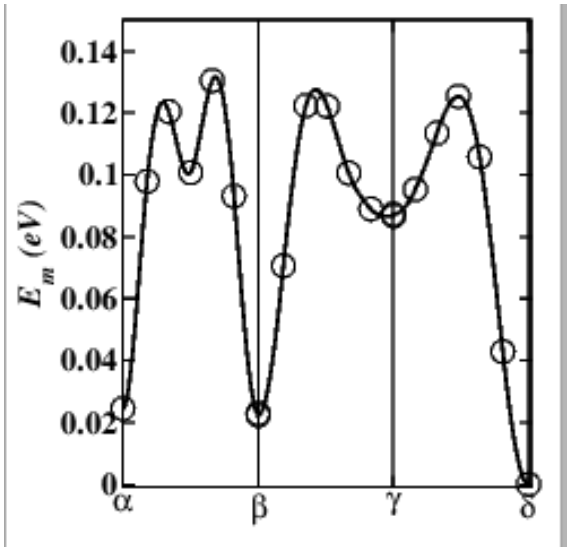

Models of Idealized Interfaces

Crystal structure of bulk Li_3PS_4 – γ-form $Pmn2_1$ (#31)

Note: Li_3PS_4 is also found in the β-form with Pnma (#62) structure

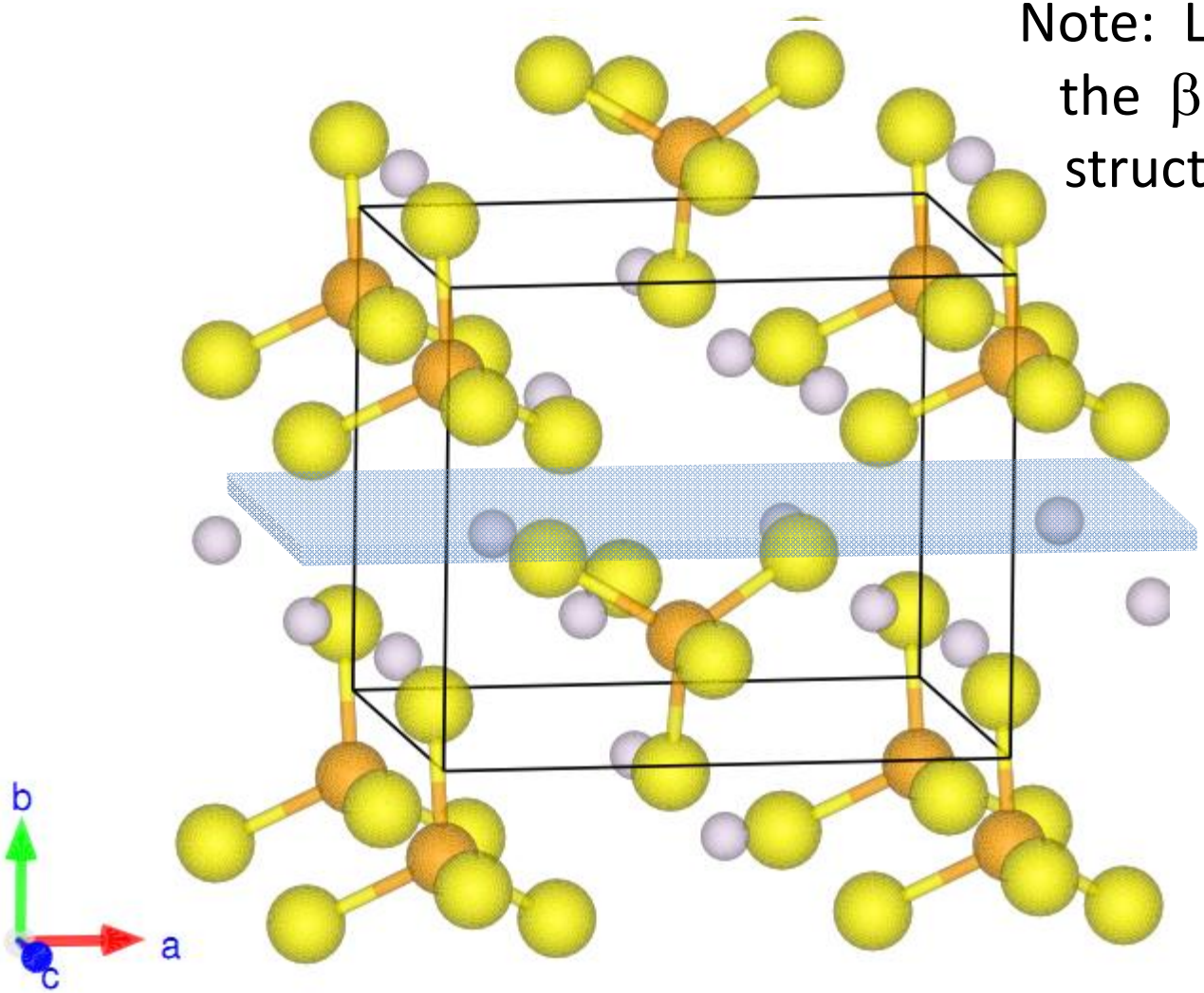

Li
N
O
P
S

γ-Li_3PS_4 [0 1 0] surface

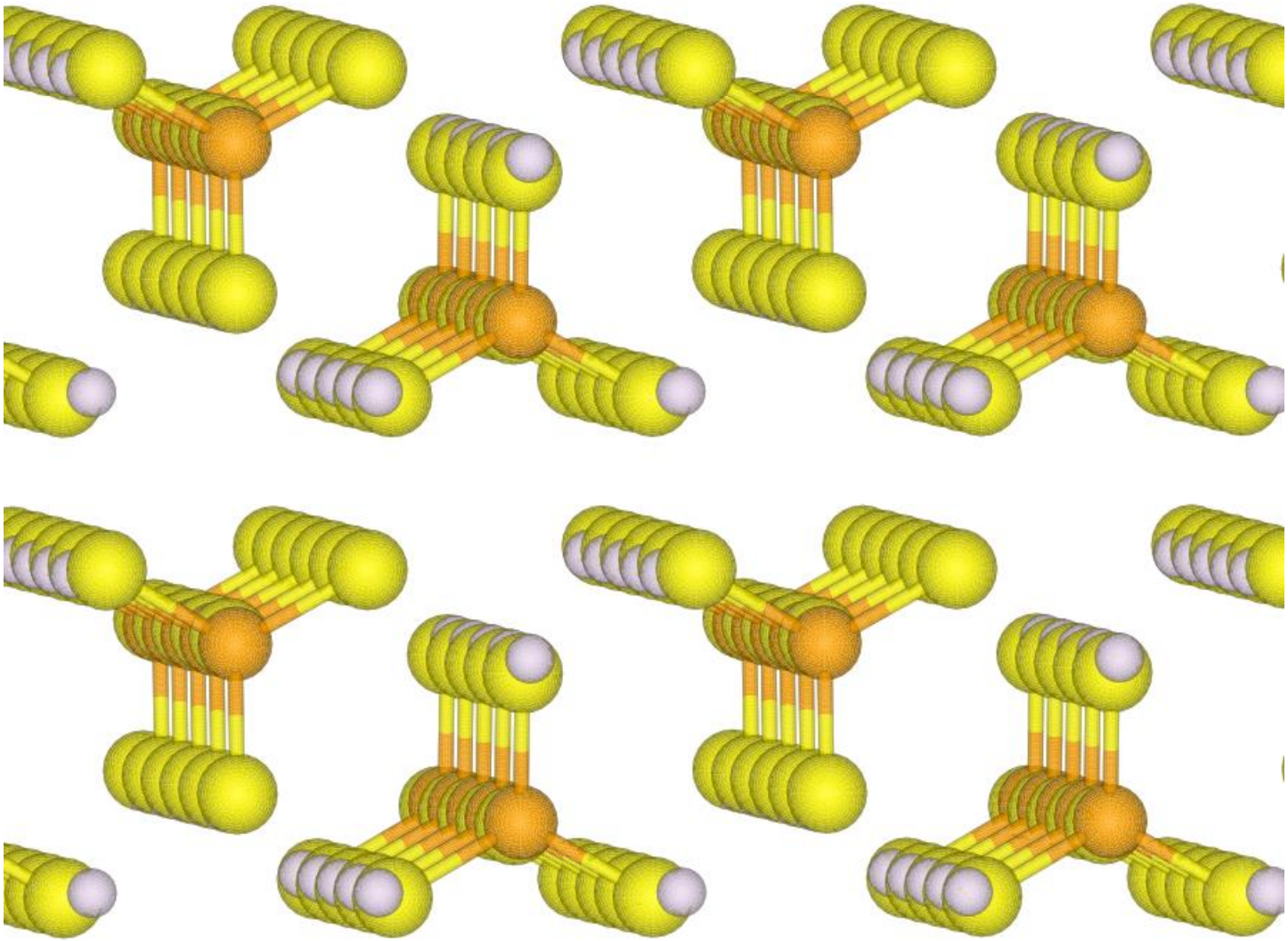

Simulations of ideal γ-Li_3PS_4 [0 1 0] surface in the presence of Li

Initial configuration:

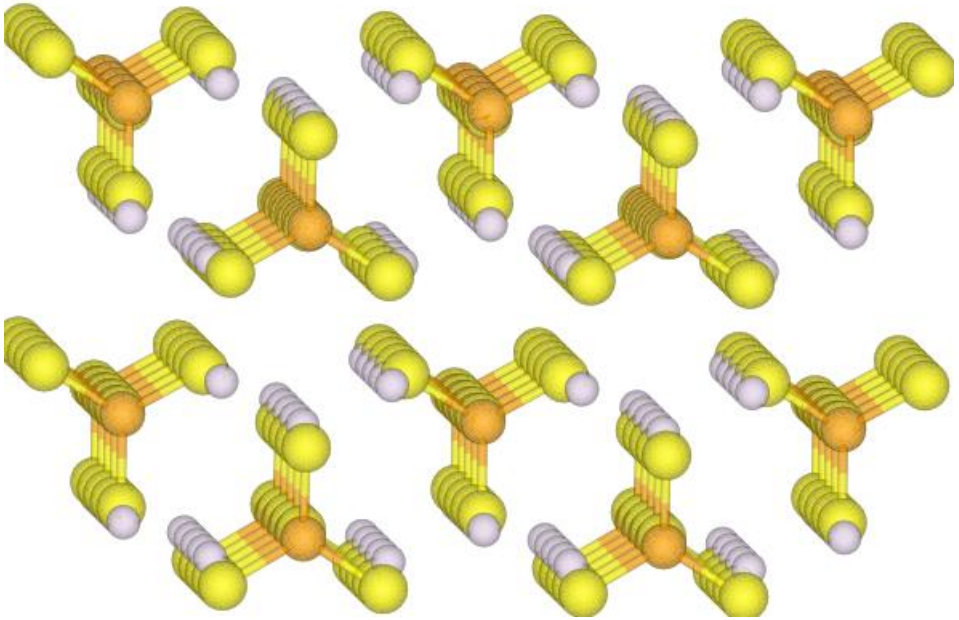

Computed optimized structure:

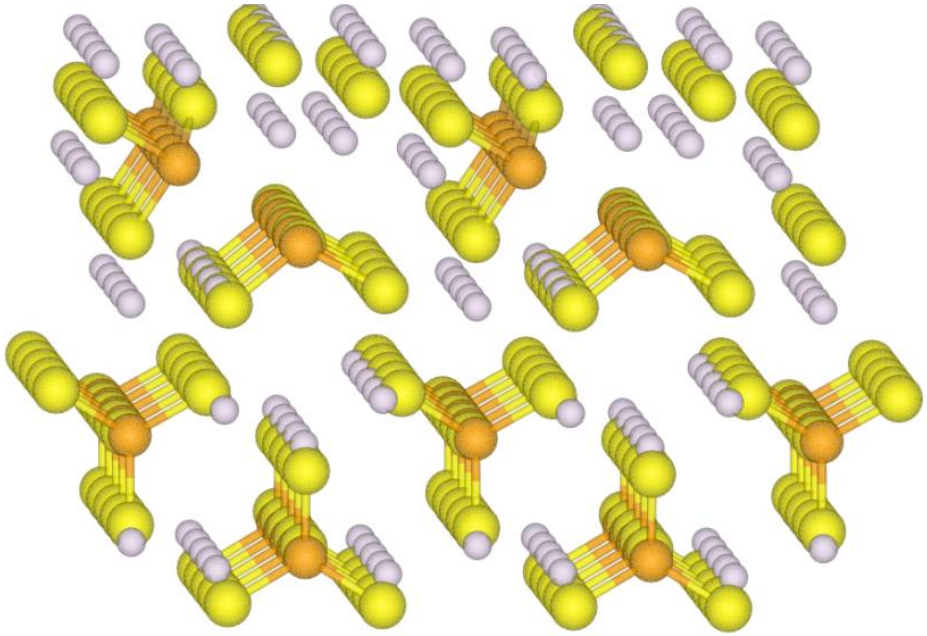

More simulations of ideal γ-Li_3PS_4 [0 1 0] surface in the presence of Li – supercells containing

12 Li atoms and

2 or 4 electrolyte layers

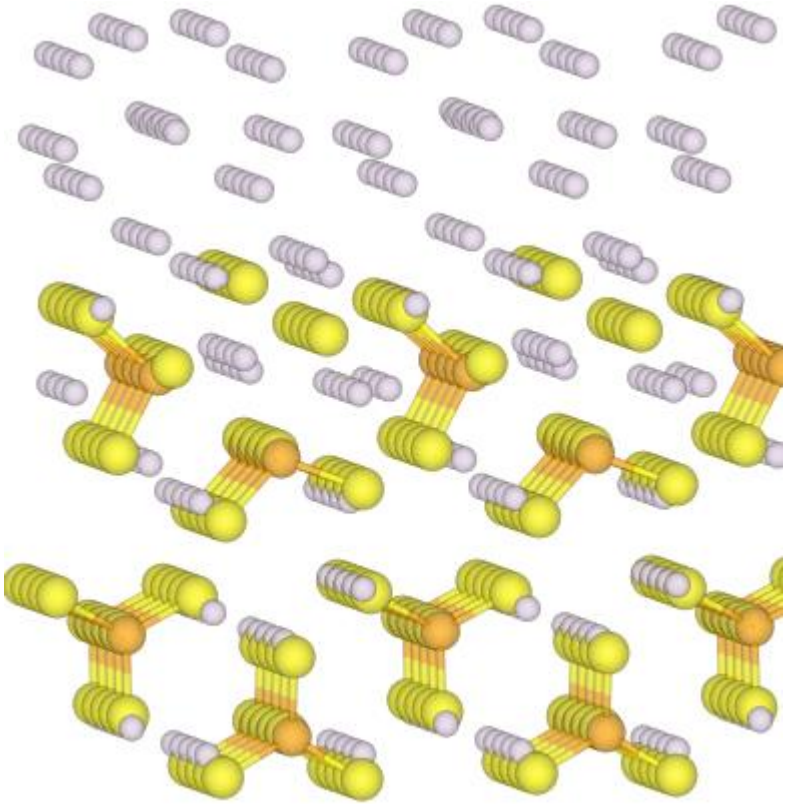

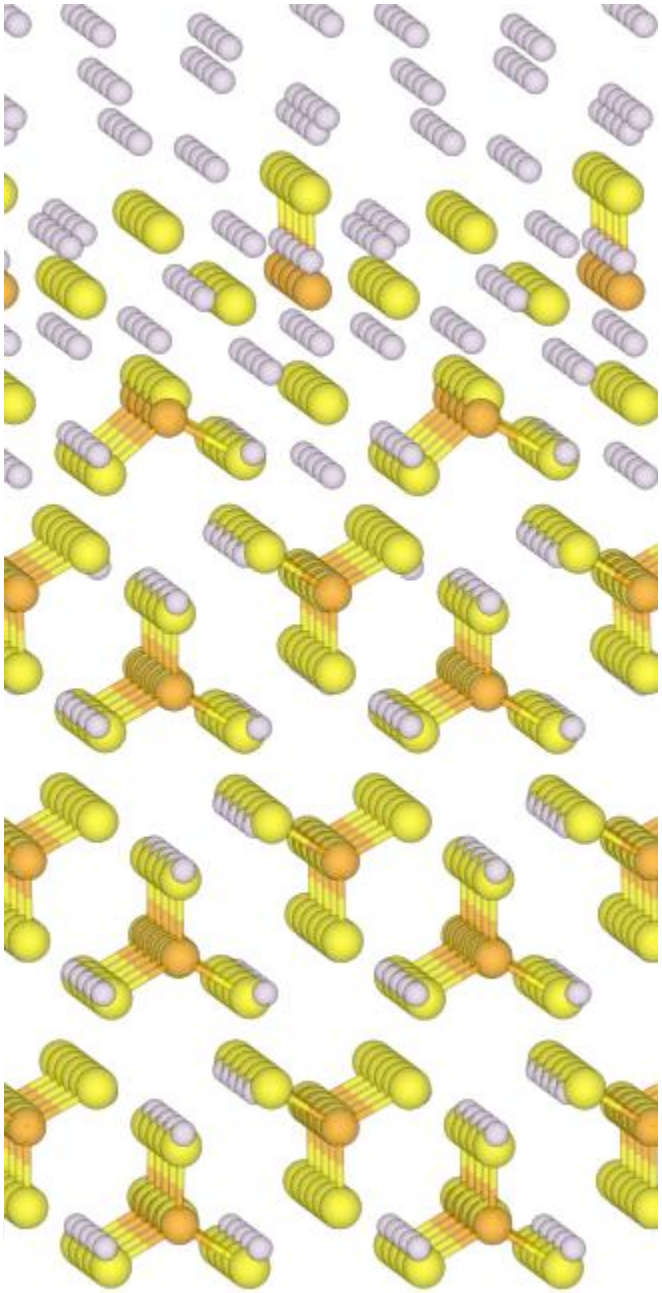

γ-Li_3PS_4 [0 1 0] surface in the presence of Li – supercells containing 12 Li atoms and 2 or 4 electrolyte layers (greater detail)

2 electrolyte layers

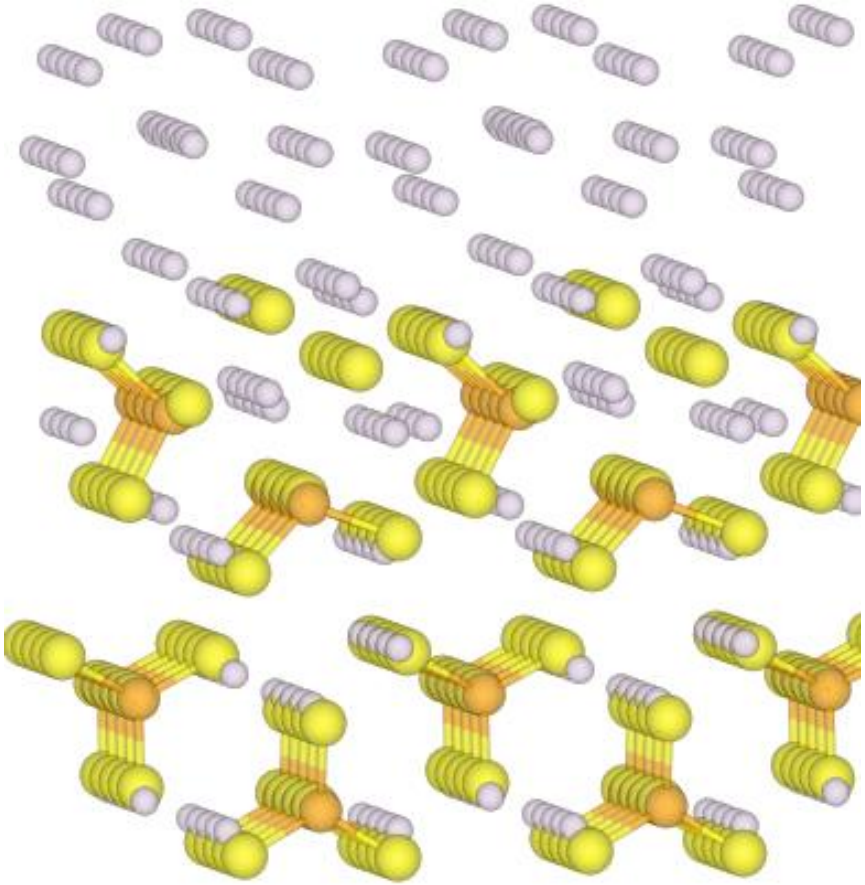

4 electrolyte layers

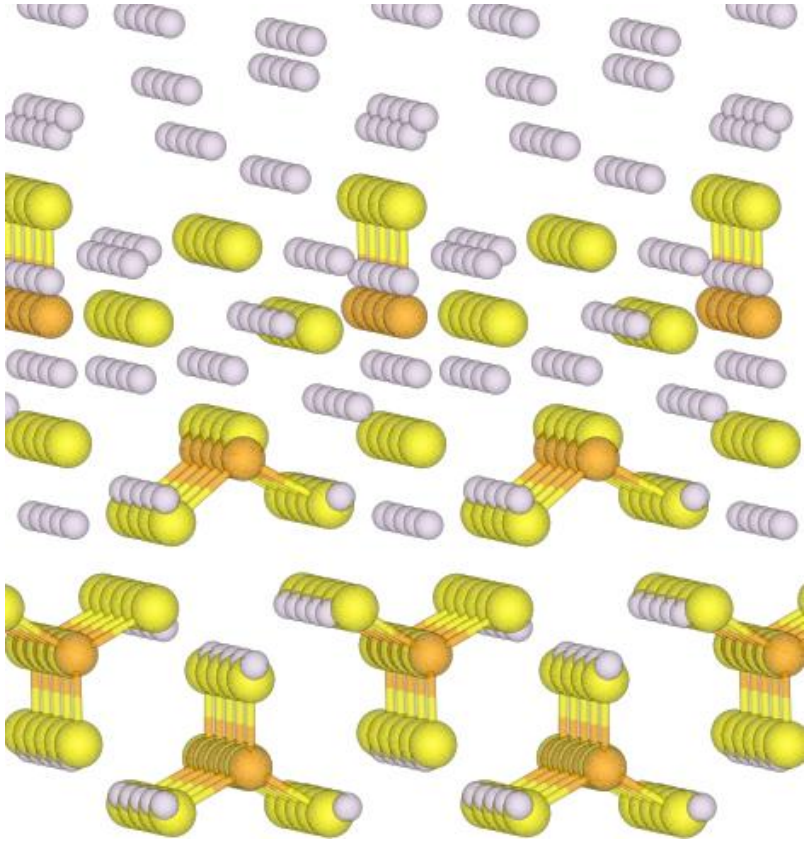

Computational counter example – stable interface: Li/β-Li_3PO_4

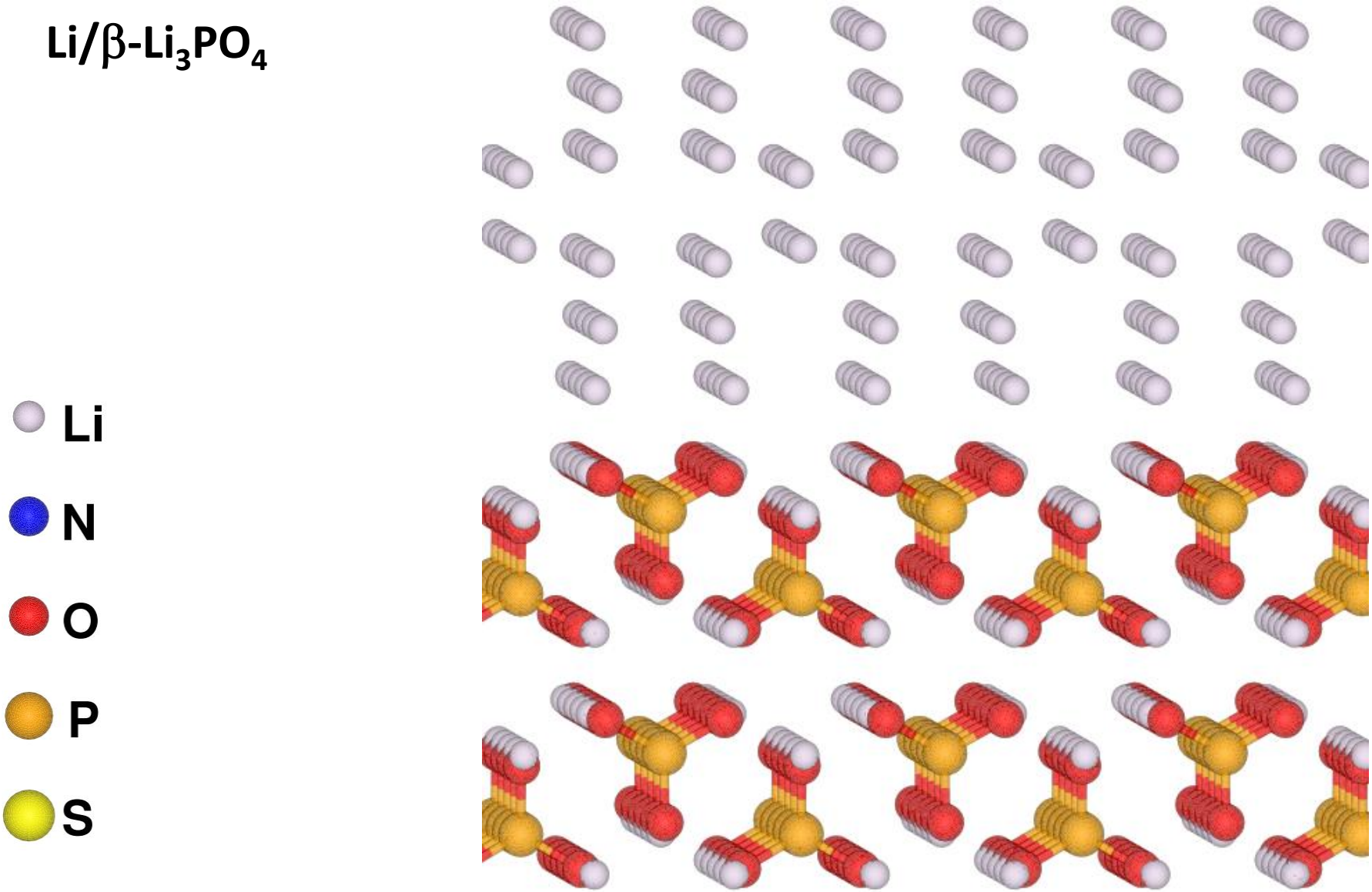

Computational counter example – stable interface: Li/*SD*-Li_2PO_2N

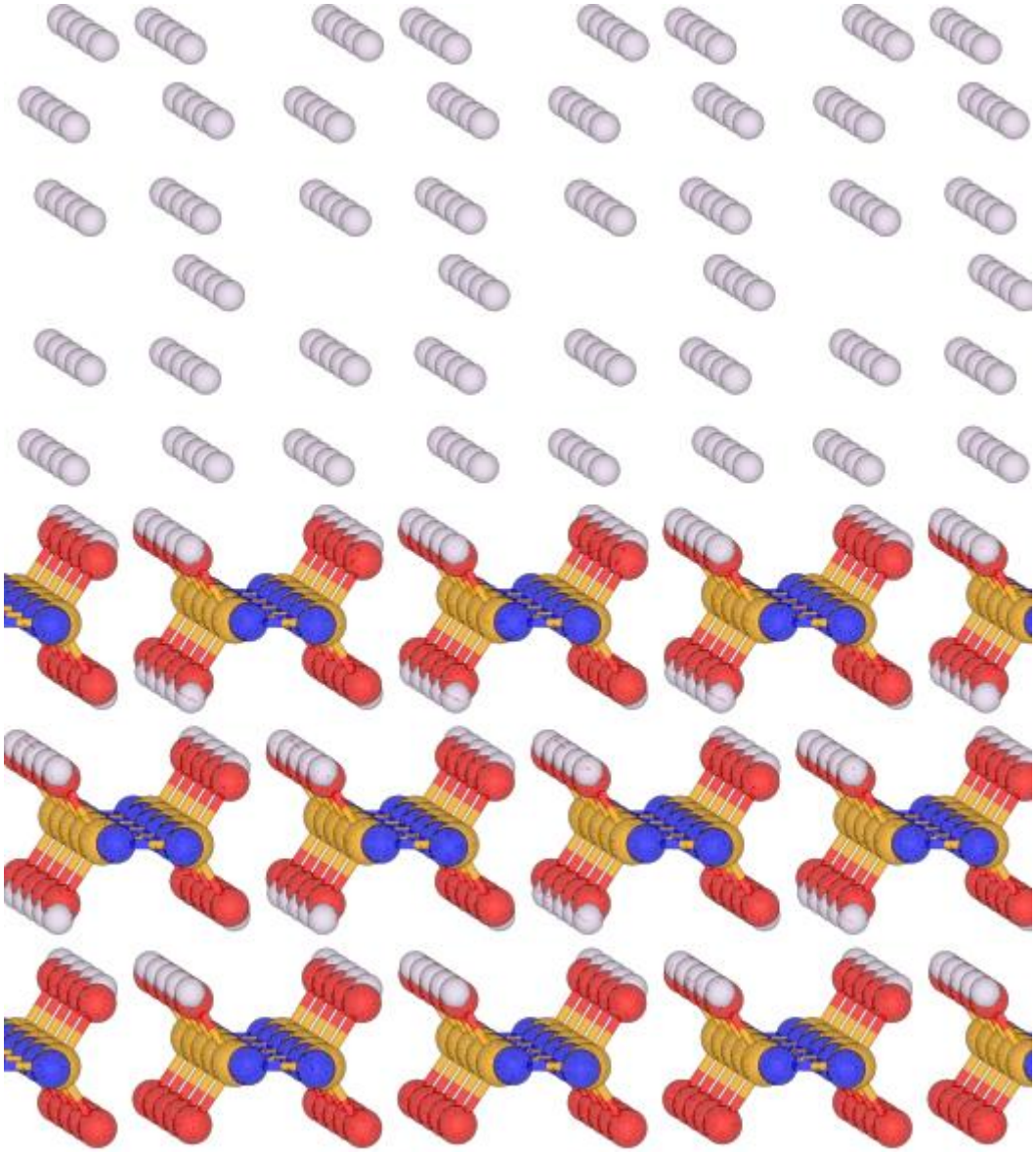

Li

N

O

P

S

Mystery:

- **Models of ideal Li_3PS_4 surfaces are computational found to be structurally (and chemically) altered by the presence of Li metal. (Also found for β-Li_3PS_4 and for various initial configurations of Li metal.)**
- **Experimentally, the ORNL group has found that solid Li_3PS_4 electrolyte samples can be prepared in Li/ Li_3PS_4/Li cells and cycled many times**

Possible solution:

- **Thin protective buffer layer at Li_3PS_4 surface can stabilize electrolyte – for example $Li_2S/Li_3PS_4/Li_2S$**

Idealized $Li_2S/Li_3PS_4/Li_2S$ system

Details:
Thin film of cubic Li_2S oriented in its non-polar [1 1 0] direction, optimized on [0 1 0] surface of γ-Li_3PS_4. While the Li_2S film was slightly strained, the binding energy of the composite was found to be stable with a binding energy of -0.9 eV.

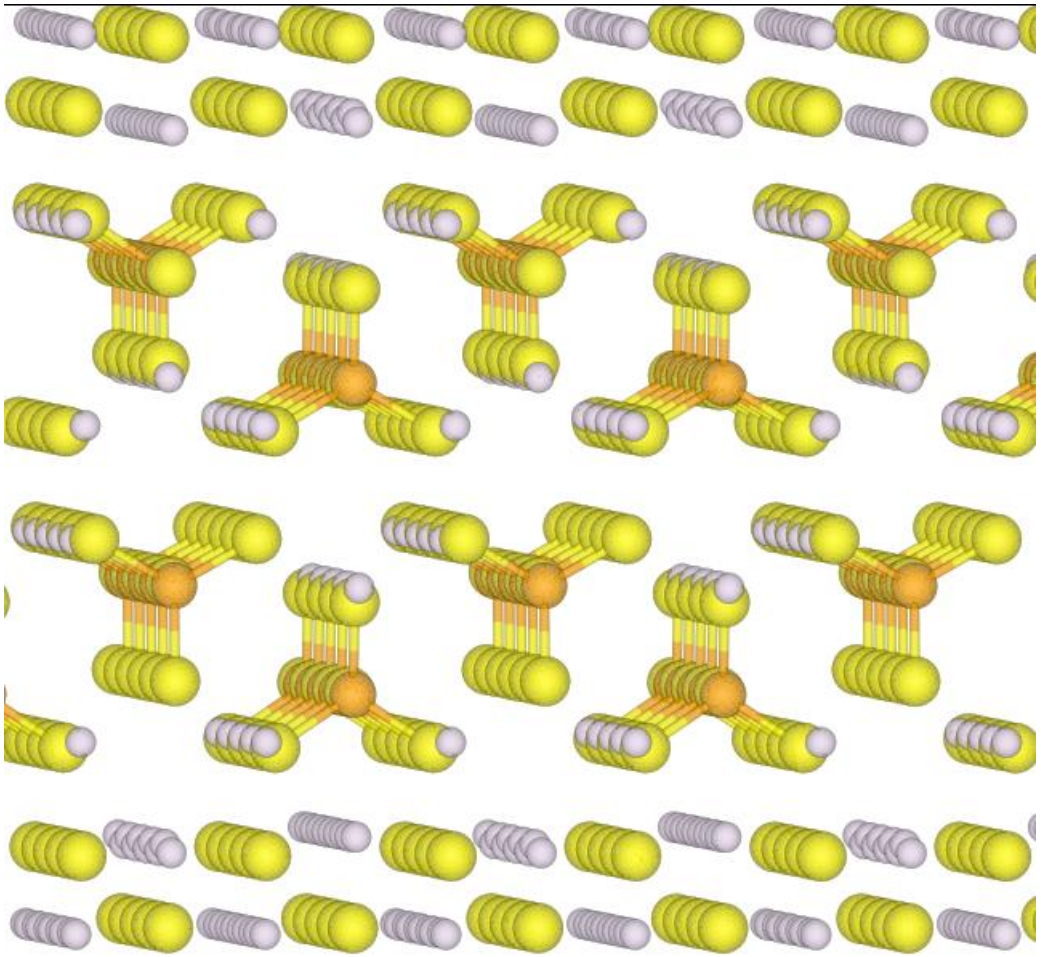

Plausible explanation --

Idealized $Li_2S/Li_3PS_4/Li_2S$ system optimized in presence of Li

In practice, a single Li_2S buffer layer may not be sufficient. These are not explicitly prepared in constructing β-Li3PS4 electrolytes, but may be formed during the first few cycles.

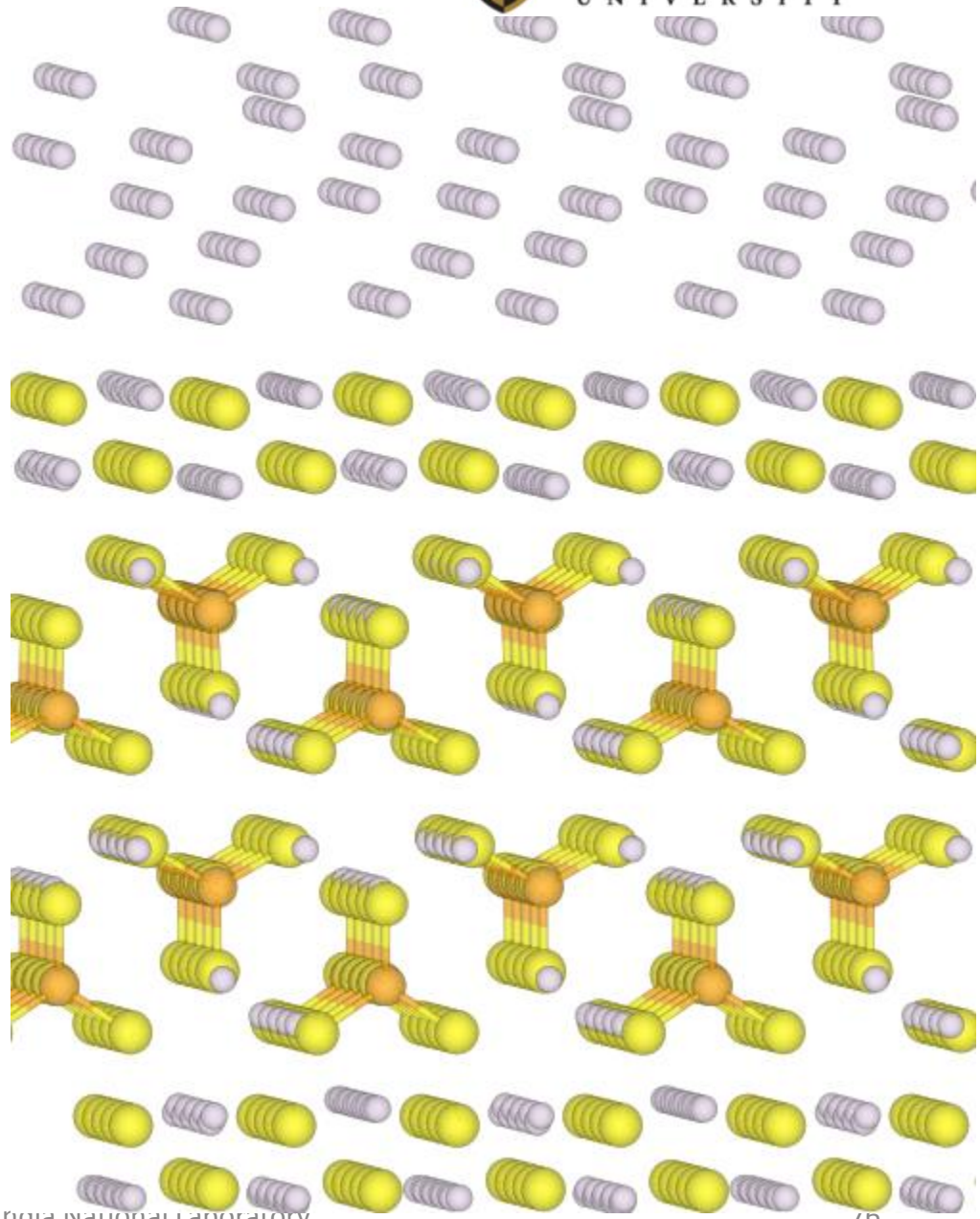

$Li/Li_4P_2S_6/Li$ interfaces

Models of $Li_4P_2S_6$/Li interfaces -- Surface parallel to P-P bonds:

Surface with vacuum

Surface with lithium

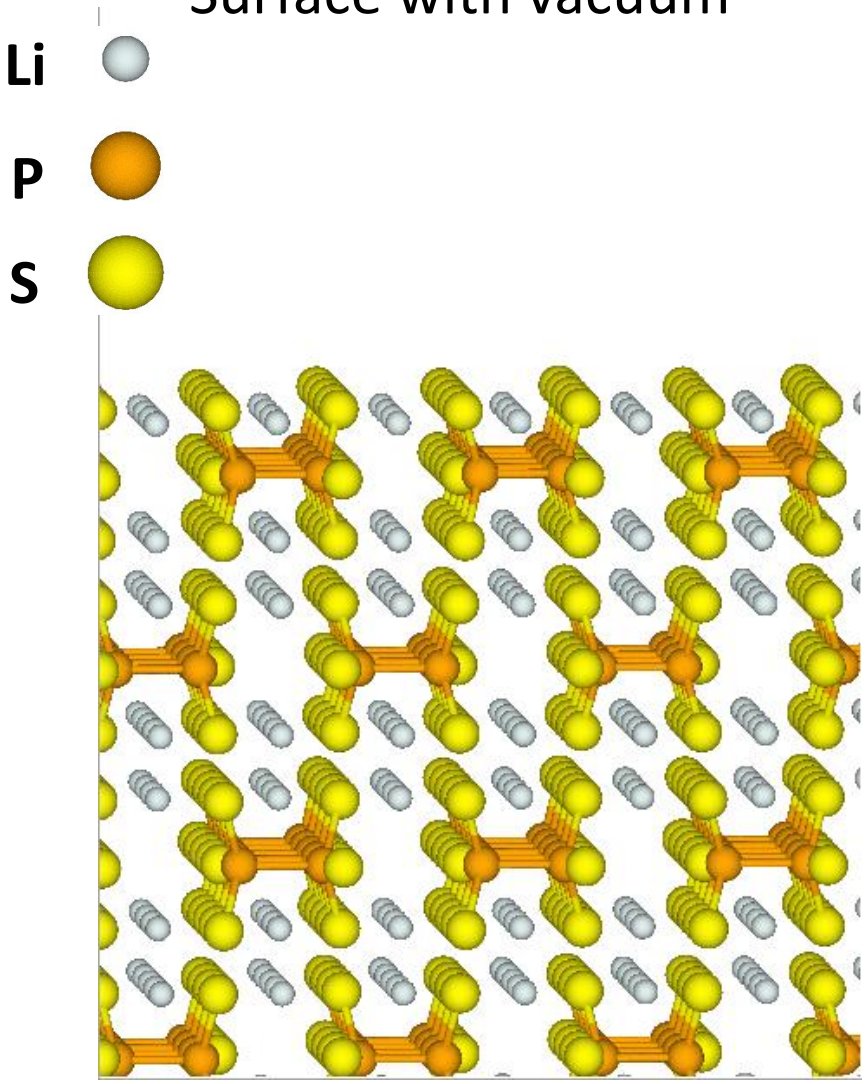

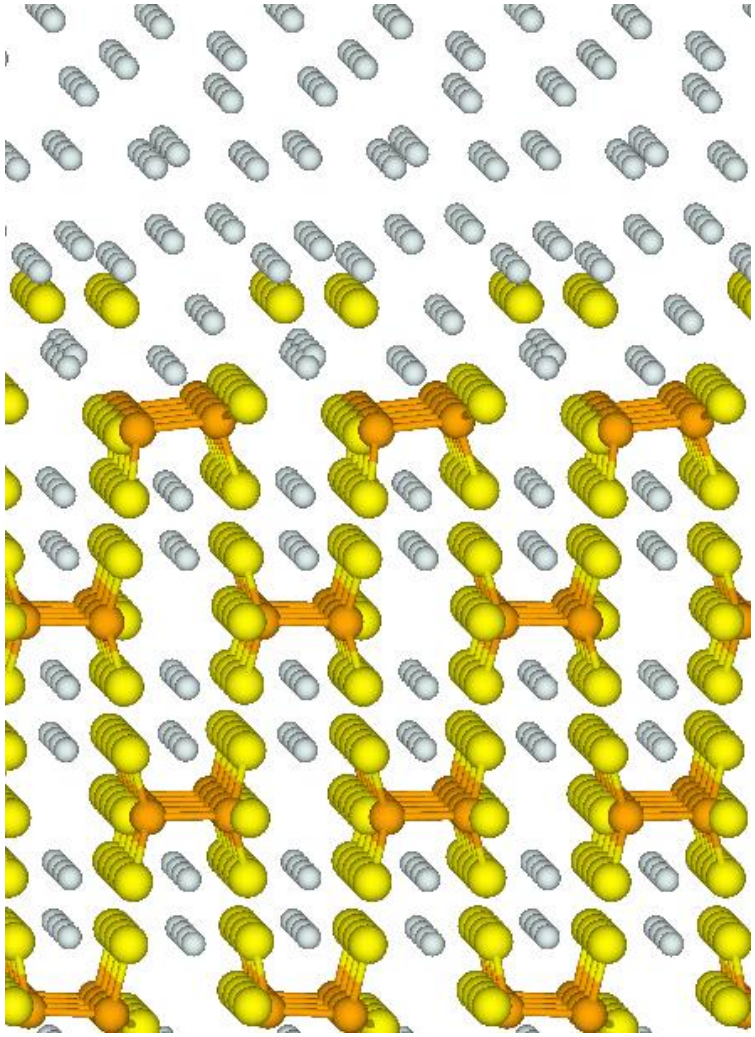

Models of $Li_4P_2S_6$/Li interfaces -- Surface perpendicular to P-P bonds:

Surface with vacuum

Surface with lithium

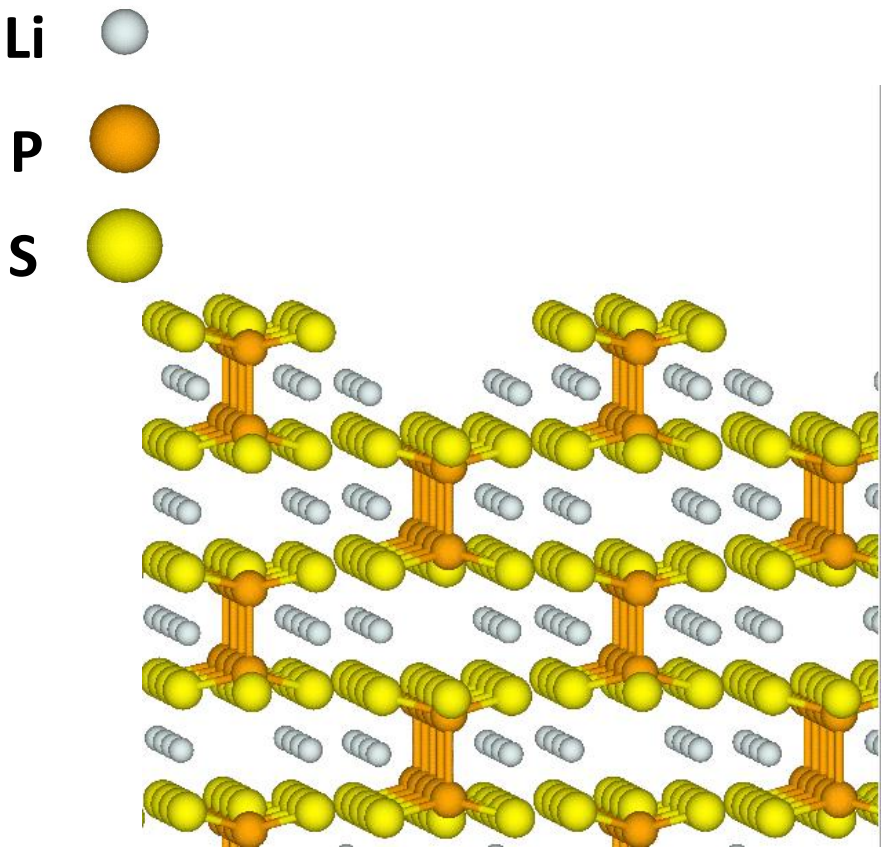

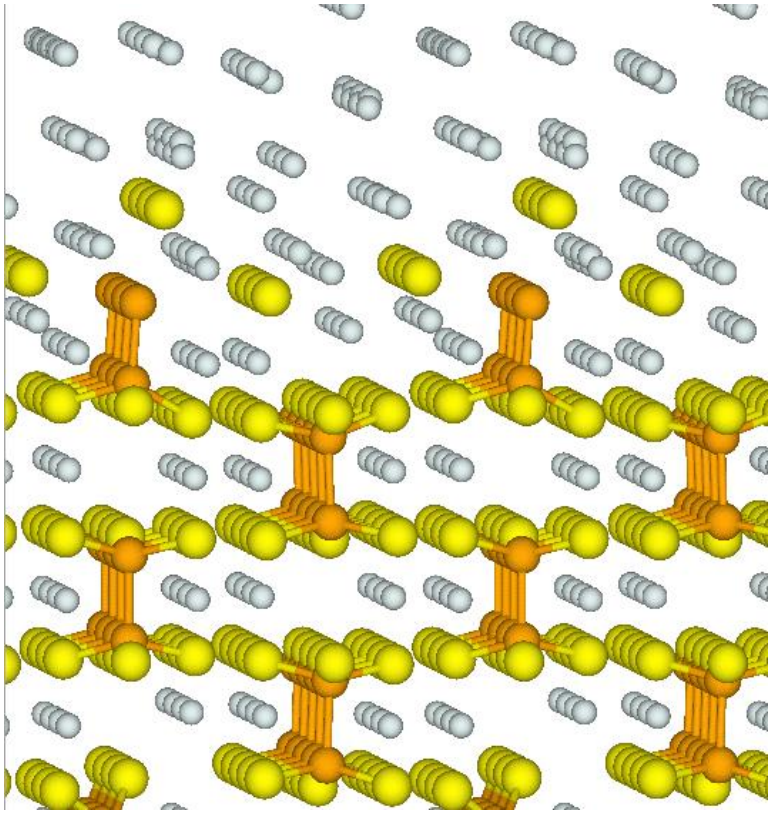

Experimentally, $Li_4P_2S_6$/Li has not been stably cycled (yet).

Things we have learned so far in studying the lithium phosphate and thiophosphate families of materials

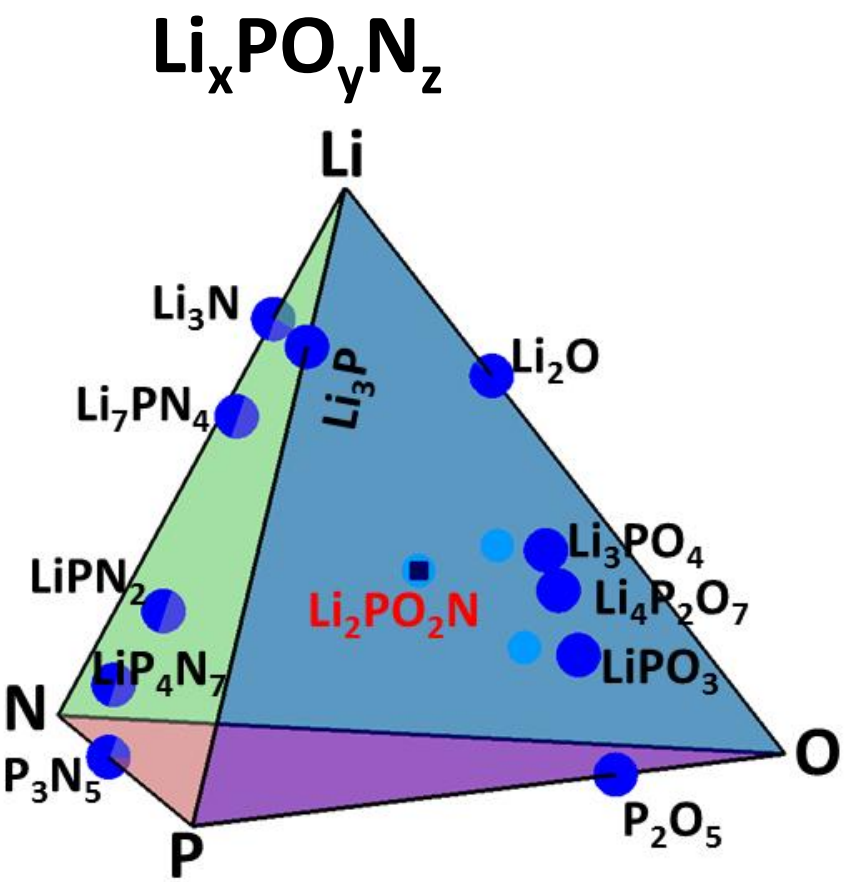

Lower conductivity & greater stability

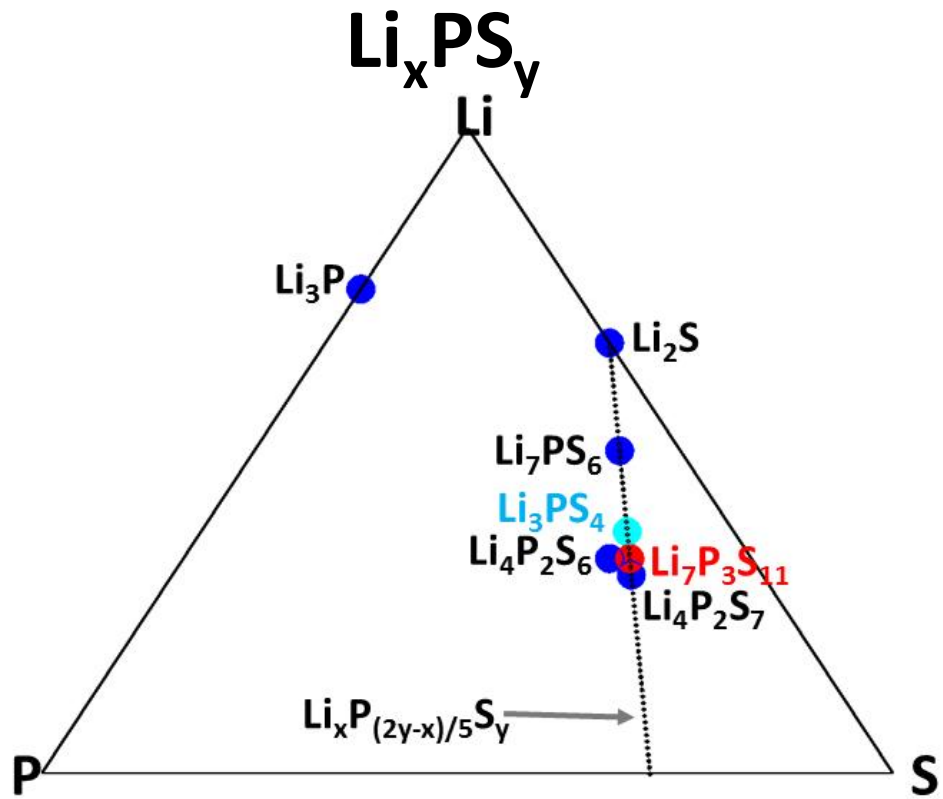

Higher conductivity & lesser stability

Additional thoughts

- Limitations of first principles modeling
  - Small simulation cells
  - Zero temperature
- Possible extensions
  - Develop approximation schemes for treatment of larger supercells
  - Use molecular dynamics and/or Monte Carlo techniques
- Ideal research effort in materials includes close collaboration of both simulations and experimental measurements.
- For battery technology, there remain many opportunities for new materials development.